Title
A Suppressor of Quenching Regulates Photosynthetic Light Harvesting

Author
Brooks, Matthew Dakota

Publication Date
2012

Peer reviewed|Thesis/dissertation

A Suppressor of Quenching Regulates Photosynthetic Light Harvesting

By

Matthew Dakota Brooks

A dissertation submitted in partial satisfaction of the

requirements for the degree of

Doctor of Philosophy

in

Plant Biology

in the

Graduate Division

of the

University of California, Berkeley

Committee in charge

Professor Krishna K. Niyogi, Chair
Professor Bob B. Buchanan
Professor Graham R. Fleming

Fall 2012

Abstract

A Suppressor of Quenching Regulates Photosynthetic Light Harvesting

by

Matthew Dakota Brooks

Doctor of Philosophy in Plant Biology

University of California, Berkeley

Professor Krishna K. Niyogi, Chair

Plants are able to dissipate excess absorbed energy as heat through several mechanisms collectively termed non-photochemical quenching (NPQ). Because these pathways can compete with photochemistry, they must be tightly regulated in order to optimize photosynthesis. In high light, the primary component of NPQ is feedback de-excitation (qE), which is known to require the protein PsbS. In order to investigate additional NPQ pathways and to identify novel proteins involved, I performed a suppressor screen in PsbS-deficient *(npq4)* mutants of *Arabidopsis thaliana*. One of the mutants identified, called *suppressor of quenching 1 (soq1),* displayed considerably higher NPQ relative to *npq4* plants after illumination with high light.

The characteristics of the NPQ demonstrated by the *soq1* mutant point to a new component of NPQ that has not been previously described. The NPQ seen in *soq1* plants had slower induction and relaxation kinetics relative to qE, relaxing over the course of several hours. Additionally, fluorescence measurements of *soq1* single mutants in an otherwise wild-type background demonstrated an additive capacity for quenching, and this quenching was dependent on the light intensity. The additional quenching formed independently of both changes in the pH gradient and zeaxanthin formation based on treatments with nigericin and dithiothreitol, respectively. The additional NPQ in *soq1* was also still observed in xanthophyll mutants, and the pigment composition was identical in wild type and *soq1* leaves before and after illumination. State transitions are also not involved in *soq1* quenching, as quenching occurred in the absence of the STN7 kinase and did not cause changes in phosphorylation of thylakoid proteins or the 77 K fluorescence spectra when compared to wild type. Increased damage to reaction centers is unlikely to be the cause of quenching, as determined by treatment with lincomycin, light curves, and a seemingly wild-type growth phenotype in high light. Using time-resolved fluorescence, it was shown that quenching in *soq1* mutants was the result of a decrease in average lifetime of excited chlorophyll.

The *soq1* mutation was mapped to an uncharacterized chloroplast protein containing three domains: a haloacid dehalogenase-like hydrolase (HAD), a thioredoxin-like (Trx-like) fold and a beta-propeller. The NPQ phenotype of T-DNA lines and complementation with the wild-type *SOQ1* gene confirmed that this locus was responsible for the *soq1* phenotype, and that the *soq1* mutants obtained by mutagenesis were loss-of-function alleles. *SOQ1* is found in all green plants with the exception of prasinophytes and certain species of algae and monocots that have unique domain architecture. Trx-like and beta-propeller domains are also found together in diverse

groups of organisms including animals, bacteria and archaea. I demonstrated that SOQ1 is a thylakoid membrane protein with both Trx-like and beta-propeller domains located in the lumen and the HAD domain in the stroma. Successful complementation with a truncated SOQ1 protein lacking the HAD domain indicated that it did not contribute to the formation of the NPQ seen in *soq1* plants.

To determine the role of SOQ1 in the thylakoid and how it prevents NPQ, biochemical and high-resolution imaging techniques were used to explore differences between *soq1* and wild-type plants. SOQ1 was shown to bind thylakoid proteins in plants treated with high light, however these interactions did not affect the composition of supercomplexes. To identify these interacting proteins, co-immunoprecipitation and yeast two-hybrid analysis were performed and indicated that SOQ1 might interact with HCF136 and At2G26340. Fluorescent labeling of reduced thiols using monobromobimane could lead to additional targets of SOQ1. Electron microscopy (EM) showed that *soq1* plants did not appear to have significantly different chloroplast or thylakoid structures, except for a possible accumulation of plastoglobules in the *soq1* background. When investigated using atomic force microscopy (AFM), the organization of supercomplexes within the grana was unique in *soq1* mutants in both dark-adapted and high light-treated plants.

The role of the HAD domain of SOQ1 has also been investigated. I have shown that both the full-length protein and the HAD domain alone can act as phosphatases on small molecules. Initially, I demonstrated that SOQ1 removed phosphate groups from a general phosphate substrate, *p*-nitrophenyl phosphate. Using the malachite green assay, I narrowed SOQ1's substrate specificity to a pentose sugar phosphate. The highest activity was seen using ribose-5-phosphate as the substrate, and this activity was redox regulated and had a pH optimum near 7. Initial characterization of the sugar content of wild type and *soq1* mutants may improve our understanding of the role of the HAD domain *in vivo*.

Other aspects of NPQ that I have investigated include the dynamic mechanical changes to the thylakoid that occur upon illumination. Using a modified AFM instrument, changes in the stiffness and height of thylakoid membranes were followed in real time. Upon illumination with photosystem II-specific light, an immediate increase in membrane stiffness was observed that was attributed to lumen expansion. Visco-elastic measurements suggest that some undetermined interaction between opposing lumen membranes was involved in this change. After a short delay, the change in stiffness was followed by an increase in the height of the membrane. Both the change in stiffness and height required formation of the pH gradient as determined by the addition of an uncoupler during the measurements. Using measurements on the *stn7* mutant that is incapable of phosphorylating antenna complexes, the height change was shown to result from membrane unstacking.

The identification and characterization of a novel quenching pathway and the use of new AFM techniques to monitor dynamic changes in the thylakoid membrane will lead to a better understanding of how plants regulate photosynthesis.

Table of Contents

List of Figures

List of Tables

Chapter 1

Light Harvesting and Photoprotection in Plants

Introduction

Phototrophic organisms harvest light from the sun in order to provide energy for metabolic processes. In plants and cyanobacteria, the source of electrons for photosynthesis is the oxidation of water, which generates oxygen. Plants form large antenna complexes with several hundred chlorophyll (Chl) and pigment molecules in order to maximize their light harvesting ability in low light conditions. As light intensities increase and light harvesting exceeds the rate of photochemistry, an unavoidable consequence of oxygenic photosynthesis is the production of reactive oxygen species (ROS) by photosensitizers such as Chl and strong reductants such as Photosystem I (PSI) [15,138,140,159]. ROS will oxidize many types of important molecules within the cell and can be toxic to the plant if left unchecked [9,16].

When Chl absorbs light and is excited to the singlet state ($^1Chl^*$), there are several pathways through which it can return to the ground state. It can transfer that energy to the reaction center and undergo charge separation, be dissipated as heat, or decay through intrinsic pathways such as fluorescence and intersystem crossing, which forms triplet Chl ($^3Chl^*$) [159]. $^3Chl^*$ is relatively long-lived and when it interacts with oxygen, it can produce singlet oxygen ($^1O_2$) [65]. When plants are exposed to light intensities where the amount of light captured by the antenna exceeds that which can be used by photochemistry, the yield of $^3Chl^*$ and therefore $^1O_2$ and damage will increase. Most of the $^1O_2$ formation in the thylakoid happens at photosystem II (PSII) due to a longer $^1Chl^*$ lifetime compared to PSI [50,159].

Plants have many systems in the chloroplast in order to scavenge the ROS that are inevitably made [9,13,151]. Enzymatic scavengers are present to prevent damage on the acceptor side of PSI, where the low redox potential required to reduce ferredoxin can also reduce oxygen to the superoxide anion and subsequently form hydrogen peroxide and hydroxyl radicals [16]. In order to prevent the formation of these extremely toxic molecules, thylakoid-bound superoxide dismutase [38] and ascorbate-specific peroxidase [147,148] detoxify superoxide and hydrogen peroxide, respectively [16]. Several small antioxidant molecules can also act as scavengers. Tocopherols, ascorbate, glutathione and carotenoids can all protect the chloroplast by directly quenching ROS, chemical scavenging of ROS, or inhibiting lipid peroxidation [11, 84,46,66,70,183]. Of particular interest are the carotenoids, hydrophobic molecules that are often bound to membrane proteins such as the light-harvesting complexes (LHCs) [132] and reaction centers of PSI [24] and PSII [51,108,192]. Besides their role in quenching $^1O_2$, carotenoids are also involved in light harvesting [77,182], thermal dissipation [137,176] and the structure of photosynthetic complexes [133]. When damage does occur, an elaborate and specific repair pathway exists for PSII in order for plants to quickly and efficiently allocate resources and maximize productivity [205].

Just as plants have several ways to deal with ROS once they are formed, they also have several mechanisms that they use to limit the formation of ROS [146,151,187]. This can be accomplished by increasing carbon fixation [31,44], movement of leaves [110,162] and chloroplasts [41,113,160], or decreasing light harvesting [131,139,196]. These mechanisms work

by limiting the mismatch between the amount of light absorbed and that which can be utilized by photosynthesis. These responses tend to be relatively slow and are involved in plants acclimating to their light environment. Because plants live in habitats where the light intensities can rapidly vary over several orders of magnitude, mechanisms that can respond more quickly are essential in order to deal with the excess light that is unavoidable. Therefore plants also have many pathways by which they can dissipate the excess energy.

Measuring Non-Photochemical Quenching

The thermal dissipation of excess energy is measured and referred to as non-photochemical quenching of Chl fluorescence (NPQ). As mentioned previously, fluorescence is one pathway by which excited Chl molecules can return to the ground state. As early as 1960, Kautsky and his collaborators were able to show that by measuring the amount of Chl fluorescence, one could obtain information on the photochemical reactions themselves [114]. Since then the measurement of Chl fluorescence, as a rapid and non-invasive technique, has become an indispensable tool for assessing photosynthesis. The most common method used is the pulse-amplitude modulated (PAM) fluorometry technique [178,179]. PAM fluorometers isolate and amplify the signal from a weak modulated light source to give information on fluorescence yield in a background of much larger changes in fluorescence intensity due to the actinic light and saturating pulses. Conservation of energy dictates that changes in the yield of fluorescence is the result of changes in the amount of energy quenched by other processes. Because the lifetime of $^1Chl^*$ is much longer for Chls associated with PSII than PSI, under ambient conditions changes in fluorescence can be attributed to changes in the PSII unit [50, 159].

Photochemical quenching of Chl fluorescence is the result of charge separation and occurs when an electron is transferred to the primary acceptor within PSII, Q_A [62]. When a leaf is dark-adapted, electrons are emptied from the electron transport chain and NPQ pathways relax. As a result Q_A is fully oxidized, and all the reaction centers are said to be open, resulting in the minimal fluorescence in the dark (F_o). If a short pulse of light strong enough to briefly reduce all the Q_A sites is then given to the leaf, the reaction centers are closed, and a maximal fluorescence (F_m) can be measured. The variable florescence (F_v) is the difference between the F_o and F_m and the F_v/F_m is equivalent to the the maximum photochemical efficiency of PSII [72]. The F_v/F_m is remarkably consistent between the leaves of unstressed plants [33], and decreases in this value are used as a sign that the plant is stressed [2].

Upon exposure to an actinic light, fluorescence rises due to the closure of reaction centers, and then quickly decreases again as Q_A is reoxidized and NPQ pathways are activated. To separate the contribution of photochemical quenching from NPQ, reaction centers are closed again with saturating pulses, and a light-adapted maximal fluorescence level (F_m') is measured. The difference between the F_m and F_m' is due to non-photochemical processes and it has typically been expressed using the Stern-Volmer equation for quenching calculated as $(F_m-F_m')/F_m'$, often referred to simply as NPQ [33].

There are several mechanisms that contribute to NPQ, and they have traditionally been separated based on how long they take to relax once the actinic light is removed and by using mutants that disrupt specific pathways. In recent years there has been a surge in more sophisticated techniques being used to study NPQ, such as transient absorption [4,18,19,88],

time-resolved fluorescence [10,89,103,112], two-photon excitation [35,128,129] and fluorescence lifetime imaging microscopy [97]. These methods can yield detailed information on the mechanisms contributing to NPQ and can be used to separate the different components by means other than their kinetics.

Feedback De-excitation (qE)

Much of the research done on NPQ has focused on the feedback de-excitation (qE) component due to the fact that more than 75% of the energy absorbed by the plant can be dissipated via this pathway [58]. qE is the fastest component of NPQ, inducing and relaxing within seconds to minutes and is thought to be the primary mechanism by which plants cope with excess energy in fluctuating light conditions [99,146,177]. Feedback de-excitation is thought to limit the production of reactive oxygen species by decreasing the lifetime of $^1Chl^*$ and reducing the excitation pressure on PSII [151]. The signal that activates qE is the low lumen pH, which occurs when the proton gradient is being formed faster than it can be dissipated by ATP synthase [109,189]. In this way qE acts as a feedback mechanism, switching the PSII antenna to a quenching state in response to the light perceived.

There are at least three requirements for the activation of qE in vascular land plants. The first is the transthylakoid pH gradient which forms in the light [200]. Preventing the formation of the pH gradient by the addition of uncouplers inhibits the formation of qE [40], while using chemicals [104,189] or decreasing CO_2 fixation [178,185] to increase the pH gradient will increase the amount of qE. Through changes in the pH gradient, qE can also be modulated *in vivo* by cyclic electron transport [85,143] or changes to the conductivity of ATP synthase [18,109].

The second requirement for qE *in vivo* is the xanthophyll cycle, and specifically the conversion of the symmetrical carotenoid violaxanthin (Vio) to antheraxanthin and zeaxanthin (Zea) [56,151]. Vio is converted to Zea through the action of violaxanthin de-epoxidase (VDE), a lumenal enzyme of the lipocalin family of proteins [80,204]. VDE itself is activated by the transthylakoid proton gradient in several ways. A conformational change occurring within the VDE protein at low pH [115] causes dimerization [14] and binding to its ascorbic acid cofactor, resulting in a low pH optimum [39,81]. The low pH also causes VDE to bind to thylakoid membrane where its substrate is located associated with LHCs [202]. This binding is thought to be mediated through histidine residues at the C-terminal of the protein [76,86]. VDE is also redox regulated, most likely through a cysteine-rich N-terminal domain [86]. In contrast to most redox-regulated proteins, which are located in the stroma [180], VDE is active when oxidized and can be inhibited by reducing agents such as dithiothreitol (DTT) [201].

The first evidence for the role of the xanthophyll cycle in qE came from the correlation between Zea levels and the amount of quenching upon exposure of leaves to high light [54]. This relationship was confirmed by the identification of mutants in VDE (*npq1*) and zeaxanthin epoxidase (*npq2*) that also affected NPQ [150]. Despite years of study, the exact role of Zea in qE remains controversial, owing largely to the lack of consensus on the molecular mechanism of qE (see below) [87,99,177] and the presence of separate protein-bound and lipid-soluble pools of carotenoids that complicate kinetic relationships [49,203]. A direct role in qE has been proposed for Zea through either an energy transfer [68,137,158] or charge-transfer [4,19,20,88] mechanism from Chl to a Zea. Alternatively, an indirect role for Zea in qE has been put forward

in which it acts as an allosteric regulator, controlling the sensitivity of qE to the pH gradient and/or conformational changes within the LHCs where qE occurs [47,102,106,177]. These roles for Zea are not necessarily mutually exclusive, and models have been put forth that explain qE by giving Zea different functions depending on the site of quenching [99].

The third requirement for qE *in vivo* is the thylakoid protein PsbS, a 22 kDa subunit of PSII whose involvement in qE was identified through a screen for mutants with lower amounts of NPQ [124]. PsbS is a member of the LHC superfamily of proteins, unique in that it contains four transmembrane helices and lacks some of the conserved Chl-binding residues present in other LHCs [30]. It was originally hypothesized that PsbS was the site of quenching [124] but because of conflicting reports on its ability to bind Chl and pigments *in vivo* or *in vitro* [17, 60,71], a role as a regulator of qE is now favored. This view is supported by evidence that PsbS binds dicyclohexylcarbodiimide (DCCD), a chemical that will bind acidic amino acid residues in hydrophobic environments [60]. Through site-directed mutagenesis, lumen-exposed glutamate residues were identified that are critical for the formation of qE [125] and DCCD binding [126]. These results suggest that the glutamate residues act as pH sensors, causing a conformational change in PsbS that turns qE on or off. The pH may also act as a signal for PsbS dimerization, which has been observed in solubilized membranes from *Zea mays* and appears to be favored at higher pH [30].

As mentioned above, the mechanism of qE in higher plants is heavily debated. Most of the current research indicates that quenching occurs in the LHCs associated with PSII (LHCII), however there is some evidence that PSII reaction centers can also form quenching complexes, important during photoinhibitory stress (see below) [96]. Higher plants have six LHCII proteins associated with PSII (Lhcb1-6), with Lhcb1-3 forming the major trimeric antenna while Lhcb4-6 exist as monomers [100,119,165,167]. The observation that isolated LHCII trimers formed aggregates *in vitro* with spectroscopic features that have been correlated with qE *in vivo* [166,174,177,197] has led to the proposal of the "LHCII aggregation model" [91,93,177]. In this four-state model, aggregation of LHCII trimers is controlled cooperatively by PsbS protonation and Zea formation. Recent findings that diaminodurene, a chemical that can artificially lower the lumen pH beyond physiological values by artificial cyclic electron flow around PSI [83], can induce quenching in the absence of both PsbS [104] and xanthophylls [106] suggest that both play allosteric roles controlling levels of LHCII aggregation. This would also suggest that the pH is sensed through other proteins as well, possibly the different LHCIIs which have been shown to bind DCCD [164,197]. Support for this model also comes from freeze-fracture electron microscopy which indicated that clusters of PSII cores and LHCII aggregates form upon light exposure and were influenced by pre-illumination to convert Vio to Zea [105].

Another model put forth and in many ways complementary to the aggregation model, proposes the presence of two distinct quenching sites, Q1 and Q2 [89,99]. This model is based on spectroscopic [89] and biochemical evidence [32] suggesting the PsbS-dependent detachment of a subset of LHCII trimers and the minor complexes Lhcb4 and Lhcb6, which can then aggregate and lead to the formation of Q1. The formation of a far-red spectral component assigned to Q1 has been seen in during qE formation in both aggregated LHCII [141,173] and intact leaves [122]. Zea was shown to enhance this effect but not be required, again suggesting an allosteric role [103]. The Q2 site in their model remains associated with PSII and is Zea-dependent but does not require PsbS [89]. More kinetic information will be required to determine if the quenching at this site is in fact qE or if it would more accurately fit with one of the slower components.

The molecular mechanism that is responsible for qE is much more contentious. One proposed mechanism involves an aggregation-dependent conformational change affecting a lutein located in the L1 site of trimeric LHCII, which positions it as a quencher of Chl through an energy transfer mechanism [176]. Alternatively it has been suggested that the same conformational change results in quenching through a Chl-Chl charge transfer mechanism [141,144]. In contrast to these scenarios where Zea plays a strictly allosteric role, mechanisms for qE based on direct involvement either through energy or electron transfer from Chl to Zea have been proposed [56,61,67,87]. Evidence for a carotenoid charge-transfer mechanism came from observations of the formation of Zea radical cation formed under qE conditions in isolated thylakoids [88] and purified Lhcb4-6 [4,19,20]. Interestingly a lutein cation radical was also formed in Lhcb5 and was allosterically enhanced by Zea, but no evidence of any radical cation could be found in isolated LHCII trimers [20]. Recently it has been shown that in plants lacking Zea, over-accumulation of lutein can partially restore qE that is associated with formation of a lutein cation radical [127]. Excitionic coupling between the S1 state of carotenoids and Chl has been observed to be correlated with the amount of quenching and the formation of the red shifted band in isolated LHCs [35,128,129] and *in vivo* [35]. This has led to the proposal that when electronic coupling between the two molecules is sufficient, energy can be trapped in this short-lived state and further increases in coupling can lead to the charge transfer state [35,130]. As the Q2 site is also assigned to the minor LHCII, it has been proposed that carotenoid-dependent mechanisms of quenching occur only at this site [89,99]. Quenching by a carotenoid mechanism in detached LHCII can not be excluded however, as quenching by excitionic coupling of carotenoid and Chl could still occur and the possible presence of Lhcb4 and Lhb6 in those complexes would also allow charge transfer quenching. One appealing way to integrate the various experimental observations is to suggest that multiple qE mechanisms occur at different sites surrounding the PSII supercomplex in order to provide dynamic protection.

Zeaxanthin-Dependent Quenching (qZ)

The most recently identified component of NPQ is called zeaxanthin-dependent quenching (qZ). This component was identified as being distinct from qE, by its slow kinetics, PsbS-independence and close correlation to Zea formation and re-epoxidation [149]. qZ forms and relaxes on the timescale of 15 to 30 minutes, similar to state transitions, but it does not require the STN7 kinase (see below). The slower kinetics seen in the qZ component could serve as a form of 'memory' of light conditions so that the plant is prepared for longer periods of high light. The finding that Zea re-epoxidation is slowed at higher light intensities supports this view [170]. Since the rate of conversion of Vio into Zea in the major LHCII trimers [98] is presumed to be faster than in the minor complexes [198], it has been proposed that qZ quenching occurs in the latter [149]. The identification of the qZ component also possibly explains the observation of a PsbS- and pH-independent quenching mechanism in Lhcb5 that was prevalent in *npq2* mutants but absent in *npq1* plants [48]. The assignment of qZ to the minor complexes and its being independent of PsbS have led to the suggestion that it is in fact responsible for the quenching at Q2 [99]. Further characterization of the kinetics of qZ, especially in the various mutants could help elucidate its contribution to NPQ under various conditions and its role in photoprotection.

State Transitions (qT)

Due to the different action spectra of the two photosystems, plants can experience light conditions where either PSI or PSII is preferentially excited. State transitions (qT) were discovered when it was observed that preferential excitation of PSII led to an increase in PSI and decrease in PSII fluorescence, and this was assumed to be a response by which plants balance excitation between the two photosystems [36,145]. In the dark, far-red light, or high light, LHCII is associated with PSII (state 1). When PSII is preferentially excited, which can happen in low light, a subset of LHCII will migrate and attach to PSI (state 2). This process is thought to prevent over-reduction of intermediates in the electron transport chain and the formation of ROS [12].

Understanding the mechanism leading to state transitions began with the observation that phosphorylation of threonine residues on LHCs [25] was correlated with the decrease in Chl fluorescence of PSII and changes in the 77K fluorescence yield that were signatures of qT [27,43,90]. By inhibition of PSII using 3-(3,4-dichlorophenyl)-1,1-dimethylurea (DCMU) [6] and reduction of the plastoquinone (PQ) pool using different electron donors [7,8,26], the phosphorylation of LHCs was shown to be dependent not on the light itself, but on the redox state of the electron transport chain. These results indicated that the redox status of the PQ pool acted as an indicator of the relative rates of PSI and PSII excitation. Further work demonstrated that the binding of reduced PQ to cytochrome b_6f (Cyt*bf*), and not reduced PQ itself, was in fact the signal to activate the LHC kinase [28,199,209].

The kinase responsible for phosphorylating LHCs was identified by screening for *Chlamydomonas reinhardtii* mutants defective in qT [64]. The Stt7 protein (STN7 in higher plants) is a thylakoid membrane serine/threonine kinase that interacts with Cyt*bf* and PSI subunits [23,123]. Stt7/STN7 also contains conserved N-terminal cysteine residues [123] that may be responsible for the observed inhibition of qT in high light [94,171]. This inhibition is possibly mediated through thioredoxin, however the topology of the protein indicates that the cysteines are within the lumen, and point mutants converting the cysteines to other amino acids result in permanent inactivation of the kinase [123], suggesting that the protein may be active when oxidized, similar to VDE. While it is clear the STN7 has a role in qT, it remains possible that it is part of a signal cascade with other kinases.

The reversible phosphorylation of LHCs suggests the presence of at least one phosphatase. This activity was shown to depend on divalent cations and to be resistant to inhibition by microcystin and okadaic acid [82,186], indicating that it would be a PP2C-type phosphatase. A targeted screen for Arabidopsis mutants resulted in the identification of PPH1/TAP38 [169,181]. Loss of function mutants in this phosphatase resulted in plants with a larger PSI antenna, while overexpression prevented phosphorylation of LHCs [169,181].

Work from several labs has also gone into characterizing the interaction between LHCII and PSI. The PsaH, PsaL [135] and PsaO [101] subunits of PSI were identified as being involved in docking of phosphorylated LHCs to the PSI complex. The specific LHCII complexes that migrate to PSI were also identified as being the Lhcb1/Lhcb2 heterotrimer by crosslinking experiments in *Arabidopsis thaliana* [208], and later a PSI supercomplex containing Lhcb4 and Lhcb5 was found in Chlamydomonas [188], though this complex has not been characterized in higher plants.

While it has long been assumed that the quenching associated with qT was the result of

LHCs migrating from PSII and attaching to PSI where Chl fluorescence is rapidly quenched, recent evidence suggests this may not be the whole story. Using fluorescent lifetime imaging microscopy to study qT in Chlamydomonas, it was observed that some phosphorylated LHCs form aggregates unbound to either photosystem and with fluorescent lifetimes that are shorter than complexes associated with PSII [97]. The similarities between the PsbS-dependent dissociation of LHCs in qE and formation of redox-dependent quenched aggregates during qT raise the question of whether these two components of NPQ have the same quenching mechanism but are activated by different signals [97,142]. Further experiments will be required to clarify this point, and it remains to be seen if higher plants behave similarly, as in Arabidopsis only 25% LHCs are mobile [29] compared to up to 80% in Chlamydomonas [52].

Photoinhibition (qI)

The processes of NPQ that relax on the longest timescales, usually greater than an hour, are labeled as photoinhibitory quenching (qI). While the term photoinhibition often refers specifically to light-induced damage to PSII reaction centers, in the context of NPQ it is most often used to describe all of the slowly reversible mechanisms that decrease PSII efficiency [3, 156]. The phenomenon of qI has been recognized for nearly a century as a response to stresses to the plant such as high light, UV radiation and temperature [63,117,168]. The F_v/F_m parameter is the most often used to assess qI due to the ease with which it can be determined, and it has been shown to correlate to the efficiency of photosynthetic oxygen evolution [55,34].

Photo-oxidative damage to PSII follows first-order kinetics and as a result the rate is light-intensity dependent [22,191]. Damage can lead to the irreversible inactivation of PSII charge separation and electron transport [45,53], and if the rate of repair cannot match the rate of damage, photosynthetic yield will be reduced [79]. Most of the photo-oxidative damage that occurs seems to be targeted to the D1 protein of the PSII reaction center [121,153], and plants have therefore evolved a complex repair system that selectively removes D1 and replaces it with a newly synthesized protein [205]. Because of the organization of the thylakoid into grana stacks, this process is complicated and involves disassembly of the damaged reaction center, transport to the stroma lamellae, cleavage and removal of the damaged D1, reassembly of the complex after insertion of the new D1 peptide and transport back to the grana [205]. Photoinhibited and pre-assembled reaction centers may also form quenching sites themselves in order to protect against further damage in the absence of charge separation [95,184,193]. Though several proteins involved in PSII repair have been discovered [111,118,134,152,161], more work remains in order to fully understand the mechanisms involved, especially in how the damage is localized to D1, how reaction centers switch between active and quenched forms and how damaged reaction centers are specifically transported to the stromal exposed regions through the densely packed grana membrane.

The idea that different forms of qI can also serve a photoprotective role has only been widely appreciated in the last couple decades, based largely on studies of non-model species [3]. Sustained thermal dissipation can protect the plant when downstream utilization of energy is limited during long periods of stress such as winter or the transfer of shade-grown plants to high light [2,3,154]. In some cases, it appears likely that this qI has the same mechanism as qE and is the result of the plant maintaining the ΔpH in the dark at low temperatures [195]. Warming of the leaves or addition of uncouplers will cause the quick relaxation of this type of qI [74]. Forms of

photoprotective qI that are pH-independent have also been observed and correlated closely to the amount of Zea present [1,59,75,195].

Based on the correlation between pH-independent qI and Zea content, it has been proposed that qI may have the same mechanism as qZ and that the distinction is an arbitrary one based on Zea epoxidation rates [89,99,149]. If this is true it would suggest that this type of quenching can form in LHCII complexes unattached to the reaction center, as many of these evergreen species will degrade reaction center components under these conditions [157,206,207]. Unfortunately, research in this area is relatively limited, and genetic manipulation on many of these organisms is undeveloped, making it difficult to mechanistically define qI.

NPQ Variation Between Organisms and Impact on Plant Fitness

Much of the work characterizing the different components of NPQ described above comes from work done on a limited number of organisms. There is a a great deal of variation in the amount of NPQ between species, and even within a species acclimated to different conditions [42,57,155,172]. Between closely related species this variation likely arises from adaptation to different environments and alterations in gene expression to fine tune the amount and kinetics of NPQ [107]. Across larger evolutionary distances, the specific mechanisms of NPQ may differ or the role that a specific component plays can be dramatically different. Two of the most well studied model organisms, Arabidopsis and Chlamydomonas, highlight these differences. While Chlamydomonas has a qE component of NPQ that is also pH-dependent, the mechanism appears to be different as it does not require PsbS but rather another LHC-like protein, LHCSR, which is able to bind Chl and pigments [37,163]. The qT mechanism also appears to play a larger role in Chlamydomonas where up to 80% of LHCII can attach to PSI [52]. In *Physcomitrella patens,* a moss species basal to land plants, both the PsbS-dependent and LHCSR-dependent forms are present and contribute additively to qE [5,73]. The differences between land plants and cyanobacteria are even greater, as one would expect given the difference between the membrane LHCs of plants and soluble phycobilisome antenna of cyanobacteria [21,116].

The apparent ubiquitous nature of NPQ in plants would suggest that it has a critical role in their survival. Yet many mutants that lack proteins essential for these components are able to grow just as well as wild type in laboratory conditions [23,124,136] and even in high light [190]. This is likely due to the overlapping roles of the different NPQ mechanisms [69,78,190] and the ability of these plants to acclimate by accumulating antioxidant molecules [84, Golan]. Growth phenotypes in mutants become apparent when plants are subjected to changing light conditions [23,120,190] or additional stresses [84]. Growth defects were even more pronounced in double mutants lacking both the qT and qE components [190]. Field experiments also demonstrated that fitness was decreased in mutant plants defective in qT or qE [69, 120].

Maintenance of the photosynthetic machinery is of critical importance to a plant's survival. In order to minimize the formation of damaging ROS, many mechanisms have evolved that are used to dissipate excess absorbed energy. These pathways are able to respond rapidly to sudden changes in light (qE), 'remember' previous stresses and light conditions (qZ and qI) and accurately estimate the quality of light the plant receives (qT). NPQ as a whole is therefore both robust and dynamic, managing to integrate multiple signals to balance the need for light harvesting with the damaging consequences that come with the absorption of excess light. There

are several important questions that remain concerning how plants accomplish this remarkable feat. With hundreds of chloroplast proteins still without a known function, there could very well be additional factors involved. Only after establishing the set of proteins that are critical for both optimizing light harvesting and NPQ will it be possible to understand these processes. Characterizing the structural changes that occur on many levels during NPQ will also be of critical importance. What are the conformational changes within proteins that can switch them from light harvesters to quenchers? How does the organization of complexes within the membrane optimize and direct energy transfer depending on the plants needs? And how does the stacking of membranes and the division grana and lamellae play a role? The following work aims to address these questions and others through a variety of approaches including genetics, biochemistry, molecular biology, and spectroscopy.

References

1. Adams, W.W., and Demmig-Adams, B. (1995). The xanthophyll cycle and sustained thermal energy dissipation activity in Vinca minor and Euonymus kiautschovicus in winter. Plant, Cell & Environment *18*, 117–127.
2. Adams III, W.W., Demmig-Adams, B. (2004) Chlorophyll fluorescence as a tool to monitor plant response to the environment, in Chlorophyll a Fluorescence: A Signature of Photosynthesis. pp. 583–604.
3. Adams III, W.W., Zarter, C.R., Mueh, K.E., Amiard, V., and Demmig-Adams, B. (2006). Energy Dissipation and Photoinhibition: A Continuum of Photoprotection. Photoprotection, Photoinhibition, Gene Regulation, and Environment. pp. 49–64.
4. Ahn, T.K., Avenson, T.J., Ballottari, M., Cheng, Y.-C., Niyogi, K.K., Bassi, R., and Fleming, G.R. (2008). Architecture of a Charge-Transfer State Regulating Light Harvesting in a Plant Antenna Protein. Science *320*, 794 –797.
5. Alboresi, A., Gerotto, C., Giacometti, G.M., Bassi, R., and Morosinotto, T. (2010). Physcomitrella patens mutants affected on heat dissipation clarify the evolution of photoprotection mechanisms upon land colonization. Proc. Natl. Acad. Sci. U.S.A. *107*, 11128–11133.
6. Allen, J.F., Bennett, J. (1981) Photosynthetic protein phosphorylation in intact chloroplasts: Inhibition by DCMU and by the onset of CO2 fixation. FEBS Lett. *123,* 67–70.
7. Allen, J.F., Bennett, J., Steinback,, K.E., Arntzen, C.J. (1981) Chloroplast protein phosphorylation couples plastoquinone redox state to distribution of excitation energy between photosystems. Nature *291*, 25–29.
8. Allen, J.F., and Horton, P. (1981). Chloroplast protein phosphorylation and chlorophyll fluorescence quenching. Activation by tetramethyl-p-hydroquinone, an electron donor to plastoquinone. Biochimica Et Biophysica Acta (BBA) - Bioenergetics *638*, 290–295.
9. Alscher, R.G., Donahue, J.L., and Cramer, C.L. (1997). Reactive oxygen species and antioxidants: Relationships in green cells. Physiologia Plantarum *100*, 224–233.
10. Amarnath, K., Zaks, J., Park, S.D., Niyogi, K.K., and Fleming, G.R. (2012). Fluorescence lifetime snapshots reveal two rapidly reversible mechanisms of photoprotection in live cells of Chlamydomonas reinhardtii. Proc. Natl. Acad. Sci. U.S.A. *109*, 8405–

8410.
11. Anderson, I.C., and Robertson, D.S. (1960). Role of Carotenoids in Protecting Chlorophyll From Photodestruction. Plant Physiology *35*, 531 –534.
12. Anderson, J.M., and Andersson, B. (1988). The dynamic photosynthetic membrane and regulation of solar energy conversion. Trends Biochem. Sci. *13*, 351–355.
13. Apel, K., and Hirt, H. (2004). Reactive Oxygen Species: Metabolism, Oxidative Stress, and Signal Transduction. Annu. Rev. Plant Biol. *55*, 373–399.
14. Arnoux, P., Morosinotto, T., Saga, G., Bassi, R., and Pignol, D. (2009). A Structural Basis for the pH-Dependent Xanthophyll Cycle in Arabidopsis thaliana. The Plant Cell *21*, 2036 –2044.
15. Aro, E.-M., Virgin, I., and Andersson, B. (1993). Photoinhibition of Photosystem II. Inactivation, protein damage and turnover. Biochimica Et Biophysica Acta (BBA) - Bioenergetics *1143*, 113–134.
16. Asada K. (1994). Production and action of active oxygen species in photosynthetic tissues. Causes of Photooxidative Stress and Amelioration of Defense Systems in Plants. 77–104.
17. Aspinall-O'Dea, M., Wentworth, M., Pascal, A., Robert, B., Ruban, A., and Horton, P. (2002). *In vitro* reconstitution of the activated zeaxanthin state associated with energy dissipation in plants. Proceedings of the National Academy of Sciences *99*, 16331 –16335.
18. Avenson, T.J., Cruz, J.A., and Kramer, D.M. (2004). Modulation of energy-dependent quenching of excitons in antennae of higher plants. Proceedings of the National Academy of Sciences of the United States of America *101*, 5530 –5535.
19. Avenson, T.J., Ahn, T.K., Zigmantas, D., Niyogi, K.K., Li, Z., Ballottari, M., Bassi, R., and Fleming, G.R. (2008). Zeaxanthin Radical Cation Formation in Minor Light-harvesting Complexes of Higher Plant Antenna. Journal of Biological Chemistry *283*, 3550 –3558.
20. Avenson, T.J., Ahn, T.K., Niyogi, K.K., Ballottari, M., Bassi, R., and Fleming, G.R. (2009). Lutein can act as a switchable charge transfer quencher in the CP26 light-harvesting complex. J. Biol. Chem. *284*, 2830–2835.
21. Bailey, S., and Grossman, A. (2008). Photoprotection in cyanobacteria: regulation of light harvesting. Photochem. Photobiol. *84*, 1410–1420.
22. Baroli, I., and Melis, A. (1996). Photoinhibition and repair in *Dunaliella salina* acclimated to different growth irradiances. Planta *198*, 640–646.
23. Bellafiore, S., Barneche, F., Peltier, G., and Rochaix, J.-D. (2005). State transitions and light adaptation require chloroplast thylakoid protein kinase STN7. Nature *433*, 892–895.
24. Ben-Shem, A., Frolow, F., and Nelson, N. (2003). Crystal structure of plant photosystem I. Nature *426*, 630–635.
25. Bennett, J. (1977). Phosphorylation of chloroplast membrane polypeptides. Nature *269*, 344– 346.
26. Bennett, J. (1979). Chloroplast phosphoproteins. The protein kinase of thylakoid membranes is light-dependent. FEBS Lett. *103*, 342–344.
27. Bennett, J., Steinback, K.E., and Arntzen, C.J. (1980). Chloroplast phosphoproteins: regulation of excitation energy transfer by phosphorylation of thylakoid membrane polypeptides. Proc. Natl. Acad. Sci. U.S.A. *77*, 5253–5257.

28. Bennett, J., Shaw, E.K., and Michel, H. (1988). Cytochrome b6f complex is required for phosphorylation of light-harvesting chlorophyll a/b complex II in chloroplast photosynthetic membranes. Eur. J. Biochem. *171*, 95–100.
29. Bennett, J. (1991). Protein Phosphorylation in Green Plant Chloroplasts. Annu. Rev. Plant. Physiol. Plant. Mol. Biol. *42*, 281–311.
30. Bergantino, E., Segalla, A., Brunetta, A., Teardo, E., Rigoni, F., Giacometti, G.M., and Szabò, I. (2003). Light- and pH-dependent structural changes in the PsbS subunit of photosystem II. Proceedings of the National Academy of Sciences *100*, 15265 – 15270.
31. Besford, R.T. (1986). Changes in some Calvin Cycle Enzymes of the Tomato during Acclimation to Irradiance. Journal of Experimental Botany *37*, 200 –210.
32. Betterle, N., Ballottari, M., Zorzan, S., de Bianchi, S., Cazzaniga, S., Dall'osto, L., Morosinotto, T., and Bassi, R. (2009). Light-induced dissociation of an antenna hetero-oligomer is needed for non-photochemical quenching induction. J. Biol. Chem. *284*, 15255–15266.
33. Bilger, W., and Björkman, O. (1990). Role of the xanthophyll cycle in photoprotection elucidated by measurements of light-induced absorbance changes, fluorescence and photosynthesis in leaves of Hedera canariensis. Photosynthesis Research *25*, 173–185.
34. Björkman, O. and Demmig, B. (1987) Photon yield of O2 evolution and chlorophyll fluorescence characteristics at 77 K among vascular plants of diverse origins. Planta 170, 489-504.
35. Bode, S., Quentmeier, C.C., Liao, P.-N., Hafi, N., Barros, T., Wilk, L., Bittner, F., and Walla, P.J. (2009). On the regulation of photosynthesis by excitonic interactions between carotenoids and chlorophylls. Proceedings of the National Academy of Sciences *106*, 12311 –12316.
36. Bonaventura, C., and Myers, J. (1969). Fluorescence and oxygen evolution from Chlorella pyrenoidosa. Biochimica Et Biophysica Acta (BBA) - Bioenergetics *189*, 366–383.
37. Bonente, G., Ballottari, M., Truong, T.B., Morosinotto, T., Ahn, T.K., Fleming, G.R., Niyogi, K.K., and Bassi, R. (2011). Analysis of LhcSR3, a protein essential for feedback de- excitation in the green alga Chlamydomonas reinhardtii. PLoS Biol. *9*, e1000577.
38. Bowler, C., Montagu, M.V., and Inze, D. (1992). Superoxide Dismutase and Stress Tolerance. Annu. Rev. Plant. Physiol. Plant. Mol. Biol. *43*, 83–116.
39. Bratt, C.E., Arvidsson, P.-O., Carlsson, M., and Åkerlund, H.-E. (1995). Regulation of violaxanthin de-epoxidase activity by pH and ascorbate concentration. Photosynthesis Research *45*, 169–175.
40. Briantais, J.M., Vernotte, C., Picaud, M., and Krause, G.H. (1979). A quantitative study of the slow decline of chlorophyll a fluorescence in isolated chloroplasts. Biochim. Biophys. Acta *548*, 128–138.
41. Brugnoli, E., and Björkman, O. (1992). Chloroplast movements in leaves: Influence on chlorophyll fluorescence and measurements of light-induced absorbance changes related to ΔpH and zeaxanthin formation. Photosynthesis Research *32*, 23–35.
42. Brugnoli, E., Cona, A., and Lauteri, M. (1994). Xanthophyll cycle components and capacity f or non-radiative energy dissipation in sun and shade leaves of*Ligustrum*

ovalifolium exposed to conditions limiting photosynthesis. Photosynthesis Research *41*, 451–463.
43. Chow, W.S., Telfer, A., Chapman, D.J., and Barber, J. (1981). State 1-state 2 transition in leaves and its association with ATP-induced chlorophyll fluorescence quenching. Biochimica Et Biophysica Acta (BBA) - Bioenergetics *638*, 60–68.
44. Chow, W., and Anderson, J. (1987). Photosynthetic Responses of Pisum sativum to an Increase in Irradiance During Growth. II. Thylakoid Membrane Components. Functional Plant Biol. *14*, 9–19.
45. Cleland, R.E., and Melis, A. (1987). Probing the events of photoinhibition by altering electron- transport activity and light-harvesting capacity in chloroplast thylakoids. Plant, Cell & Environment *10*, 747–752.
46. Conklin, P.L., Williams, E.H., and Last, R.L. (1996). Environmental stress sensitivity of an ascorbic acid-deficient Arabidopsis mutant. Proceedings of the National Academy of Sciences *93*, 9970 –9974.
47. Crouchman, S., Ruban, A., and Horton, P. (2006). PsbS enhances nonphotochemical fluorescence quenching in the absence of zeaxanthin. FEBS Letters *580*, 2053–2058.
48. Dall'Osto, L., Caffarri, S., and Bassi, R. (2005). A Mechanism of Nonphotochemical Energy Dissipation, Independent from PsbS, Revealed by a Conformational Change in the Antenna Protein CP26. The Plant Cell Online *17*, 1217 –1232.
49. Dall'Osto, L., Cazzaniga, S., Havaux, M., and Bassi, R. (2010). Enhanced Photoprotection by Protein-Bound vs Free Xanthophyll Pools: A Comparative Analysis of Chlorophyll b and Xanthophyll Biosynthesis Mutants. Molecular Plant.
50. Dau, H. (1994). Molecular Mechanisms and Qquantitative Models of Variable Photosystem II Fluorescence. Photochemistry and Photobiology *60*, 1–23.
51. Deisenhofer, J., Epp, O., Miki, K., Huber, R., and Michel, H. (1985). Structure of the protein subunits in the photosynthetic reaction centre of Rhodopseudomonas viridis at 3[angst] resolution. Nature *318*, 618–624.
52. Delosme, R., Olive, J., and Wollman, F.-A. (1996). Changes in light energy distribution upon state transitions: an *in vivo* photoacoustic study of the wild type and photosynthesis mutants from Chlamydomonas reinhardtii. Biochimica Et Biophysica Acta (BBA) - Bioenergetics *1273*, 150–158.
53. Demeter, S., Neale, P.J., and Melis, A. (1987). Photoinhibition: Impairment of the primary charge separation between P-680 and pheophytin in photosystem II of chloroplasts. FEBS Letters *214*, 370–374.
54. Demmig, B., Winter, K., Krüger, A., and Czygan, F.C. (1987). Photoinhibition and zeaxanthin formation in intact leaves : a possible role of the xanthophyll cycle in the dissipation of excess light energy. Plant Physiol. *84*, 218–224.
55. Demmig, B., and Björkman, O. (1987). Comparison of the effect of excessive light on chlorophyll fluorescence (77K) and photon yield of O_2 evolution in leaves of higher plants. Planta *171*, 171–184.
56. Demmig-Adams, B. (1990). Carotenoids and photoprotection in plants: A role for the xanthophyll zeaxanthin. Biochimica Et Biophysica Acta (BBA) - Bioenergetics *1020*, 1–24.
57. Demmig-Adams, B., and Adams, W.I. (1994). Capacity for Energy Dissipation in the Pigment Bed in Leaves With Different Xanthophyll Cycle Pools. Functional Plant Biol. *21*, 575–588.

58. Demmig-Adams, B., Adams III, W.W., Barker, D.H., Logan, B.A., Bowling, D.R., and Verhoeven, A.S. (1996). Using chlorophyll fluorescence to assess the fraction of absorbed light allocated to thermal dissipation of excess excitation. Physiologia Plantarum *98*, 253– 264.
59. Demmig-Adams, B., Moeller, D.L., Logan, B.A., and Adams III, W.W. (1998). Positive correlation between levels of retained zeaxanthin + antheraxanthin and degree of photoinhibition in shade leaves of *Schefflera arboricola* (Hayata) Merrill. Planta *205*, 367– 374.
60. Dominici, P., Caffarri, S., Armenante, F., Ceoldo, S., Crimi, M., and Bassi, R. (2002). Biochemical Properties of the PsbS Subunit of Photosystem II Either Purified from Chloroplast or Recombinant. Journal of Biological Chemistry *277*, 22750 –22758.
61. Dreuw, A., Fleming, G.R., and Head-Gordon, M. (2003). Charge-Transfer State as a Possible Signature of a Zeaxanthin−Chlorophyll Dimer in the Non-photochemical Quenching Process in Green Plants. J. Phys. Chem. B *107*, 6500–6503.
62. Duysens, L. N. M., Sweers, H. E. (1963) Mechanism of two photochemical reactions in algae as studied by means of fluorescence. Studies on Microalgae and Photosynthetic Bacteria. pp. 353–372.
63. Emerson, R. (1935). The Effect of Intense Light on the Assimilatory Mechanism of Green Plants and its Bearing on the Carbon Dioxide Factor. Cold Spring Harbor Symposia on Quantitative Biology *3*, 128 –137.
64. Fleischmann, M.M., Ravanel, S., Delosme, R., Olive, J., Zito, F., Wollman, F.-A., and Rochaix, J.-D. (1999). Isolation and Characterization of Photoautotrophic Mutants of Chlamydomonas reinhardtii Deficient in State Transition. Journal of Biological Chemistry *274*, 30987 –30994.
65. Foote, C.S. (1976). Photosensitized oxidation and singlet oxygen: consequences in biological systems. Free Radicals in Biology, 2:85–133.
66. Foyer, C.H., and Halliwell, B. (1976). The presence of glutathione and glutathione reductase in chloroplasts: A proposed role in ascorbic acid metabolism. Planta *133*, 21–25.
67. Frank, H., Cua, A., Chynwat, V., Young, A., Gosztola, D., and Wasielewski, M. (1994). Photophysics of the carotenoids associated with the xanthophyll cycle in photosynthesis. Photosynthesis Research *41*, 389–395.
68. Frank, H.A., Bautista, J.A., Josue, J.S., and Young, A.J. (2000). Mechanism of Nonphotochemical Quenching in Green Plants: Energies of the Lowest Excited Singlet States of Violaxanthin and Zeaxanthin. Biochemistry *39*, 2831–2837.
69. Frenkel, M., Bellafiore, S., Rochaix, J.-D., and Jansson, S. (2007). Hierarchy amongst photosynthetic acclimation responses for plant fitness. Physiologia Plantarum *129*, 455–459.
70. Fryer, M..J. (1992). The antioxidant effects of thylakoid Vitamin E (α-tocopherol). Plant, Cell & Environment *15*, 381–392.
71. Funk, C., Schroeder, W.P., Napiwotzki, A., Tjus, S.E., Renger, G., and Andersson, B. (1995). The PSII-S Protein of Higher Plants: A New Type of Pigment-Binding Protein. Biochemistry *34*, 11133–11141.
72. Genty, B., Briantais, J. and Baker, N.R. (1989) The relationship between the quantum yield of photosynthetic electron transport and quenching of chlorophyll fluorescence. Biochim. Biophys. Acta 990, 87-92.

73. Gerotto, C., Alboresi, A., Giacometti, G.M., Bassi, R., and Morosinotto, T. (2011). Role of PSBS and LHCSR in Physcomitrella patens acclimation to high light and low temperature. Plant Cell Environ. *34*, 922–932.
74. Gilmore, A.M., and Björkman, O. (1995). Temperature-sensitive coupling and uncoupling of ATPase-mediated, nonradiative energy dissipation: Similarities between chloroplasts and leaves. Planta *197*, 646–654.
75. Gilmore, A.M., and Ball, M.C. (2000). Protection and storage of chlorophyll in overwintering evergreens. Proceedings of the National Academy of Sciences *97*, 11098 –11101.
76. Gisselsson, A., Szilágyi, A., and Åkerlund, H.-E. (2004). Role of histidines in the binding of violaxanthin de-epoxidase to the thylakoid membrane as studied by site-directed mutagenesis. Physiologia Plantarum *122*, 337–343.
77. Goedheer, J.C. (1959). Energy transfer between carotenoids and bacteriochlorophyll in chromatophores of purple bacteria. Biochimica Et Biophysica Acta *35*, 1–8.
78. Graßes, T., Pesaresi, P., Schiavon, F., Varotto, C., Salamini, F., Jahns, P., and Leister, D. (2002). The role of ΔpH-dependent dissipation of excitation energy in protecting photosystem II against light-induced damage in Arabidopsis thaliana. Plant Physiology and Biochemistry *40*, 41–49.
79. Greer, D.H., Berry, J.A., and Björkman, O. (1986). Photoinhibition of photosynthesis in intact bean leaves: role of light and temperature, and requirement for chloroplast-protein synthesis during recovery. Planta *168*, 253–260.
80. Hager, A. (1969). Lichtbedingte pH-Erniedrigung in einem Chloroplasten-Kompartiment als Ursache der enzymatischen Violaxanthin-→ Zeaxanthin-Umwandlung; Beziehungen zur Photophosphorylierung. Planta *89*, 224–243.
81. Hager, A., and Holocher, K. (1994). Localization of the xanthophyll-cycle enzyme violaxanthin de-epoxidase within the thylakoid lumen and abolition of its mobility by a (light-dependent) pH decrease. Planta *192*, 581–589.
82. Hammer, M.F., Markwell, J., and Sarath, G. (1997). Purification of a protein phosphatase from chloroplast stroma capable of dephosphorylating the light-harvesting complex-II. Plant Physiol. *113*, 227–233.
83. Hauska, G.A., and Prince, R.C. (1974). Lipophilicity and catalysis of photophosphorylation Artificial proton translocation by lipophilic, quinoid hydrogen carriers in chloroplasts and liposomes. FEBS Letters *41*, 35–39.
84. Havaux, M., and Niyogi, K.K. (1999). The violaxanthin cycle protects plants from photooxidative damage by more than one mechanism. Proceedings of the National Academy of Sciences *96*, 8762 –8767.
85. Heber, U., and Walker, D. (1992). Concerning a Dual Function of Coupled Cyclic Electron Transport in Leaves. Plant Physiology *100*, 1621 –1626.
86. Hieber, D., Bugos, R., Verhoeven, A., and Yamamoto, H. (2002). Overexpression of violaxanthin de-epoxidase: properties of C-terminal deletions on activity and pH-dependent lipid binding. Planta *214*, 476–483.
87. Holt, N.E., Fleming, G.R., and Niyogi, K.K. (2004). Toward an Understanding of the Mechanism of Nonphotochemical Quenching in Green Plants. Biochemistry *43*, 8281–8289.
88. Holt, N.E., Zigmantas, D., Valkunas, L., Li, X.-P., Niyogi, K.K., and Fleming, G.R. (2005). Carotenoid Cation Formation and the Regulation of Photosynthetic Light

Harvesting. Science *307*, 433 –436.
89. Holzwarth, A.R., Miloslavina, Y., Nilkens, M., and Jahns, P. (2009). Identification of two quenching sites active in the regulation of photosynthetic light-harvesting studied by time- resolved fluorescence. Chemical Physics Letters *483*, 262–267.
90. Horton, P., and Black, M.T. (1981). Light-dependent quenching of chlorophyll fluorescence in pea chloroplasts induced by adenosine 5'-triphosphate. Biochim. Biophys. Acta *635*, 53–62.
91. Horton, P., Ruban, A.V., Rees, D., Pascal, A.A., Noctor, G., and Young, A.J. (1991). Control of the light-harvesting function of chloroplast membranes by aggregation of the LHCII chlorophyll—protein complex. FEBS Letters *292*, 1–4.
92. Horton, P., Ruban, A.V., and Walters, R.G. (1996). Regulation of Light Harvesting in Green Plants. Annu. Rev. Plant. Physiol. Plant. Mol. Biol. *47*, 655–684.
93. Horton, P., Johnson, M.P., Perez-Bueno, M.L., Kiss, A.Z., and Ruban, A.V. (2008). Photosynthetic acclimation: Does the dynamic structure and macro-organisation of photosystem II in higher plant grana membranes regulate light harvesting states? FEBS Journal *275*, 1069–1079.
94. Hou, C.-X., Pursiheimo, S., Rintamäki, E., and Aro, E.-M. (2002). Environmental and metabolic control of LHCII protein phosphorylation: revealing the mechanisms for dual regulation of the LHCII kinase. Plant, Cell & Environment *25*, 1515–1525.
95. Huner, N., Öquist, G., Hurry, V., Krol, M., Falk, S., and Griffith, M. (1993). Photosynthesis, photoinhibition and low temperature acclimation in cold tolerant plants. Photosynthesis Research *37*, 19–39.
96. Huner, N.P.A., Ivanov, A.G., Sane, P.V., Pocock, T., Król, M., Balseris, A., Rosso, D., Savitch, L.V., Hurry, V.M., and Öquist, G. (2006). Photoprotection of Photosystem II: Reaction Center Quenching Versus Antenna Quenching. Photoprotection, Photoinhibition, Gene Regulation, and Environment. pp. 155–173.
97. Iwai, M., Yokono, M., Inada, N., and Minagawa, J. (2010). Live-cell imaging of photosystem II antenna dissociation during state transitions. Proceedings of the National Academy of Sciences *107*, 2337 –2342.
98. Jahns, P., Wehner, A., Paulsen, H., and Hobe, S. (2001). De-epoxidation of Violaxanthin after Reconstitution into Different Carotenoid Binding Sites of Light-harvesting Complex II. Journal of Biological Chemistry *276*, 22154 –22159.
99. Jahns, P., and Holzwarth, A.R. (2012). The role of the xanthophyll cycle and of lutein in photoprotection of photosystem II. Biochim. Biophys. Acta *1817*, 182–193.
100. Jansson, S. (1999). A guide to the Lhc genes and their relatives in Arabidopsis. Trends Plant Sci. *4*, 236–240.
101. Jensen, P.E., Haldrup, A., Zhang, S., and Scheller, H.V. (2004). The PSI-O Subunit of Plant Photosystem I Is Involved in Balancing the Excitation Pressure between the Two Photosystems. Journal of Biological Chemistry *279*, 24212 –24217.
102. Johnson, M.P., Davison, P.A., Ruban, A.V., and Horton, P. (2008). The xanthophyll cycle pool size controls the kinetics of non-photochemical quenching in Arabidopsis thaliana. FEBS Letters *582*, 262–266.
103. Johnson, M.P., and Ruban, A.V. (2009). Photoprotective Energy Dissipation in Higher Plants Involves Alteration of the Excited State Energy of the Emitting Chlorophyll(s) in the Light Harvesting Antenna II (LHCII). Journal of Biological Chemistry 284, 23592 –23601.

104. Johnson, M.P., and Ruban, A.V. (2011). Restoration of Rapidly Reversible Photoprotective Energy Dissipation in the Absence of PsbS Protein by Enhanced ΔpH. Journal of Biological Chemistry 286, 19973 –19981.
105. Johnson, M.P., Goral, T.K., Duffy, C.D.P., Brain, A.P.R., Mullineaux, C.W., and Ruban, A.V. (2011). Photoprotective Energy Dissipation Involves the Reorganization of Photosystem II Light-Harvesting Complexes in the Grana Membranes of Spinach Chloroplasts. The Plant Cell 23, 1468 –1479.
106. Johnson, M., Zia, A., and Ruban, A. (2012). Elevated ΔpH restores rapidly reversible photoprotective energy dissipation in *Arabidopsis* chloroplasts deficient in lutein and xanthophyll cycle activity. Planta *235*, 193–204.
107. Jung, H.-S., and Niyogi, K.K. (2009). Quantitative Genetic Analysis of Thermal Dissipation in Arabidopsis. Plant Physiology *150*, 977 –986.
108. Kamiya, N., and Shen, J.-R. (2003). Crystal structure of oxygen-evolving photosystem II from Thermosynechococcus vulcanus at 3.7-Å resolution. Proceedings of the National Academy of Sciences *100*, 98 –103.
109. Kanazawa, A., and Kramer, D.M. (2002). *In vivo* modulation of nonphotochemical exciton quenching (NPQ) by regulation of the chloroplast ATP synthase. Proceedings of the National Academy of Sciences *99*, 12789 –12794.
110. Kao, W.Y., and Forseth, I.N. (1992). Dirunal leaf movement, chlorophyll fluorescence and carbon assimilation in soybean grown under different nitrogen and water availabilities. Plant, Cell & Environment *15*, 703–710.
111. Kapri-Pardes, E., Naveh, L., and Adam, Z. (2007). The Thylakoid Lumen Protease Deg1 Is Involved in the Repair of Photosystem II from Photoinhibition in Arabidopsis. The Plant Cell Online *19*, 1039 –1047.
112. Karukstis, K.K., and Sauer, K. (1983). Fluorescence decay kinetics of chlorophyll in photosynthetic membranes. J. Cell. Biochem. *23*, 131–158.
113. Kasahara, M., Kagawa, T., Oikawa, K., Suetsugu, N., Miyao, M., and Wada, M. (2002). Chloroplast avoidance movement reduces photodamage in plants. Nature *420*, 829–832.
114. Kautsky H, Apel W, Amann H. (1960) Chlorophyllfluoreszenz und kohlensäureassimilation. XIII. Die fluoreszenkurve und die photochemie der pflanze. Biochem. Zeit. 322, 277–292
115. Kawano, M., and Kuwabara, T. (2000). pH-dependent reversible inhibition of violaxanthin de- epoxidase by pepstatin related to protonation-induced structural change of the enzyme. FEBS Letters *481*, 101–104.
116. Kerfeld, C.A., and Kirilovsky, D. (2011). Photoprotection in Cyanobacteria: The Orange Carotenoid Protein and Energy Dissipation. Bioenergetic Processes of Cyanobacteria. pp. 395–421.
117. Kok, B. (1956). On the inhibition of photosynthesis by intense light. Biochimica Et Biophysica Acta *21*, 234–244.
118. Komenda, J., Knoppová, J., Krynická, V., Nixon, P.J., and Tichý, M. (2010). Role of FtsH2 in the repair of Photosystem II in mutants of the cyanobacterium Synechocystis PCC 6803 with impaired assembly or stability of the CaMn(4) cluster. Biochim. Biophys. Acta *1797*, 566–575.
119. Kühlbrandt, W., and Wang, D.N. (1991). Three-dimensional structure of plant light-harvesting complex determined by electron crystallography. Nature *350*, 130–134.

120. Külheim, C., Ågren, J., and Jansson, S. (2002). Rapid Regulation of Light Harvesting and Plant Fitness in the Field. Science *297*, 91 –93.
121. Kyle, D.J., Ohad, I., and Arntzen, C.J. (1984). Membrane protein damage and repair: Selective loss of a quinone-protein function in chloroplast membranes. Proceedings of the National Academy of Sciences *81*, 4070 –4074.
122. Lambrev, P.H., Nilkens, M., Miloslavina, Y., Jahns, P., and Holzwarth, A.R. (2010). Kinetic and Spectral Resolution of Multiple Nonphotochemical Quenching Components in Arabidopsis Leaves. Plant Physiology *152*, 1611 –1624.
123. Lemeille, S., Willig, A., Depège-Fargeix, N., Delessert, C., Bassi, R., and Rochaix, J.-D. (2009). Analysis of the Chloroplast Protein Kinase Stt7 during State Transitions. PLoS Biol *7*, e1000045.
124. Li, X.-P., Bjorkman, O., Shih, C., Grossman, A.R., Rosenquist, M., Jansson, S., and Niyogi, K.K. (2000). A pigment-binding protein essential for regulation of photosynthetic light harvesting. Nature *403*, 391–395.
125. Li, X.-P., Phippard, A., Pasari, J., and Niyogi, K.K. (2002). Structure–function analysis of photosystem II subunit S (PsbS) *in vivo*. Functional Plant Biol. *29*, 1131–1139.
126. Li, X.-P., Gilmore, A.M., Caffarri, S., Bassi, R., Golan, T., Kramer, D., and Niyogi, K.K. (2004). Regulation of Photosynthetic Light Harvesting Involves Intrathylakoid Lumen pH Sensing by the PsbS Protein. Journal of Biological Chemistry *279*, 22866 –22874.
127. Li, Z., Ahn, T.K., Avenson, T.J., Ballottari, M., Cruz, J.A., Kramer, D.M., Bassi, R., Fleming, G.R., Keasling, J.D., and Niyogi, K.K. (2009). Lutein Accumulation in the Absence of Zeaxanthin Restores Nonphotochemical Quenching in the Arabidopsis thaliana npq1 Mutant. The Plant Cell Online *21*, 1798 –1812.
128. Liao, P.-N., Bode, S., Wilk, L., Hafi, N., and Walla, P.J. (2010a). Correlation of electronic carotenoid–chlorophyll interactions and fluorescence quenching with the aggregation of native LHC II and chlorophyll deficient mutants. Chemical Physics *373*, 50–55.
129. Liao, P.-N., Holleboom, C.-P., Wilk, L., Kühlbrandt, W., and Walla, P.J. (2010b). Correlation of Car S1 → Chl with Chl → Car S1 Energy Transfer Supports the Excitonic Model in Quenched Light Harvesting Complex II. J. Phys. Chem. B *114*, 15650–15655.
130. Liao, P.-N., Pillai, S., Kloz, M., Gust, D., Moore, A., Moore, T., Kennis, J., van Grondelle, R., and Walla, P. (2012). On the role of excitonic interactions in carotenoid–phthalocyanine dyads and implications for photosynthetic regulation. Photosynthesis Research *111*, 237–243.
131. Lindahl, M., Yang, D.-H., and Andersson, B. (1995). Regulatory Proteolysis of the Major Light- Harvesting Chlorophyll a/b Protein of Photosystem II by a Light-Induced Membrane- Associated Enzymic System. European Journal of Biochemistry *231*, 503–509.
132. Liu, Z., Yan, H., Wang, K., Kuang, T., Zhang, J., Gui, L., An, X., and Chang, W. (2004). Crystal structure of spinach major light-harvesting complex at 2.72[thinsp]A resolution. Nature *428*, 287–292.
133. Lokstein, H., Tian, L., Polle, J.E.W., and DellaPenna, D. (2002). Xanthophyll biosynthetic mutants of Arabidopsis thaliana: altered nonphotochemical quenching of chlorophyll fluorescence is due to changes in Photosystem II antenna size and stability. Biochimica Et Biophysica Acta (BBA) - Bioenergetics *1553*, 309–319.

134. Lu, Y., Hall, D.A., and Last, R.L. (2011). A Small Zinc Finger Thylakoid Protein Plays a Role in Maintenance of Photosystem II in Arabidopsis thaliana. The Plant Cell Online *23*, 1861 – 1875.
135. Lunde, C., Jensen, P.E., Haldrup, A., Knoetzel, J., and Scheller, H.V. (2000). The PSI-H subunit of photosystem I is essential for state transitions in plant photosynthesis. Nature 408, 613–615.
136. Lunde, C., Jensen, P.E., Rosgaard, L., Haldrup, A., Gilpin, M.J., and Scheller, H.V. (2003). Plants Impaired in State Transitions Can to a Large Degree Compensate for their Defect. Plant and Cell Physiology *44*, 44 –54.
137. Ma, Y.-Z., Holt, N.E., Li, X.-P., Niyogi, K.K., and Fleming, G.R. (2003). Evidence for direct carotenoid involvement in the regulation of photosynthetic light harvesting. Proceedings of the National Academy of Sciences *100*, 4377 –4382.
138. Mehler, A.H. (1951). Studies on reactions of illuminated chloroplasts: I. Mechanism of the reduction of oxygen and other hill reagents. Archives of Biochemistry and Biophysics *33*, 65–77.
139. Melis, A. (1991). Dynamics of photosynthetic membrane composition and function. Biochimica Et Biophysica Acta (BBA) - Bioenergetics *1058*, 87–106.
140. Melis, A. (1999). Photosystem-II damage and repair cycle in chloroplasts: what modulates the rate of photodamage *in vivo*? Trends in Plant Science *4*, 130–135.
141. Miloslavina, Y., Wehner, A., Lambrev, P.H., Wientjes, E., Reus, M., Garab, G., Croce, R., and Holzwarth, A.R. (2008). Far-red fluorescence: A direct spectroscopic marker for LHCII oligomer formation in non-photochemical quenching. FEBS Letters *582*, 3625–3631.
142. Minagawa, J. (2011). State transitions—The molecular remodeling of photosynthetic supercomplexes that controls energy flow in the chloroplast. Biochimica Et Biophysica Acta (BBA) - Bioenergetics *1807*, 897–905.
143. Miyake, C., Miyata, M., Shinzaki, Y., and Tomizawa, K. (2005). CO2 Response of Cyclic Electron Flow around PSI (CEF-PSI) in Tobacco Leaves—Relative Electron fluxes through PSI and PSII Determine the Magnitude of Non-photochemical Quenching (NPQ) of Chl Fluorescence. Plant and Cell Physiology *46*, 629 –637.
144. Müller, M.G., Lambrev, P., Reus, M., Wientjes, E., Croce, R., and Holzwarth, A.R. (2010). Singlet Energy Dissipation in the Photosystem II Light-Harvesting Complex Does Not Involve Energy Transfer to Carotenoids. ChemPhysChem *11*, 1289–1296.
145. Murata, N. (1969). Control of excitation transfer in photosynthesis I. Light-induced change of chlorophyll a fluoresence in Porphyridium cruentum. Biochimica Et Biophysica Acta (BBA) - Bioenergetics *172*, 242–251.
146. Murchie, E.H., and Niyogi, K.K. (2011). Manipulation of Photoprotection to Improve Plant Photosynthesis. Plant Physiology *155*, 86 –92.
147. Nakano, Y., and Asada, K. (1980). Spinach chloroplasts scavenge hydrogen peroxide on illumination. Plant and Cell Physiology *21*, 1295 –1307.
148. Nakano, Y., and Asada, K. (1981). Hydrogen Peroxide is Scavenged by Ascorbate-specific Peroxidase in Spinach Chloroplasts. Plant and Cell Physiology *22*, 867 –880.
149. Nilkens, M., Kress, E., Lambrev, P., Miloslavina, Y., Müller, M., Holzwarth, A.R., and Jahns, P. (2010). Identification of a slowly inducible zeaxanthin-dependent component of non- photochemical quenching of chlorophyll fluorescence generated under steady-state conditions in Arabidopsis. Biochimica Et Biophysica Acta (BBA)

- Bioenergetics *1797*, 466–475.
150. Niyogi, K.K., Grossman, A.R., and Björkman, O. (1998). Arabidopsis Mutants Define a Central Role for the Xanthophyll Cycle in the Regulation of Photosynthetic Energy Conversion. The Plant Cell Online *10*, 1121 –1134.
151. Niyogi, K.K. (1999). Photoprotection Revisited: Genetic and Molecular Approaches. Annu. Rev. Plant. Physiol. Plant. Mol. Biol. *50*, 333–359.
152. Nixon, P.J., Barker, M., Boehm, M., de Vries, R., and Komenda, J. (2005). FtsH-mediated repair of the photosystem II complex in response to light stress. Journal of Experimental Botany *56*, 357 –363.
153. Ohad, I., Kyle, D.J., and Arntzen, C.J. (1984). Membrane protein damage and repair: removal and replacement of inactivated 32-kilodalton polypeptides in chloroplast membranes. The Journal of Cell Biology *99*, 481 –485.
154. Öquist, G., and Huner, N.P.A. (2003). Photosynthesis of Overwintering Evergreen Plants. Annu. Rev. Plant Biol. *54*, 329–355.
155. Osmond, C.B., Ramus, J., Levavasseur, G., Franklin, L.A., and Henley, W.J. (1993). Fluorescence quenching during photosynthesis and photoinhibition of Ulva rotundata blid. Planta 190, 97–106.
156. Osmond CB (1994) What is photoinhibition? Some insights from comparisons of shade and sun plants. Photoinhibition of Photosynthesis from Molecular Mechanisms to the Field. Pp 1– 24.
157. Ottander, C., Campbell, D., and Öquist, G. (1995). Seasonal changes in photosystem II organisation and pigment composition in *Pinus sylvestris*. Planta *197*, 176–183.
158. Owens, T,G. (1994). Excitation energy transfer between chlorophylls and carotenoids. A proposed molecular mechanism for non-photochemical quenching. Photoinhibition of Photosynthesis: From Molecular Mechanisms to the Field. pp 95-109
159. Owens, T.G. (2004). Processing of excitation energy by antenna pigments. Photosynthesis and the Environment. pp. 1–23.
160. Park, Y.I., Chow, W.S., and Anderson, J.M. (1996). Chloroplast Movement in the Shade Plant Tradescantia albiflora Helps Protect Photosystem II against Light Stress. Plant Physiology *111*, 867 –875.
161. Park, S., Khamai, P., Garcia-Cerdan, J.G., and Melis, A. (2007). REP27, a tetratricopeptide repeat nuclear-encoded and chloroplast-localized protein, functions in D1/32-kD reaction center protein turnover and photosystem II repair from photodamage. Plant Physiol. *143*, 1547–1560.
162. Pastenes, C., Pimentel, P., and Lillo, J. (2005). Leaf movements and photoinhibition in relation to water stress in field-grown beans. Journal of Experimental Botany *56*, 425 –433.
163. Peers, G., Truong, T.B., Ostendorf, E., Busch, A., Elrad, D., Grossman, A.R., Hippler, M., and Niyogi, K.K. (2009). An ancient light-harvesting protein is critical for the regulation of algal photosynthesis. Nature *462*, 518–521.
164. Pesaresi, P., Sandonà, D., Giuffra, E., and Bassi, R. (1997). A single point mutation (E166Q) prevents dicyclohexylcarbodiimide binding to the photosystem II subunit CP29. FEBS Letters *402*, 151–156.
165. Peter, G.F., and Thornber, J.P. (1991). Biochemical composition and organization of higher plant photosystem II light-harvesting pigment-proteins. J. Biol. Chem. *266*, 16745–16754.

166. Phillip, D., Ruban, A.V., Horton, P., Asato, A., and Young, A.J. (1996). Quenching of chlorophyll fluorescence in the major light-harvesting complex of photosystem II: a systematic study of the effect of carotenoid structure. Proceedings of the National Academy of Sciences *93*, 1492 –1497.
167. Pichersky, E., and Jansson, S. (2004).Structure, protein and pigment composition of LHC II, LHC I and other CAB species. Oxygenic Photosynthesis: The Light Reactions. pp. 507– 521.
168. Powles, S.B. (1984). Photoinhibition of Photosynthesis Induced by Visible Light. Annu. Rev. Plant. Physiol. *35*, 15–44.
169. Pribil, M., Pesaresi, P., Hertle, A., Barbato, R., and Leister, D. (2010). Role of Plastid Protein Phosphatase TAP38 in LHCII Dephosphorylation and Thylakoid Electron Flow. PLoS Biol *8*, e1000288.
170. Reinhold, C., Niczyporuk, S., Beran, K.C., and Jahns, P. (2008). Short-term down-regulation of zeaxanthin epoxidation in Arabidopsis thaliana in response to photo-oxidative stress conditions. Biochimica Et Biophysica Acta (BBA) - Bioenergetics *1777*, 462–469.
171. Rintamäki, E., Martinsuo, P., Pursiheimo, S., and Aro, E.-M. (2000). Cooperative regulation of light-harvesting complex II phosphorylation via the plastoquinol and ferredoxin-thioredoxin system in chloroplasts. Proceedings of the National Academy of Sciences *97*, 11644 –11649.
172. Roberts, A., Borland, A.M., Maxwell, K., and Griffiths, H. (1998). Ecophysiology of the C3- CAM intermediate Clusia minor L. in Trinidad: seasonal and short-term photosynthetic characteristics of sun and shade leaves. Journal of Experimental Botany *49*, 1563 –1573.
173. Ruban, A.V., and Horton, P. (1992). Mechanism of ΔpH-dependent dissipation of absorbed excitation energy by photosynthetic membranes. I. Spectroscopic analysis of isolated light- harvesting complexes. Biochimica Et Biophysica Acta (BBA) - Bioenergetics 1102, 30–38.
174. Ruban, A.V., Rees, D., Pascal, A.A., and Horton, P. (1992). Mechanism of ΔpH-dependent dissipation of absorbed excitation energy by photosynthetic membranes. II. The relationship between LHCII aggregation *in vitro* and qE in isolated thylakoids. Biochimica Et Biophysica Acta (BBA) - Bioenergetics 1102, 39–44.
175. Ruban, A.V., Young, A.J., and Horton, P. (1996). Dynamic Properties of the Minor Chlorophyll a/b Binding Proteins of Photosystem II, an *in Vitro* Model for Photoprotective Energy Dissipation in the Photosynthetic Membrane of Green Plants. Biochemistry 35, 674–678.
176. Ruban, A.V., Berera, R., Ilioaia, C., van Stokkum, I.H.M., Kennis, J.T.M., Pascal, A.A., van Amerongen, H., Robert, B., Horton, P., and van Grondelle, R. (2007). Identification of a mechanism of photoprotective energy dissipation in higher plants. Nature *450*, 575–578.
177. Ruban, A.V., Johnson, M.P., and Duffy, C.D.P. (2012). The photoprotective molecular switch in the photosystem II antenna. Biochim. Biophys. Acta *1817*, 167–181.
178. Schreiber, U., Schliwa, U. and Bilger, W. (1986) Continuous recording of photochemical and non-photochemical chlorophyll fluorescence quenching with a new type of modulation fluorometer. Photosynth. Res. 10, 51-62.
179. Schreiber, U. (2004) Pulse-Amplitude-Modulation (PAM) fluorometry and saturation

pulse method: an overview, in Chlorophyll a Fluorescence: A Signature of Photosynthesis. pp. 279–319.
180. Schürmann, P., and Buchanan, B.B. (2008). The ferredoxin/thioredoxin system of oxygenic photosynthesis. Antioxid. Redox Signal. *10*, 1235–1274.
181. Shapiguzov, A., Ingelsson, B., Samol, I., Andres, C., Kessler, F., Rochaix, J.-D., Vener, A.V., and Goldschmidt-Clermont, M. (2010). The PPH1 phosphatase is specifically involved in LHCII dephosphorylation and state transitions in Arabidopsis. Proceedings of the National Academy of Sciences *107*, 4782 –4787.
182. Siefermann-Harms, D. (1987). The light-harvesting and protective functions of carotenoids in photosynthetic membranes. Physiologia Plantarum *69*, 561–568.
183. Sirikhachornkit, A., Shin, J.W., Baroli, I., and Niyogi, K.K. (2009). Replacement of α-Tocopherol by β-Tocopherol Enhances Resistance to Photooxidative Stress in a Xanthophyll-Deficient Strain of Chlamydomonas reinhardtii. Eukaryotic Cell *8*, 1648 – 1657.
184. Somersalo, S., and Krause, G.H. (1990). Reversible photoinhibition of unhardened and cold- acclimated spinach leaves at chilling temperatures. Planta *180*, 181–187.
185. Stitt, M., Quick, W.P., Schurr, U., Schulze, E.-D., Rodermel, S.R., and Bogorad, L. (1991). Decreased ribulose-1,5-bisphosphate carboxylase-oxygenase in transgenic tobacco transformed with "antisense" *rbcS*. Planta *183*, 555–566.
186. Sun, G., Bailey, D., Jones, M.W., and Markwell, J. (1989). Chloroplast Thylakoid Protein Phosphatase Is a Membrane Surface-Associated Activity. Plant Physiology *89*, 238 – 243.
187. Takahashi, S., and Badger, M.R. (2011). Photoprotection in plants: a new light on photosystem II damage. Trends in Plant Science *16*, 53–60.
188. Takahashi, H., Iwai, M., Takahashi, Y., and Minagawa, J. (2006). Identification of the mobile light-harvesting complex II polypeptides for state transitions in Chlamydomonas reinhardtii. Proceedings of the National Academy of Sciences of the United States of America *103*, 477 –482.
189. Takizawa, K., Kanazawa, A., and Kramer, D.M. (2008). Depletion of stromal Pi induces high "energy-dependent" antenna exciton quenching (qE) by decreasing proton conductivity at CFO-CF1 ATP synthase. Plant, Cell & Environment *31*, 235–243.
190. Tikkanen, M., Grieco, M., Kangasjärvi, S., and Aro, E.-M. (2010). Thylakoid Protein Phosphorylation in Higher Plant Chloroplasts Optimizes Electron Transfer under Fluctuating Light. Plant Physiology *152*, 723 –735.
191. Tyystjärvi, E., and Aro, E.M. (1996). The rate constant of photoinhibition, measured in lincomycin-treated leaves, is directly proportional to light intensity. Proceedings of the National Academy of Sciences *93*, 2213 –2218.
192. Umena, Y., Kawakami, K., Shen, J.-R., and Kamiya, N. (2011). Crystal structure of oxygen- evolving photosystem II at a resolution of 1.9[thinsp]A. Nature *473*, 55–60.
193. van Wijk, K.J., and van Hasselt, P.R. (1993). Kinetic resolution of different recovery phases of photoinhibited photosystem II in cold-acclimated and non-acclimated spinach leaves. Physiologia Plantarum *87*, 187–198.
194. Verhoeven, A.S., Adams, W.W., and Demmig-Adams, B. (1996). Close relationship between the state of the xanthophyll cycle pigments and photosystem II efficiency during recovery from winter stress. Physiologia Plantarum *96*, 567–576.
195. Verhoeven, A.S., Adams, W.W., and Demmig-Adams, B. (1998). Two forms of sustained

xanthophyll cycle-dependent energy dissipation in overwintering Euonymus kiautschovicus. Plant, Cell & Environment *21*, 893–903.
196. Walters, R.G., and Horton, P. (1994). Acclimation of *Arabidopsis thaliana* to the light environment: Changes in composition of the photosynthetic apparatus. Planta *195*, 248–256.
197. Walters, R.G., Ruban, A.V., and Horton, P. (1994). Higher Plant Light-Harvesting Complexes LHCIIa and LHCIIc are Bound by Dicyclohexylcarbodiimide During Inhibition of Energy Dissipation. European Journal of Biochemistry *226*, 1063–1069.
198. Wehner, A., Grasses, T., and Jahns, P. (2006). De-epoxidation of Violaxanthin in the Minor Antenna Proteins of Photosystem II, LHCB4, LHCB5, and LHCB6. Journal of Biological Chemistry *281*, 21924 –21933.
199. Wollman, F.-A., and Lemaire, C. (1988). Studies on kinase-controlled state transitions in Photosystem II and b6f mutants from Chlamydomonas reinhardtii which lack quinone- binding proteins. Biochimica Et Biophysica Acta (BBA) - Bioenergetics *933*, 85–94.
200. Wraight, C.A., and Crofts, A.R. (1970). Energy-Dependent Quenching of Chlorophyll a Fluorescence in Isolated Chloroplasts. European Journal of Biochemistry *17*, 319–327.
201. Yamamoto, H.Y., and Kamite, L. (1972). The effects of dithiothreitol on violaxanthin de-epoxidation and absorbance changes in the 500-nm region. Biochimica Et Biophysica Acta (BBA) - Bioenergetics 267, 538–543.
202. Yamamoto, H.Y., and Higashi, R.M. (1978). Violaxanthin de-epoxidase: Lipid composition and substrate specificity. Archives of Biochemistry and Biophysics *190*, 514–522.
203. Yamamoto, H.Y., and Bassi, R. (2004). Carotenoids: location and function. Oxygenic Photosynthesis: The Light Reactions. pp. 539–563.
204. Yamamoto, H., Bugos, R., and David Hieber, A. (2004). Biochemistry and Molecular Biology of the Xanthophyll Cycle. The Photochemistry of Carotenoids. pp. 293–303.
205. Yokthongwattana, K., and Melis, A. (2006). Photoinhibition and Recovery in Oxygenic Photosynthesis: Mechanism of a Photosystem II Damage and Repair Cycle. Photoprotection, Photoinhibition, Gene Regulation, and Environment. pp. 175–191.
206. Zarter, C.R., Adams, W.W., 3rd, Ebbert, V., Cuthbertson, D.J., Adamska, I., and Demmig-Adams, B. (2006). Winter down-regulation of intrinsic photosynthetic capacity coupled with up-regulation of Elip-like proteins and persistent energy dissipation in a subalpine forest. New Phytol. *172*, 272–282.
207. Zarter, C.R., Adams, W.W., 3rd, Ebbert, V., Adamska, I., Jansson, S., and Demmig-Adams, B. (2006). Winter acclimation of PsbS and related proteins in the evergreen Arctostaphylos uva-ursi as influenced by altitude and light environment. Plant Cell Environ. *29*, 869–878.
208. Zhang, S., and Scheller, H.V. (2004). Light-harvesting Complex II Binds to Several Small Subunits of Photosystem I. Journal of Biological Chemistry *279*, 3180 –3187.
209. Zito, F., Finazzi, G., Delosme, R., Nitschke, W., Picot, D., and Wollman, F.-A. (1999). The Qo site of cytochrome b6f complexes controls the activation of the LHCII kinase. Embo J *18*, 2961–2969.

Chapter 2

A Conserved Thioredoxin-like/Beta-Propeller Protein in the Thylakoid Lumen Maintains Photosynthetic Efficiency

Summary

The light-harvesting complexes of plants have evolved the ability to switch between efficient light harvesting and quenching forms in order to optimize photosynthesis in response to the environment. Here I describe the isolation and characterization of an *Arabidopsis thaliana* mutant, *soq1*, that increases non-photochemical quenching (NPQ) in the presence or absence of PsbS, which is normally required for feedback de-excitation (qE). The kinetics of NPQ formation and relaxation in this mutant are slower than qE, and its formation is light intensity dependent. Through chemical treatments, crosses to other mutants, and analysis of fluorescence parameters, the NPQ was shown to be independent of the factors that are known to be required for well characterized forms of NPQ. Time-resolved fluorescence showed that the mutation results in a shorter average chlorophyll excited lifetime when leaves are exposed to high light. The *soq1* mutation was mapped to a previously uncharacterized gene that encodes a chloroplast protein containing haloacid dehalogenase-like hydrolase (HAD), thioredoxin-like (Trx-like) and beta-propeller (NHL) domains. In contrast to the Trx-like and NHL domains, the HAD domain is found only in plant homologs and is not required to complement the NPQ phenotype. The protein was localized to the thylakoid membrane with the HAD domain located in the stroma and the Trx-like/NHL domains in the lumen. A role in protein folding or reducing oxidized proteins in order to maintain photosynthetic efficiency is proposed based on the structure and location of the Trx-like domain.

Preface

Kapil Amarnath, Julia Zaks, and Emily Jane Glassman contributed to the work in this chapter by performing time-resolved fluorescence measurements and interpreting the results. Wallace Chan and Kevin Li aided with plant maintenance and assisted with various experiments.

Introduction

Several mutants affecting NPQ have been found through forward genetic screens in plants and algae. Many of these screens looked for mutants that were not able to respond as expected during high light [20,45,56,57,59] or conditions that induce state transitions [24]. Reverse genetics approaches have also been instrumental in the identification of mutants affecting NPQ. Bellafiore *et al.* [6] were able to identify the Arabidopsis protein homolog of the Chlamydomonas Stt7 protein by characterizing T-DNA knockouts of similar proteins found in land plants. The phosphatase involved in state transitions was also identified by two separate groups using reverse genetics to screen chloroplast candidates for mutants that became stuck in

state 2 [61,66]. Using T-DNA and antisense lines of various LHCII proteins, it has been shown that no individual antenna protein is essential for qE [3,35,41]. These mutants have been used extensively to help understand the physiological role and molecular basis of NPQ.

Given the important role NPQ plays in protecting plants from stress and the multiple mechanisms by which it does so, it may seem strange that relatively few proteins have been identified as being required. One reason for this may be redundancy between proteins, as seen with the LHCII mutants. Another explanation is that some proteins and molecules are involved not only in multiple NPQ mechanisms, but also function in light harvesting or electron transport. Mutations in these genes may well be lethal or cause larger effects that mask any NPQ phenotype. Finally, many of the original screens were performed in wild-type backgrounds under standard laboratory growth conditions, resulting in isolation of mutants that affected the pathways that dominated under those conditions. By screening in a zeaxanthi-deficiency mutant background, Li *et al.* [47] were able to identify *szl1* and show that over-accumulation of lutein can partially compensate for the lack of zeaxanthin.

While our understanding of the mechanisms of NPQ have come a long way, without knowing all of the factors involved we we are unable to fully appreciate the complexity behind the processes of energy transfer and quenching within the antenna. This chapter describes the isolation and characterization of mutants affecting a novel protein involved in a slowly reversible type of NPQ in Arabidopsis. This mutant was isolated through a suppressor screen for plants that have rapidly forming NPQ in the absence of PsbS. We show that this additional quenching is unrelated to other forms of NPQ and due to its slow relaxation kinetics is likely prevented under most conditions in order to maintain the efficiency of light harvesting.

Methods

Suppressor Screen and Fluorescence Measurements - Mutagenized *npq4-1 gl1-1, npq4-5, npq4-6* and *npq4-7* [45,46] seeds were spread on 100 mm agar plates, and after two weeks seedlings were screened by chlorophyll fluorescence video imaging as described [56]. The actinic light intensity used was 1,200 µmol photons m^{-2} s^{-1} for 10 minutes. False-colored images were used to select mutants that had a higher level of NPQ, calculated as $(F_m-F_m')/F_m'$, than the *npq4* parent, and those plants were transferred to soil and grown in a 10-hour light and 14-hour dark cycle at 21.5ºC. Video imaging screening for the complementation experiments and crosses was done with the Maxi version of an IMAGING-PAM M-Series (Heinz Walz GmbH , Germany).

Pulse-amplitude-modulated fluorescence measurements were done using an FMS2 (Hansatech Instruments Ltd, UK) after 3-4 weeks as described [7] for the amount of time and at the light intensities indicated in the figure legends. Potential suppressors in the *npq4-5, npq4-6* and *npq4-7* backgrounds from the video imaging screen that were confirmed by PAM were checked for presence of the *npq4* mutation by the derived cleaved amplified polymorphic sequence (dCAPS) assay [55].

For nigericin treatments, leaf punches of 0.5 cm diameter were placed in a syringe with either 100 µM nigericin from a 5 mM stock in ethanol, or mock buffer without the nigericin. Leaf discs were vacuum infiltrated by covering the outlet and pulling back on the plunger gently for 10 seconds and repeated two or three times until fully infiltrated. Leaf discs were dried on cloth and dark-adapted for 20 minutes before fluorescence measurements.

For treatment with dithiothreitol (DTT), leaves were cut off with a sharp razor blade, placed in an microfuge tube with the petiole submerged in a solution of 1 mM DTT and allowed to uptake the solution overnight in very low light (<10 µmol photons m^{-2} s^{-1}). Mock-treated leaves were put in water. Leaves were dark-acclimated for 20 minutes prior to fluorescence measurements.

For lincomycin treatments, leaves were floated (adaxial side up) on a solution of 1 mM lincomycin or water and allowed to uptake the solution overnight in very low light (<10 µmol photons m^{-2} s^{-1}). F_v/F_m measurements were taken after 0, 30, 60 and 90 minutes of high light (1,200 µmol photons m^{-2} s^{-1}) and at 90, 180 1280 and 2710 minutes after being removed from high light and placed at 20 µmol photons m^{-2} s^{-1}. Before each measurement leaves were dark-acclimated for 20 minutes to allow the relaxation of qE.

Crosses and Mapping - The *soq1-1 npq4-1* mutant (strain 6-22) was backcrossed to *npq4-1* twice to remove background mutations. Both *soq1-1 npq4-1* and *soq1-2 npq4-5* (strain 3-94) were also crossed to Col-0 in order to obtain the single mutants. Because *SOQ1* was linked to *NPQ4,* plants homozygous for the *soq1* mutations but heterozygous for *npq4* were obtained initially and then selfed in order to get *soq1-1* and *soq1-2* plants. The *soq1-1* mutant was crossed to Col-0 again in order to remove any remaining background mutations. The *soq1-1* mutant was also used to make *soq1-1 npq1, soq1-1 npq2, soq1-1 stn7* and *soq1-1 stn8* double mutants. As *stn7* was also linked to *soq1*, double mutants were selected in a similar manner as that used for isolating the *soq1-1* single mutant.

For mapping, *soq1-1 npq4-1* was crossed to Landsberg erecta (Ler) and F1 plants were selfed in order to generate a mapping population. To identify mutants, F2 seeds were spread on PN plates and after two to four weeks of growth were screened by fluorescence video imaging. Plants that showed the reduced NPQ relaxation phenotype were transferred to soil and allowed to grow for another two to four weeks before being screened individually using the FMS2 to confirm the mutant phenotype. For rough mapping, bulked segregant analysis was used [51]. DNA was extracted from an initial set of 92 plants and bulked into eight pools of 11 or 12 plants per pool. Using DNA from Col-0 and an F1 plant from *soq1-1* crossed to Ler as controls, PCR was performed on each of the pools using the MapPairs primer sets (Research Genetics, discontinued).

Fine mapping was carried out by screening the individual F2 plants for recombinants between *soq1* and each marker. To narrow the region further, additional primers were made using simple sequence length polymorphisms, cleaved amplified polymorphisms or dCAPs between Ler and Col-0 [34], and an additional 125 mutants from the F2 population were used. Three candidate genes that were in the mapping interval and predicted to be targeted to the chloroplast by TargetP [21] were amplified and sequenced from Col-0 and three *soq1* mutants.

Phylogenetic Trees - Protein sequences for SOQ1 homologs were retrieved from the, Phytozome (http://www.phytozome.net/), National Center for Biotechnology Information (www.ncbi.nlm.nih.gov/) or from the Department of Energy Joint Genome Institute (http://www.jgi.doe.gov/). Alignment was done using PSI-COFFEE (http://tcoffee.crg.cat/) [39,71] and a maximum likelihood tree was generated by PhyML [4,28] and visualized by TreeDyn [12] using the Phylogeney.fr web-program (http://www.phylogeny.fr/) [18,19] .

Complementation - Total RNA was extracted from Col-0 plants using the RNeasy plant mini kit (QIAGEN Inc., USA), and RT-PCR was used to make cDNA using the Omniscript RT kit (QIAGEN Inc., USA). *SOQ1* cDNA was amplified and cloned both with and without the stop codon into the pENTR/D-TOPO vector (Invitrogen, USA). Sequence was cofirmed using the M13 forward and reverse primers as well as gene-specific primers. Entry clones were cut with the *BspHI* restriction enzyme, which cuts the backbone of the vector outside of the recombination regions and prevents transfomation of *E. coli* with the entry vector. The cDNA was then inserted into the pEarleyGate100 (with stop codon) or pEarleyGate103 vectors (without stop codon) by using LR clonase reactions (Invitrogen, USA). *E. coli* DH5-alpha cells were transformed with the LR reaction, and colony PCR using the CaMV 35S promoter primer and a gene-specific primer was used to select positive clones. The vector was then transformed into *Agrobacterium tumefaciens* GV3101 chemically competent cells, and positive clones were selected using LB plates with kanamycin, rifampacin and hygromycin. The floral dip technique [13] was used to transform *soq1-1* plants with the constructs, and transformants were selected by either plating on agar plates containing 10 µg/mL glufosinate ammonium or plating without selection and spraying with a solution containing 0.015% (v/v) Silwet L-77 and 60-fold diluted Finale (Bayer CropScience LP, USA) after germination .

T1 plants were screened by fluorescence video imaging as described. Those plants that displayed both wild-type levels and kinetics of NPQ and were able to grow with herbicide selection were transferred to soil and re-screened using the FMS2. To get stable lines, T1 lines that fully complemented were selfed and propagated through to the T3 generation, in which progeny were then screened to identify homozygous transformants.

For point mutations, tag insertions and domain deletions 'Round-the-Horn' PCR was used [25]. Genomic DNA was extracted from complemented plants and PCR was used to show that they contained the truncated transgene and also had the original *soq1-1* mutation. The FLAG and Strep epitope tags used were DYKDDDDK and WSHPQFEK, respectively.

Recombinant Protein Expression and Antibody Production - SOQ1 cDNA encoding amino acids 58-1055 (without the chloroplast transit peptide) was amplified and cloned into the pET15b His-tag expression vector (Novagen, EMD Biosciences Inc., USA) using the *NdeI* and *BamHI* cut sites. Vector was transformed into *E. coli* ER2566 (New England Biolabs, US), and a 500 mL culture containing 100 µg/mL ampicillin was inoculated from a 10 mL starter culture and incubated at 37ºC with shaking at 250 RPM. When the OD_{600} reached 0.6-0.8, expression was induced by the addition of IPTG to a concentration of 0.5 mM, and the culture was grown overnight at 20ºC with shaking at 250 RPM. On the following day, cells were pelleted by centrifugation at 5,000 g for 20 min at 4ºC and resuspended in 20 mL of 50 mM Tris-HCl, pH 7.8, 500 mM NaCl, 10% glycerol, 10 mM imidazole and 1 mM PMSF. Lysozyme was added to a final concentration 1 mg/mL and incubated on ice for 30 minutes. Cells were lysed by three passes through a French pressure cell at 20,000 lbs/in^2, and insoluble debris was pelleted by centrifugation at 20,000 g for 30 minutes at 4ºC. The soluble fraction was incubated with 3 mL of washed Pro-Bond nickel chelating resin (Invitrogen, USA) for 1 hour at 4ºC with end-over-end mixing. The resin was washed three times with 30 mL of 50 mM Tris-HCl pH 7.8, 500 mM NaCl, 10% glycerol, 30 mM imidazole and 1 mM PMSF to remove unbound proteins. Bound protein was eluted with 12 mL of elution bufer (50 mM Tris-HCl pH 7.8, 500 mM NaCl, 10% glycerol, 500 mM imidzole and 1 mM PMSF) and collected as 1 mL fractions. Fractions containing a significant amount of protein as determined by A_{280} were pooled and run on a 5%

SDS-PAGE gel with a single large well. After staining the gel with colloidal coomassie, the band containing SOQ1 was excised, and a rabbit polyclonal-antibody was produced from the gel piece (Covance, USA).

Bleeds from the two rabbits were tested by immunoblot analysis and rabbit #1 demonstrated a higher specificity, but the low titer resulted in high background. Affinity purification of the production and terminal bleeds from rabbit #1 was performed by coupling the recombinant SOQ1 protein to cyanogen bromide-activated-Sepharose (Sigma, USA) following the manufacturer's protocol. After coupling, 5-10 mL of the bleed was applied to the resin and rotated end over end at 4ºC overnight. The following day the mixture was applied to a column and rinsed three times with 10 mL of PBS. The serum flow-through was saved and can be purified again. The column was washed with 10 mL buffer A (50 mM Tris-HCl pH 8.0, 120 mM NaCl, 0.5% Triton X-100) followed by 10 mL buffer B (50 mM Tris-HCl, pH 8.0, 1 M LiCl, 0.5% Triton X-100), another 10 mL buffer A and finally 10 mL of PBS. Antibody was eluted with 50 mM glycine-HCl pH 2.5, 150 mM NaCl. Aliquots of 500 µL were collected in tubes containing enough 1 M Tris-HCl pH 8.0 to bring the pH to 7-7.5. Elutions were tested by dot and Western blots for specificity and titer.

Chloroplast and Thylakoid Isolation - For thylakoid isolation, leaves were removed from 6-8 week old plants before bolting and placed on ice in foil to cool for 1 hour. Leaves were homogenized in 0.4 M sorbitol, 5 mM EDTA, 5 mM $MgCl_2$, 10 mM $NaHCO_3$, 0.5% (w/v) BSA and 20 mM Tricine pH 8.4 with 8-10 short pulses using a commercial blender and then filtered though four layers of cheesecloth. Thylakoids were then pelleted at 2,600 g for 3 minutes at 4ºC. The supernatant was removed and the pellet was washed three times with resuspension buffer (0.3 M sorbitol, 2.5 mM EDTA, 5 mM $MgCl_2$, 10 mM $NaHCO_3$, 0.5% (w/v) BSA, 20 mM HEPES pH 7.6). The pellet was then resuspended in hypotonic buffer (2.5 mM EDTA, 5 mM $MgCl_2$, 10 mM $NaHCO_3$, 20 mM HEPES pH 7.6) for 10 minutes to rupture the chloroplasts before being centrifuged a final time at 2,600 g for 3 minutes at 4ºC and finally resuspended in a small volume of resuspension buffer. Chlorophyll concentration was measured in 80% acetone [60]. For isolated chloroplasts, the centrifugation speed was reduced to 800 g for each step, and the homogenate was washed three times in resuspension buffer without the addition of hypotonic buffer. PAM measurements on isolated chloroplasts and thylakoids were done in a 1 mL volume with constant stirring and the addition of methyl viologen to 20 µM as an electron acceptor.

Pigment Analysis - Plants were illuminated with high light for 20 minutes, and leaf disc samples were taken and immediately frozen in liquid nitrogen. The frozen disc was ground to a fine powder and extracted with 150 µL of 100% (v/v) acetone by vortexing for 1 min. The extract was centrifuged for 20 seconds, and the supernatant was saved. Another 150 µL of 100% (v/v) acetone was added to the pellet and mixed thoroughly. The extract was centrifuged again, and the supernatants were pooled. The supernatant was filtered through a 0.45-µm nylon filter. The acetone-extracted samples were stored in the dark until HPLC analysis, when 25 µl of the pigment extract was separated into individual pigments on a reverse-phase C18 Spherisorb S5 ODS1 4.6- X 250-mm cartridge column (Waters, Milford, MA) at 30°C. The carotenoids and chlorophylls were identified by their absorbance at 445 and 296 nm using a diode array detector. A standard curve of known concentrations of each purified compound was used for calculating chlorophyll and carotenoid concentrations.

Fluorescence Lifetime Analysis - Chlorophyll lifetimes were measured according to Amarnath et al. [2] with some modifications. Plants were dark adapted for 30 minutes prior to measurements, and a detached leaf was placed into a custom built holder. The adaxial surface of the leaf was angled at 45º with respect to the actinic light source and detector, and the laser hit the leaf at a 90º angle. The leaf was exposed to darkness for $T = 0$ - 50 seconds (where T refers to the time axis of the illumination sequence) followed by white light (KL1500 LCD, Schott, Germany) at 650 μmol photons m^{-2} s^{-1} for 8.5 minutes ($T = 50$ s – 560 s) and then darkness again for 20.5 minutes ($T = 560$ s – 1790 s). Fluorescence snapshots were taken at $T = 0$, 50, 80,140, 200, 260, 320, 380, 440, 500, 560, 590 and every 60 seconds until the end of the illumination sequence. Five leaves were measured using this illumination sequence for wild type and each mutant. The five fluorescence decays collected at each timepoint T for each genotype were summed to reduce noise.

Western Blots, Protein Localization and Topology - For protein localization experiments, thylakoid membranes and intact chloroplasts were isolated as described above. Samples were separated by SDS-PAGE, transferred to nitrocellulose and blotted with the antibodies indicated in the text. Blocking was done with 5% non-fat powdered milk, except when using the anti-phosphotheronine antibody in which case 3% BSA was used.

Protease protection assays were done on isolated thylakoids at 0.5 mg chlorophyll/mL in resuspension buffer by the addition of either sequence-grade trypsin (Promega, USA) or thermolysin (EMD Millipore, USA) at the concentration indicated in 300 μL reactions. After the indicated times, 50 μL were removed and added to a tube containing protease inhibitor to stop the reaction. PMSF was used at a final concentration of 1 mM to inhibit trypsin and EDTA at a final concentration of 50 mM to inhibit thermolysin. The tubes were vortexed immediately, and sample buffer was added.

Separation of grana, grana margins, and stromal lamellae fractions was done as described [43]. Thylakoids were resuspended at 0.5 mg chlorophyll/mL in resuspension buffer, and one volume of 1% digitonin was added. After mixing for 30 minutes at 4ºC, differential centrifugation at 1,000 g for 10 minutes, 10,000 g for 30 minutes, 40,000 g for 30 minutes and 144,000 g for 60 minutes was used to separate unsolubilized membranes, grana membranes, grana margins and stromal lamellae, respectively.

Results

Screen for *npq4* Suppressors

The *npq4* mutant of Arabidopsis is defective in the qE component of NPQ due to mutations in the PsbS protein. Several different alleles of *npq4* have been identified by insertional (*npq4-1)* and EMS mutagenesis (*npq4-5, npq4-6* and *npq4-7).* To identify additional proteins involved in NPQ we use chlorophyll fluorescence video imaging to screen for mutants that had increased levels of NPQ compared to *npq4* parent plants (Figure 2.1). From approximately 18,000 *npq4-1* M2 plants, three putative suppressors were found. Because the *npq4-1* mutant was crossed with *gl1-1* before mutagenesis, the presence of trichomes was used to eliminate any false positives resulting from wild-type contamination. The EMS-mutagenized population from the point mutant *npq4-6*, which had not been crossed to *gl1-1,* yielded many more putative suppressors (150 out of 7,500 plants screened), all of which proved to contain a

wild-type allele of *NPQ4* when examined using dCAPS PCR. Therefore, approximately 10,000 total plants from the EMS-mutagenized populations of *npq4-5* and *npq4-7* point mutants were also screened, and twelve more putative mutants were selected.

The fifteen putative mutants from the initial screen were grown to maturity, and M3 seeds were collected. Three putative suppressors did not produce seeds or the seeds did not germinate, three plants did not have higher NPQ when the M3 plants were rescreened, and three more were likely heterozygous for *npq4* based on their 1:2:1 segregation of the NPQ phenotype in the M3 plants. Of the six remaining putative mutants, three were shown to have wild-type *NPQ4* alleles by dCAPS PCR. The remaining three were called *suppressor of quenching (soq)* mutants and further characterized.

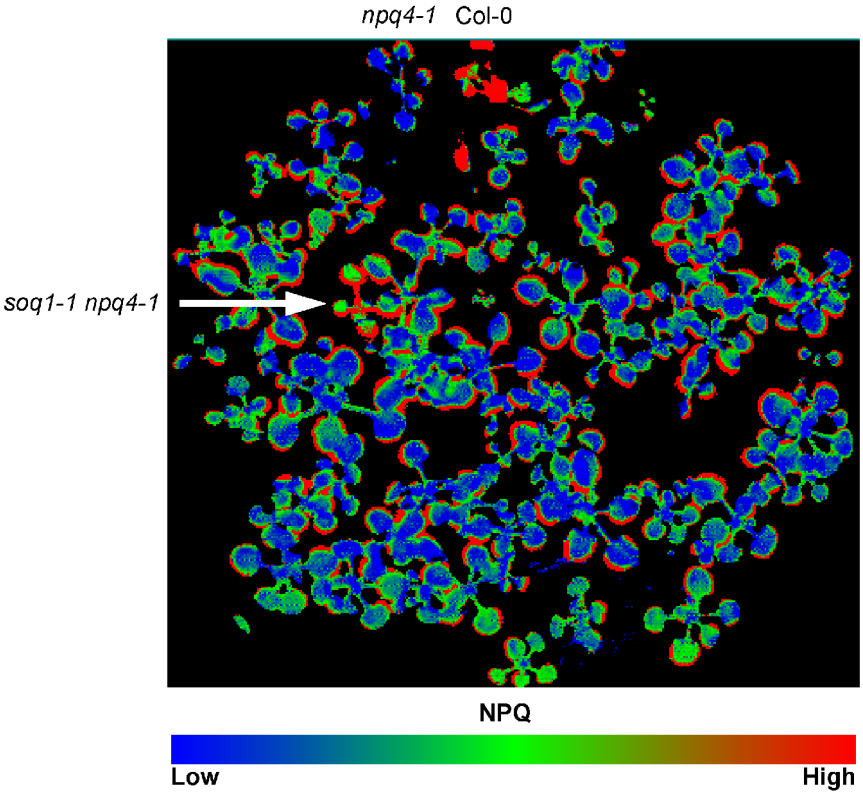

Figure 2.1: Identification of a suppressor of *npq4-1* by fluorescence video imaging
Mutagenized *npq4-1* M2 seedlings on an agar plate were exposed to 1,200 µmol photons m^{-2} s^{-1} for 10 min. Fluorescence was measured once within the first minute of illumination and again after 10 minutes. NPQ was calculated from these values and the image was false colored.

NPQ Phenotype of the Confirmed Suppressors

Two of the confirmed suppressors were from the *npq4-1* background (6-22 and 0-26) and one was from the *npq4-5* background (3-94). The mutant 6-22 (*soq1-1 npq4-1*) had a clear increase in NPQ compared to *npq4-1*, with a slower induction of NPQ than in wild-type plants but reaching nearly wild-type levels after 5-10 minutes of illumination with 1,200 µmol photons m^{-2} s^{-1} (Figure 2.2). In addition *soq1* showed slower relaxation of NPQ once the light was turned

off. The higher NPQ was accompanied by a greater quenching of F_o, which also relaxed more slowly than in wild type. As a result, the F_o' value in *soq1-1* after 10 minutes of dark relaxation was less than the initial F_o, whereas wild-type and *npq4* plants consistently had an F_o'/F_o value greater than 1.0. This phenotype, along with the higher induction and slower relaxation of NPQ, can clearly be seen in the fluorescence trace shown in Figure 2.3. The other mutants, 0-26 and 3-94, had similar NPQ phenotypes, and complementation tests between *soq1-1* and the other two mutants revealed that they resulted from defects in the same gene. This was later confirmed by mapping of the mutations (see below). Based on these results, further experiments were performed with only *soq1-1*.

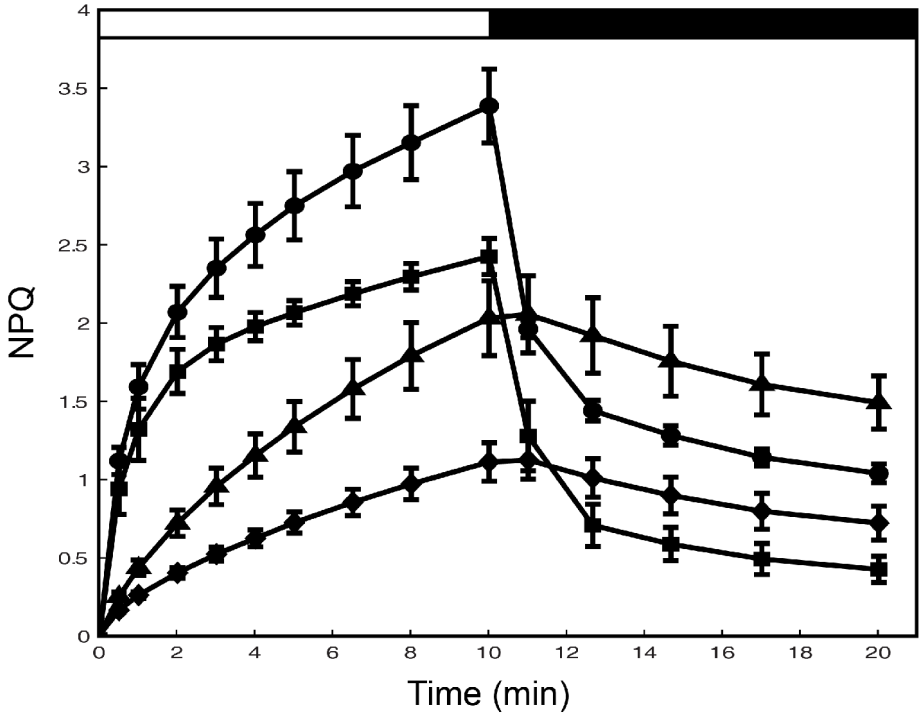

Figure 2.2: NPQ induction curve of wild type, *npq4-1*, *soq1-1 npq4-1* and *soq1-1*
Leaves were exposed to high light (1,200 µmol photons m^{-2} s^{-1}) for 10 minutes (white bar) and then allowed to relax for 10 minutes in the dark (black bar). wild-type – squares, *npq4-1*- diamonds, *soq1-1 npq4-1* – triangles, *soq1-1* – circles. Data represent means ± SD (n = 4).

The *soq1-1 npq4-1* mutant was backcrossed to *npq4-1* parent and the resulting progeny segregated 3:1 for the amount of NPQ (low:high) indicating the the *soq1* mutation is recessive. The *soq1-1 npq4-1* mutant was also crossed to Col-0 wild type and F2 progeny from this cross segregated in the expected 3:1 ratio when scoring the relaxation of NPQ (fast:slow) or F_o'/F_o (high:low) phenotypes. Given that *npq4-1* is semi-dominant and *soq1-1* is recessive, one might expect a 3:7:6 (low:intermediate:high) ratio for the level of maximum NPQ after 10 minutes of high light, however this was not the case. Rather, a ratio of 1:11:4 was observed, because the *soq1-1* mutation is linked to *NPQ4.* This was confirmed by mapping (see below). A rare recombinant plant that was homozygous for *soq1-1* and heterozygous for *npq4-1* was selfed,

resulting in one out of four plants having the *soq1-1* phenotype in a wild-type *NPQ4* background. The NPQ phenotype from this *soq1-1* single mutant is shown in Figure 2.2. The additional NPQ resulting from the *soq1-1* mutation was additive with that seen in wild type. It can also be concluded that the additional NPQ in *soq1-1* is not the result of the pH gradient across the thylakoid membrane dissipating more slowly, as the qE component of NPQ relaxed normally when the light was turned off.

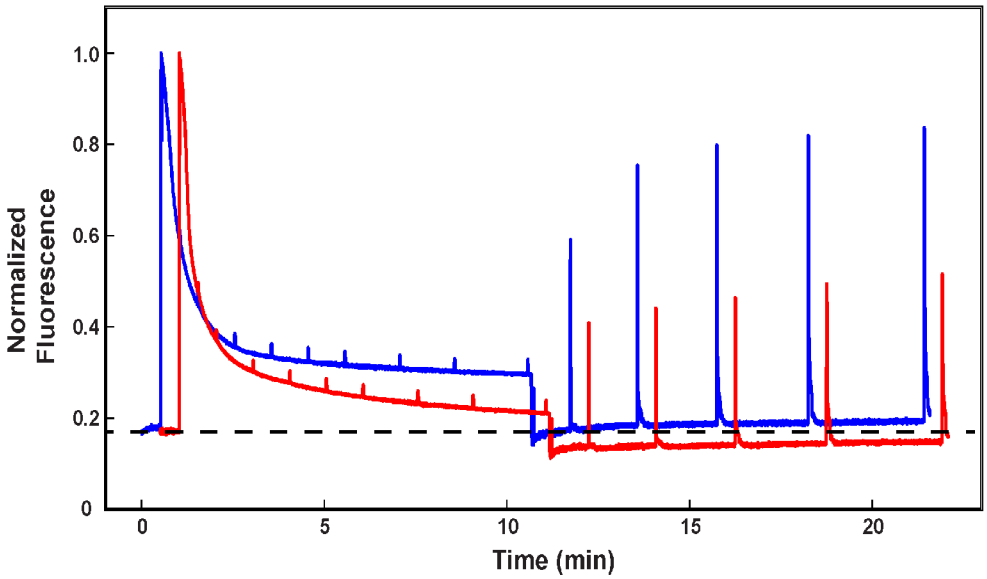

Figure 2.3: Fluorescence trace of wild-type and *soq1*
Representative PAM fluorescence trace of wild-type (blue) and *soq1-1* (red) illuminated at 1,200 µmol photons m^{-2} s^{-1} for 10 minutes and allowed to relax for 10 minutes. The *soq1-1* trace was offset by 30 seconds for clarity. A dashed line was placed at the F_o level to indicate that the F_o' in wild-type quickly recovered to the F_o level, whereas in *soq1-1* it remained lower.

The NPQ phenotype in *soq1-1* is dependent on the actinic light intensity used during the PAM measurement. At lower actinic light intensities (250 µmol photons m^{-2} s^{-1}), near levels at which the plants were grown (100-200 µmol photons m^{-2} s^{-1}), there was little difference between wild-type and mutant plants in the amount of NPQ (Figure 2.4). When the actinic light intensity was increased to 500 µmol photons m^{-2} s^{-1}, the mutant had a higher NPQ in terms of both maximum amount of NPQ attained and the level to which the NPQ relaxed. When the light intensity was further increased to 1,000 µmol photons m^{-2} s^{-1}, the difference in NPQ also increased (Figure 2.4).

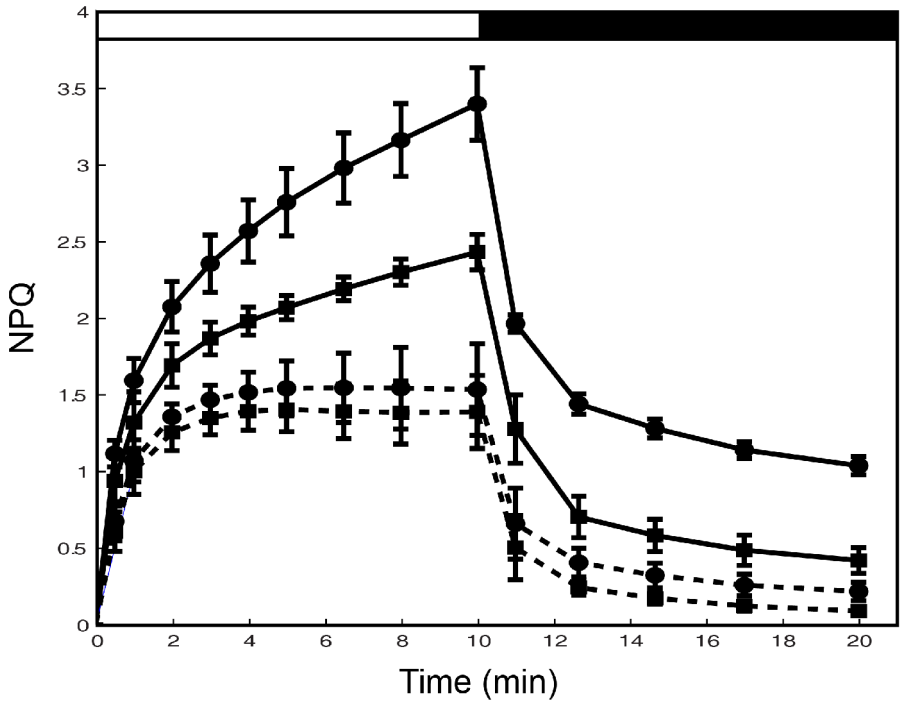

Figure 2.4: Light intensity dependence of the *soq1* NPQ phenotype
Wild-type (squares) and *soq1-1* leaves (circles) were exposed to either 1,000 µmol photons m^{-2} s^{-1} (solid lines) or low light 250 µmol photons m^{-2} s^{-1} (dashed lines) for 10 minutes (white bar), followed by dark relaxation for 10 mintues (black bar). Data represent means ± SD (n = 4).

Relationship with Known NPQ Components

To determine if the additional NPQ in *soq1-1* depends on the factors involved in known components of NPQ, we tested the formation of NPQ in the presence of different inhibitors. The low pH of the lumen protonates PsbS and activates VDE and is therefore required for the formation of qE. Uncouplers are molecules that prevent the formation of the pH gradient across the thylakoid membrane by allowing the free diffusion of ions. Figure 2.5 shows the NPQ from wild-type and *soq1-1* leaves infiltrated with either a mock solution without uncoupler or a nigericin solution. The difference in the level of NPQ at the end of the actinic light period between wild type and mutant in the mock-treated sample was not as pronounced due to the infiltration procedure and the larger variability between leaf measurements. Despite this, the amount of NPQ in the nigericin-treated mutant leaf, as well as the level to which the NPQ relaxed in both cases, were significantly higher in *soq1-1* than in the wild-type leaves. This suggests that the NPQ in *soq1-1* does not require a low lumen pH or the formation of a pH gradient in order to form this additional NPQ.

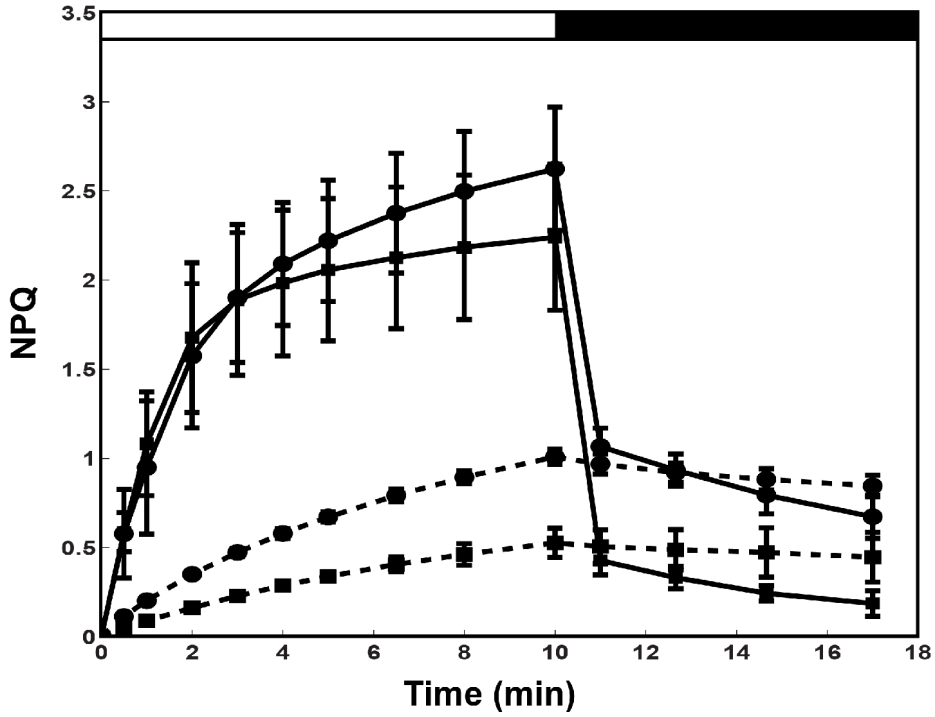

Figure 2.5: NPQ formation and relaxation in the presence of nigericin
Wild-type (squares) and *soq1-1* (circles) leaves were exposed to 1,000 µmol photons m^{-2} s^{-1} for 10 minutes (white bar) and allowed to relax in the dark for 7 minutes (black bar). Mock-treated samples (solid line) and leaves infiltrated with 100 µM nigericin (dashed line). Data represent means ± SD (n = 3).

The reducing agent, DTT is known to inhibit VDE and thereby prevent the formation of zeaxanthin, qE, and qZ. Figure 2.6 shows that the qE component of NPQ was nearly completely abolished in wild-type leaves treated with DTT (Figure 2.6). When *soq1-1* leaves were treated with DTT the qE component of NPQ was also almost completely absent, demonstrating that VDE was inhibited in the mutant as well. However, the mutant still had higher levels of NPQ than wild-type plants, indicating that the formation of zeaxanthin is not necessary for this NPQ. This also indicates that the higher NPQ seen in *soq1-1* is not due to an increase in the qZ component, which also requires zeaxanthin formation.

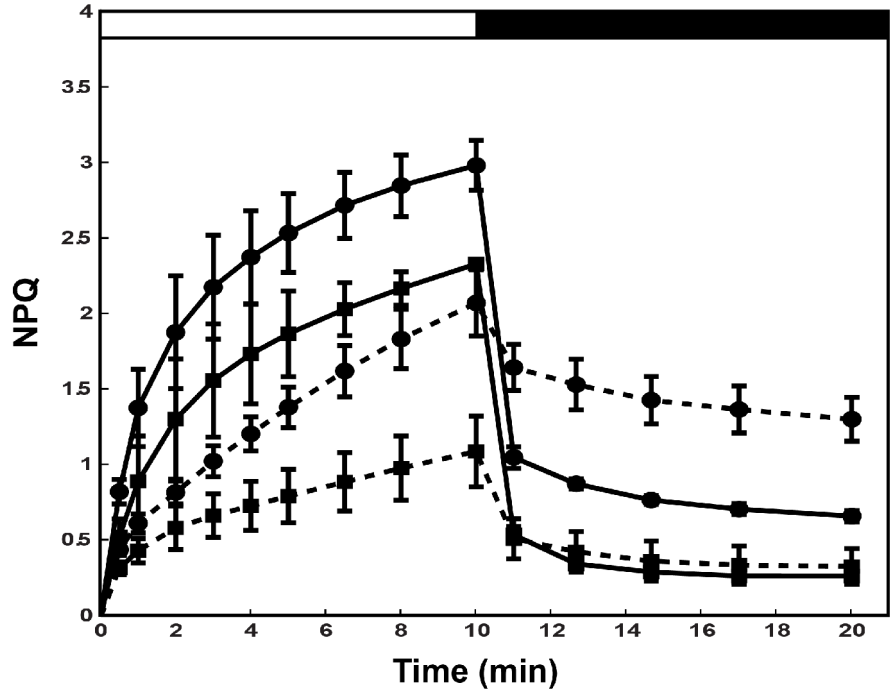

Figure 2.6: NPQ formation and relaxation in the presence of DTT
Wild-type (squares) and *soq1-1* (circles) leaves were mock-treated (solid lines) or infiltrated with 1 mM DTT (dashed lines) and then exposed to 1,000 µmol photons m^{-2} s^{-1} for 10 minutes (white bar) and allowed to relax in the dark for 10 minutes (black bar). Data represent means ± SD (n = 3).

Carotenoid and chlorophyll levels in the wildtype and the mutants were also measured using HPLC (Table 2.1). No significant differences were detected in the amount of any specific carotenoid, or the total carotenoid content. There was also no defect in the xanthophyll cycle as measured by the deepoxidation state of the xanthophylls before and after exposure to high light. The NPQ seen in *soq1-1* is also not the result of chlorophyll bleaching, as the amount of both chlorophylls *a* and *b* and the ratio between them do not change after exposure to high light (Table 2.1).

Table 2.1: Pigment content of wild type, *npq4-1, soq1-1* and *soq1-1 npq4-1* leaves

	Wild Type		*npq4-1*		*soq1-1*		*soq1-1 npq4-1*	
	LL	**HL**	**LL**	**HL**	**LL**	**HL**	**LL**	**HL**
Neoxanthin (mmol/mol Chl)	**48.4 ± 1.0**	**46.1 ± 8.3**	**45.3 ± 2.7**	**40.5 ± 6.5**	**45.7 ± 4.4**	**43.5 ± 3.2**	**42.7 ± 5.3**	**44.8 ± 4.6**
Violaxanthin (mmol/mol Chl)	**31.5 ± 3.1**	**12.5 ± 0.6**	**28.9 ± 0.6**	**11.2 ± 0.3**	**26.3 ± 1.3**	**11.9 ± 1.4**	**28.5 ± 1.3**	**11.2 ± 0.9**
Antheraxanthin (mmol/mol Chl)	**6.25 ± 2.1**	**7.23 ± 1.5**	**7.96 ± 0.7**	**8.02 ± 2.6**	**6.05 ± 2.3**	**10.2 ± 2.5**	**7.26 ± 1.4**	**6.98 ± 2.7**
Zeaxanthin (mmol/mol Chl)	***nd***	**8.57 ± 0.54**	***nd***	**12.0 ± 1.09**	***nd***	**11.6 1.65**	***nd***	**8.17 ± 0.96**
(A+Z)/(V+A+Z)	**0.17 ± 0.04**	**0.56 ± 0.02**	**0.22 ± 0.02**	**0.64 ± 0.04**	**0.19 ± 0.05**	**0.65 ± 0.01**	**0.20 ± 0.04**	**0.58 ± 0.04**
Lutein (mmol/mol Chl)	**165 ± 6**	**169 ± 11**	**159 ± 7**	**155 ± 3**	**164 ± 6**	**172 ± 15**	**159 ± 11**	**164 ± 7**
β-Carotene (mmol/mol Chl)	**94.8 ± 0.9**	**97.0 ± 3.0**	**98.9 ± 2.0**	**88.0 ± 3.3**	**90.6 ± 2.6**	**100 ± 12.9**	**93.5 ± 2.0**	**96.5 ± 3.1**
Total Carotenoids (mmol/mol Chl)	**346 ± 11**	**340 ± 21**	**340 ± 4**	**315 ± 8**	**333 ± 8**	**349 ± 32**	**331 ± 18**	**332 ± 8**
Chlorophyll *b* (mmol/mol Chl)	**266 ± 8**	**267 ± 5**	**261 ± 5**	**268 ± 7**	**264 ± 2**	**266 ± 7**	**266 ± 1**	**261 ± 1**
Chlorophyll *a* (mmol/mol Chl)	**733 ± 8**	**733 ± 5**	**739 ± 5**	**732 ± 7**	**736 ± 2**	**734 ± 7**	**734 ± 1**	**739 ± 1**
Chlorophyll *a/b*	**2.75 ± 0.12**	**2.74 ± 0.07**	**2.83 ± 0.07**	**2.74 ± 0.09**	**2.79 ± 0.02**	**2.76 ± 0.09**	**2.75 ± 0.02**	**2.83 ± 0.00**

Pigment measurements were performed before (LL) and after (HL) plants were exposed to high light (1,200 µmol photons m^{-2} s^{-1}) for 30 min. Data were normalized to total chlorophyll and are presented as the means ± SD (n = 3). V – Violaxanthin, A – Antheraxanthin, Z – zeaxanthin.

Final confirmation that the NPQ phenotype was not the result of a defect in the xanthophyll cycle was obtained by crossing *soq1-1* to the xanthophyll cycle mutants *npq1* and *npq2,* which prevent the formation of, or constitutively accumulate zeaxanthin, respectively. The additional NPQ remained in both double mutants (Figure 2.7), confirming the results from the previous experiments with DTT and indicating that the additional NPQ in *soq1-1* is not affected by changes in the xanthophyll cycle.

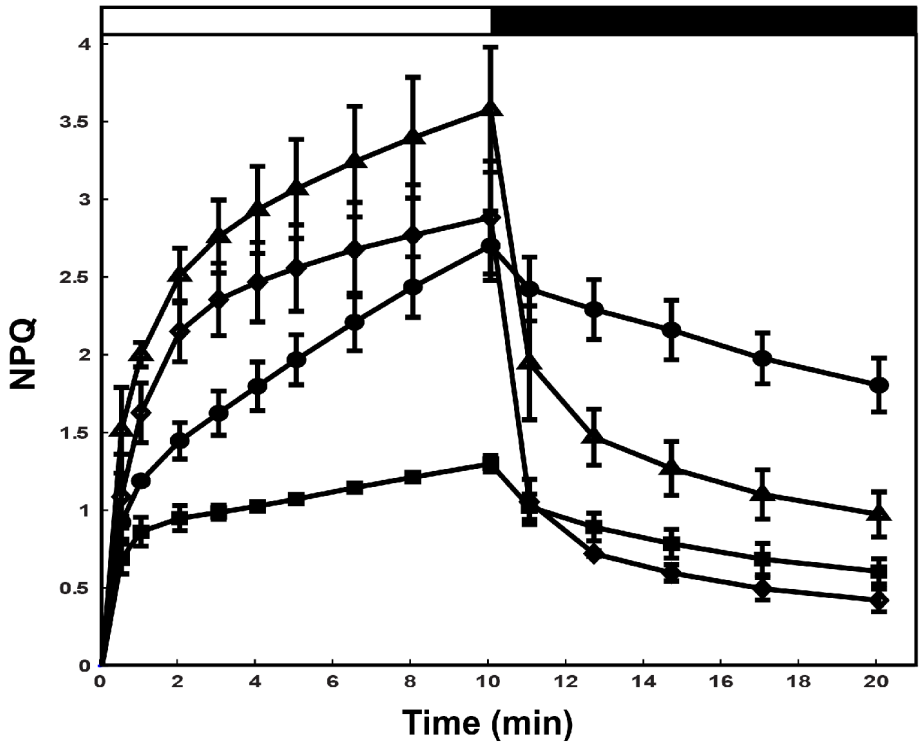

Figure 2.7: NPQ formation and relaxation in *soq1 npq1* and *soq1 npq2* double mutants
npq1 (squares), *npq1 soq1-1* (circles), *npq2* (diamonds), and *npq2 soq1-1* (triangles) leaves were exposed to 1,000 µmol photons m^{-2} s^{-1} for 10 minutes (white bar) and allowed to relax in the dark for 10 minutes (black bar). Data represent means ± SD (n = 3).

To determine if the additional NPQ in *soq1-1* is related to state transitions (qT), *soq1-1* was crossed to *stn7*, which lacks the kinase that is necessary for qT [6]. As shown in Figure 2.8A, the additional NPQ was still present in the *stn7 soq1-1* double mutant compared to the *stn7* single mutant, suggesting that this NPQ does not require STN7-dependent phosphorylation of LHCII and therefore is unlikely to be related to state transitions. To further confirm that LHCII phosphorylation is not involved, immunoblot analysis was performed using an anti-phosphothreonine antibody on proteins extracted from wild-type and *soq1-1* chloroplasts from the dark or treated with high light (Figure 2.8B). These results show that LHCII phosphorylation remained inhibited during high light in *soq1-1* and that there was no difference in the increase in reaction center phosphorylation. In addition, 77 K fluorescence measurements were performed on thylakoid samples from the dark or illuminated with high light to compare changes in PSI and PSII ratios between wild-type and *soq1-1* (Figure 2.8C). Before and after illumination with high light, there was no difference in the ratio of 77 K fluorescence between wild-type and *soq1-1* thylakoids.

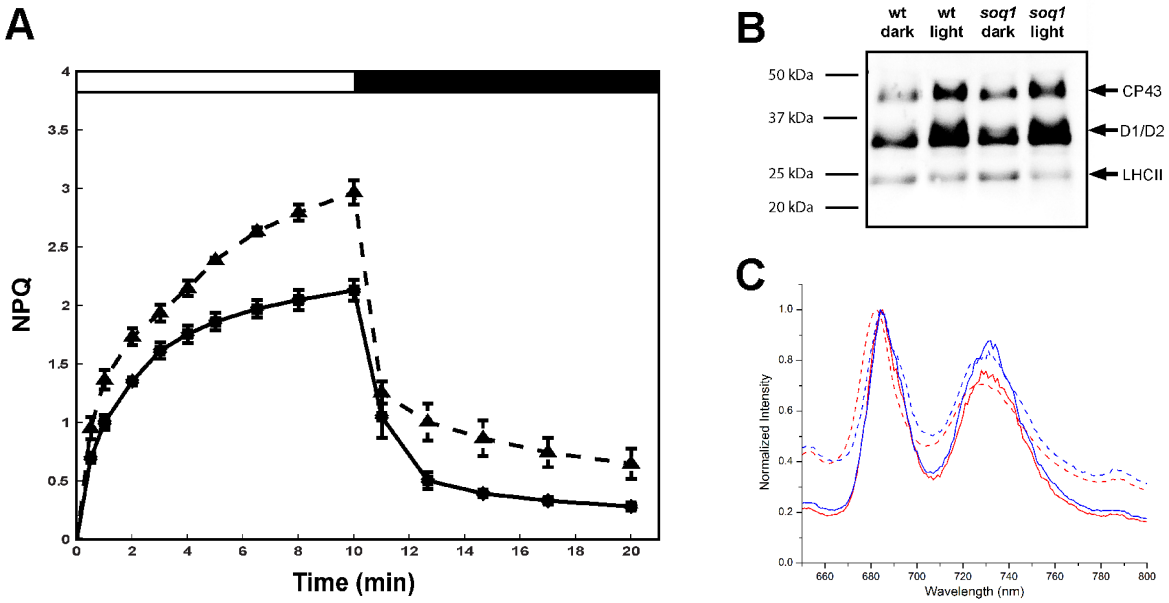

Figure 2.8: Effect of *soq1* on state transitions

A) NPQ from *soq1-1 stn7* (triangles) and *stn7* (squares) leaves exposed to high light (1,000 µmol photons m^{-2} s^{-1}) for 10 minutes (white bar) and then allowed to relax in the dark for 10 minutes (black bar). Data represent means ± SD (n = 4). B) Anti-phosphothreonine immunoblot on chloroplast proteins from dark-acclimated leaves and leaves exposed to high light (1,000 µmol photons m^{-2} s^{-1}) for 10 minutes. C) 77 K fluorescence measurements on isolated thylakoids from wild-type (blue lines) or *soq1-1* (red lines) from the dark (solid lines) or exposed to high light (500 µmol photons m^{-2} s^{-1}) for 10 minutes (dashed lines). Spectra were normalized to the peak at 680 nm.

To test the possibility that the NPQ phenotype is due to additional damage to reaction centers or a defect in D1 repair, wild-type and *soq1-1* leaves were treated with the chloroplast protein synthesis inhibitor lincomycin, and then exposed to high light for 90 minutes followed by recovery in low light for up to two days. Figure 2.9A shows that maximum photochemical efficiency of PSII (F_v/F_m) decreased dramatically as a result of treatment with lincomycin, and the rate and extent of recovery of F_v/F_m was lower in both the mutant and wild-type when compared to the mock treated sample. The decrease of F_v/F_m in the mock treated *soq1-1* mutant during exposure to high light was similar to the lincomycin-treated sample during the light treatment. The F_v/F_m in the mutant recovered to nearly the initial value when placed in low light, although this recovery took significantly longer than in wild-type plants.

A B

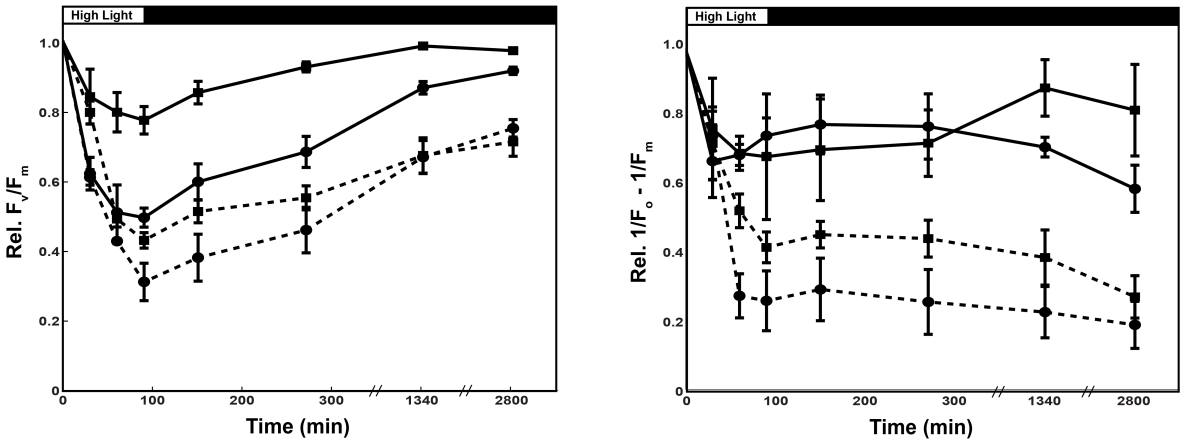

Figure 2.9: Changes in fluorescence parameters during lincomycin treatment
Wild-type (squares) and *soq1-1* (circles) leaves were treated with 1 mM lincomycin and exposed to high light (1,200 µmol photons m^{-2} s^{-1}) for 90 minutes (white bar) and then allowed to relax in very low light (20 µmol photons m^{-2} s^{-1}) for up to two days (black bar). Leaves were put in the dark for 20 minutes to allow relaxation of qE and then F_o and F_m were measured using a PAM fluorometer. A) F_v/F_m and B) $1/F_o$ -$1/F_m$ were calculated and normalized to the value obtained before the high light treatment. Data represent means $\pm$ SD (n = 3).

To determine if the changes in photochemical efficiency in the mutant are due to reaction center damage or quenching in the antenna, we also plotted the lincomycin data as described by Walters and Horton [73]. The parameter $1/F_o$-$1/F_m$ in the mock-treated mutant remained similar to mock-treated wild-type leaves during high light treatment and recovery while the lincomycin treated-leaves also behave similarly, indicating that in the untreated leaves the quenching is primarily of the antenna while in lincomycin-treated leaves the quenching is due to photoinhibited reaction centers.

Photoinhibitory damage to PSII reaction centers also generally manifests as an increased F_o' relative to the F_o, due to increased fluorescence from the antenna when reaction centers are incapable of charge separation. This is the opposite of what was seen in the *soq1* mutant (Figure 2.3). Finally, with photoinhibitory damage one would expect to see changes in the coefficient of photochemical quenching (q_P) and also possibly in the redox state of the PQ pool ($1-q_L$) or in the PSII electron transport rate (ETR), when the plant is exposed to a series of increasing light intensities. When these measurements were done with the *soq1* mutant, all three of these parameters were the same as those in wild type, even when the NPQ was significantly higher (Figure 2.10).

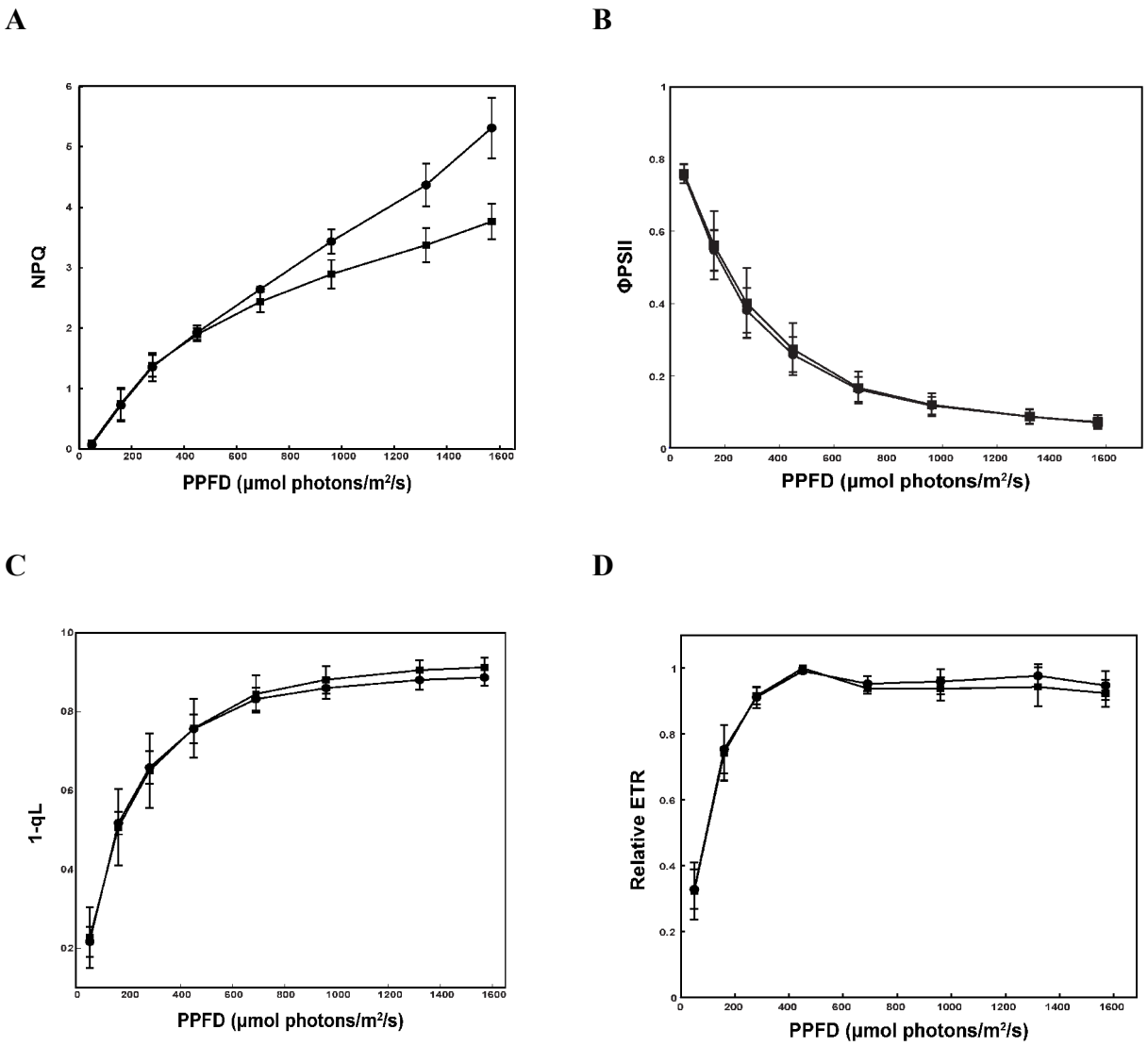

Figure 2.10: Light curve of *soq1* and wild-type leaves
Leaves from wild type (squares) and *soq1-1* (circles) were dark adapted for 30 minutes and exposed to increasing actinic light intensities. The photosynthetic parameters A) NPQ, B) ΦPSII, C) 1-q_L, which estimates the redox state of the PQ pool, and D) ETR, the electron transport rate through PSII normalized to the maximum rate for each measurement. Data represent means ± SD (n = 3).

Fluorescence Lifetimes in *soq1-1* and *soq1-1 npq4-1*

We sought to further characterize the NPQ seen in *soq1* mutants by examining the changes in chlorophyll fluorescence lifetimes using the apparatus described in Amarnath *et al.* [2]. Figure 2.11 shows that as plants adapt to light, the average fluorescence lifetime decreases, and that this decrease is partially reversible upon removal of the light. At least part of this change in chlorophyll fluorescence lifetime depends on PsbS and is therefore attributable to qE (compare green and black lines). The average lifetime in the *soq1-1* mutant is similar to wild

type in the light, but does not increase as much when the light is removed (compare black and red lines). The effects of the *soq1-1* mutation are more apparent in the *soq1-1 npq4-1* double mutant, with the average lifetime decreasing to the same value as in wild type and *soq1-1* after 5-10 minutes of illumination and showing little sign of relaxing upon return to the dark.

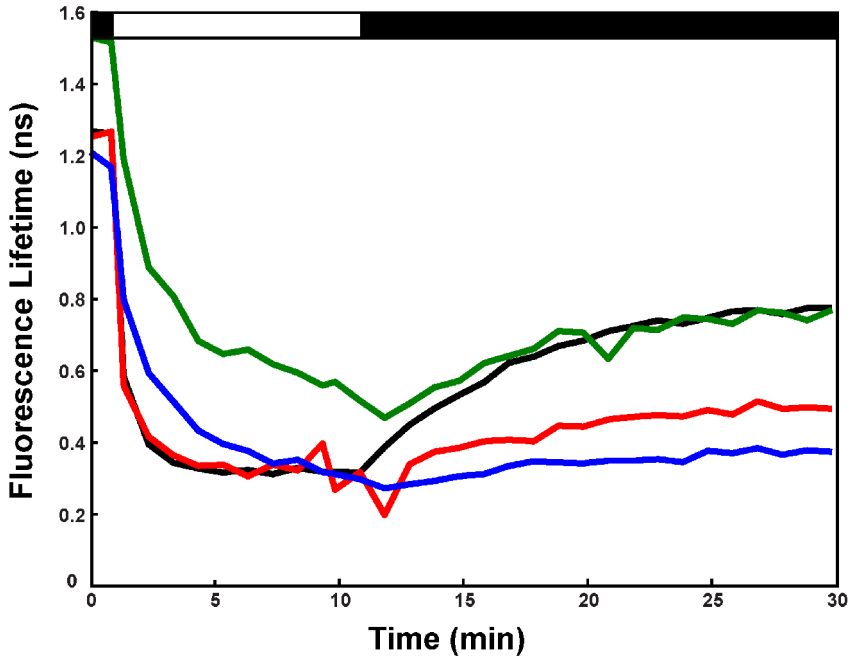

Figure 2.11: Average chlorophyll lifetime measured by time-resolved spectroscopy
Changes in the average fluorescence lifetime as measured by time-correlated single photon counting on wild type (black), *soq1-1* (red) and *npq4-1* (green) and *soq1-1 npq4-1* (blue) leaves. The data at each timepoint are result of the fitting of the sum of the fluorescence decays measured at that timepoint in 5 different leaves.

Mapping and Complementation of the *soq1-1* Mutation

To identify the genetic mutation causing the NPQ phenotype in *soq1* mutants, we used a map-based cloning strategy. Rough mapping of bulked F2 mutants from a cross between *soq1-1* and the Ler accession showed clear linkage between *soq1* and the markers nga111, nga280 and GAPB-II. This represents a 11.23 Mb region on chromosome 1 containing *NPQ4* (Figure 2.12). The interval containing the *soq1* mutation was narrowed by fine mapping to a 340 kb region between the BACs F14G9 and F12K22 containing 167 genes. Because the mutant displays an NPQ phenotype, we hypothesized that the gene would encode a protein that is targeted to the chloroplast. Searching for genes with a predicted transit peptide narrowed the candidate list to three genes. Each of these genes was sequenced from wild-type and *soq1-1* genomic DNA, and a guanine to adenine mutation was found in At1G56500 in the mutant. This mutation affects a 3' splice site before the sixth exon and likely results in premature termination of translation. When this gene was sequenced from the 0-26 mutant, the same splice site mutation was found, suggesting that they were likely siblings from the same batch of mutagenized plants. The 3-94 (*soq1-2)* allele had a guanine to adenine mutation in the 25th exon of At1G56500 that changes glutamate 895 to a lysine.

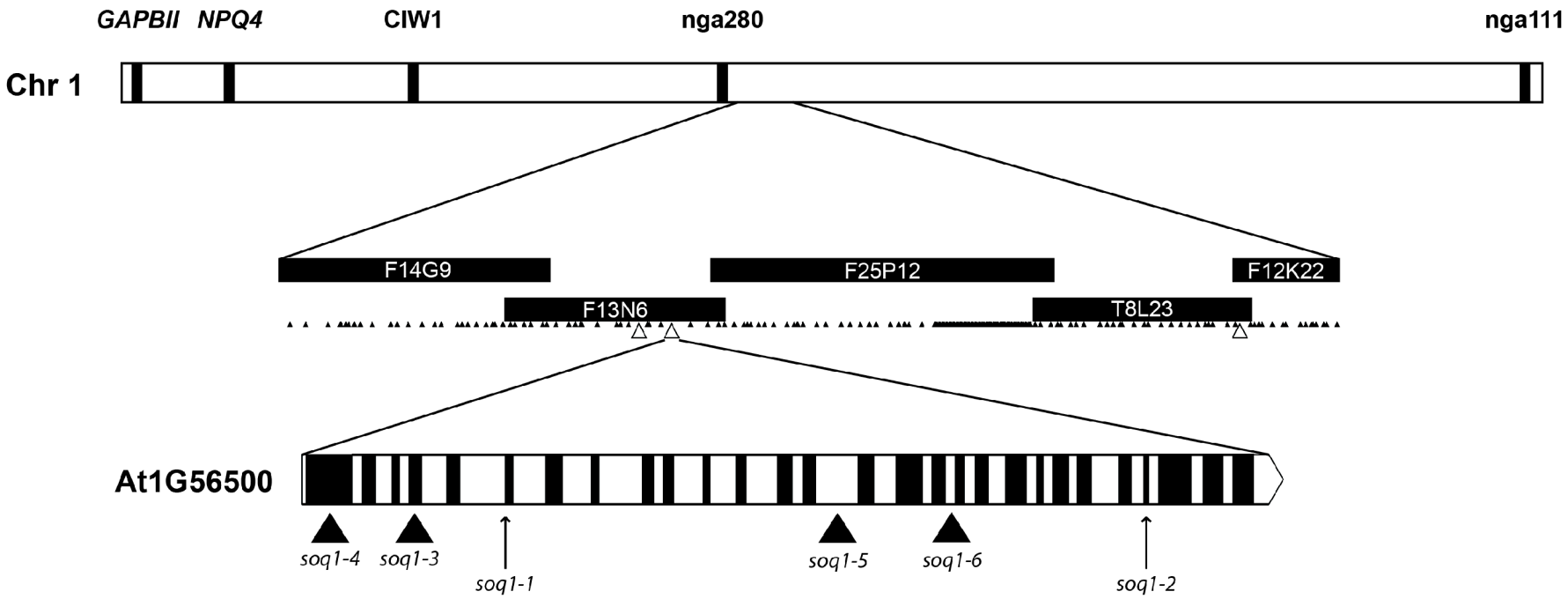

Figure 2.12: Map-based cloning of *soq1-1*
soq1-1 was linked to the molecular markers shown above the bar representing chromosome 1. Fine mapping further localized the mutation to a region between BACs F14G9 and F12K22. Small black arrowheads represent genes, and larger white arrowheads are genes that encode predicted chloroplast proteins. The gene model for At1G56500 is shown with black bars representing exons and white bars as introns. The arrows point to the location of mutations identified in this screen, and the large black triangles are the location of T-DNA insertions obtained from the ABRC.

Several potential T-DNA lines interrupting *SOQ1* were obtained from the Arabidopsis Biological Resource Center. Three homozygous T-DNA lines were confirmed: SALK_139953c, which contains an insert in the fourth exon; SALK_099167 (CS65691), which has one in the first exon; and SALK_034406C, which has an insertion after the seventeenth exon (Figure 2.12). In addition several heterozygous lines with potential insertions were screened, and a SAIL line (CS800355) with an insertion between the fourteenth and fifteenth exon was found (Figure 2.12). All four of these T-DNA insertion mutants displayed the same NPQ phenotype as *soq1-1* when screened by fluorescence video imaging, suggesting that the point mutants are likely loss-of-function alleles, as was expected from the disrupted splice site in *soq1-1* and the recessive nature of the mutations. Table 2.2 summarizes the different alleles used in this work.

Table 2.2. Summary of *soq1* alleles

Allele	Mutagen	Location of Mutation
soq1-1	EMS	Splice site before Exon 6
soq1-2	EMS	E895K in Exon 25
soq1-3	T-DNA	Exon 4
soq1-4	T-DNA	Exon 1
soq1-5	T-DNA	Between Exons 14 & 15
soq1-6	T-DNA	Between Exons 17 & 18

Final confirmation that the NPQ phenotype in *soq1-1* was due to a disruption of At1G56500 was obtained by complementing the mutation using the full-length cDNA under control of the CaMV35S promoter. In addition to transforming with a wild-type cDNA, transformed lines were also made that included a C-terminal GFP-6xHis tag, a C-terminal FLAG tag, or both N-terminal Strep and C-terminal FLAG tags. Of these, all but the GFP-6xHis construct complemented the *soq1-1* mutation and restored the NPQ phenotype to wild type (Figure 2.13).

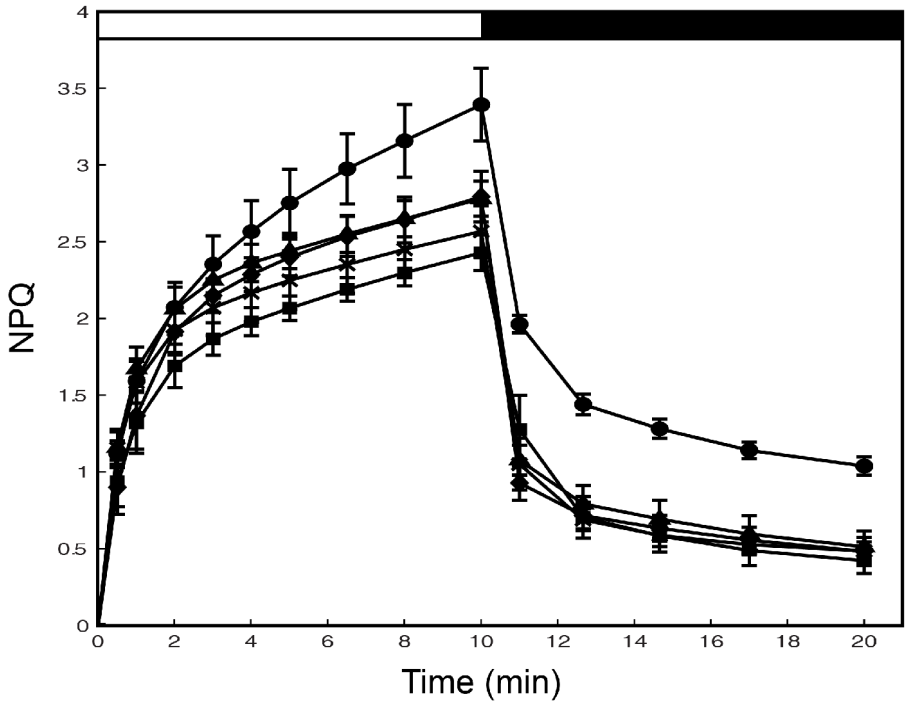

Figure 2.13: Complementation of *soq1-1* with *SOQ1* cDNA
Leaves were exposed to 1,000 µmol photons m^{-2} s^{-1} for 10 minutes (white bar) and then allowed to relax for 10 minutes in the dark (black bars). *soq1-1* – circles, wild-type – squares, *soq1-1* + 35S:*SOQ1* – triangles , *soq1-1* + 35S:*SOQ1*:FLAG – diamonds, *soq1-1* + 35S:cTP:Strep:*SOQ1*:FLAG – asterisks. Data represent means ± SD (n = 3).

SOQ1 Encodes a Multi-Domain Chloroplast Protein

The *SOQ1* gene encodes a previously uncharacterized 114-kDa protein consisting of 1055 amino acids and 28 exons. As mentioned in the previous section, SOQ1 contains a putative chloroplast transit peptide with a predicted cleavage site after 58 amino acids. The protein has three predicted functional domains: a haloacid dehalogenase-like hydrolase (HAD) domain (Pfam00702), a thioredoxin (Trx)-like fold (Pfam13905), and an NHL repeat (Pfam01436), named for the NCL-1, HT2A and Lin-41 proteins in which it was first described. Several prediction programs identifed a transmembrane helix between the HAD and Trx-like domains of SOQ1, however the strength of this prediction varied between programs.

The HAD superfamily is a large and diverse group of enzymes that use an aspartate residue in the active site as the nucleophile [40]. HAD proteins are found in all kingdoms of life, have been found to act on a wide range of substrates and typically are involved in phosphoryl group transfer reactions acting as phosphatases, ATPases, phosphonatases, and sugar phosphomutases [8]. SOQ1 further falls into the subfamily-1a-variant 3 group of HAD proteins, characterized by a capping domain between the first two catalytic motifs.

Thioredoxins are defined by the Trx fold as well as the conserved CxxC motif, where the cysteines catalyze a disulfide exchange reaction, resulting in reduction (or

oxidation) of target proteins. The Trx-like domain of SOQ1 falls into the TlpA-like family which contains a 25-residue insert forming an extra alpha helix and beta strand compared to the standard Trx domain [9]. Furthermore, all eukaryotic members of this family, including the domain found in SOQ1, fall into the DipZ-like subfamily. The DipZ subfamily shows sequence and structural homology to the soluble C-terminal Trx-like domain of the disulfide-reducing DsbD protein from *E. coli.* The bacterial Dsb proteins in this family have a role in facilitating the transfer of reducing potential across the inner membrane of bacteria to the periplasm and reducing target proteins in the this oxidizing environment [50].

The NHL repeat is a member of the beta propeller clan of domains that have a variable number of repeated beta-sheets forming blades that surround a central channel [10]. The function of beta propeller domains are diverse, with evidence of involvement in catalysis, signaling, ligand binding, protein structure, and protein-protein interactions. NHL domains are typically six-bladed structures and are found in both eukaryotic and prokaryotic species.

Species Distribution and Evolution of SOQ1

SOQ1 is found in nearly all land plants and is very highly conserved at the sequence level. The algal species *Chlorella variabilis* and *Coccomyxa subellipsoidae* contain a protein with all three domains, whereas *Chlamydomonas reinhardtii* and *Volvox carteri* only have the Trx-like and NHL domains, suggesting a loss of the HAD domain in some algal lineages. No hits were found when SOQ1 was blasted against the prasinophyte species, *Micromonas sp. RCC299* and *Ostreococcus tauri,* or any non-green algae with a published genome. Arabidopsis cDNA sequences from Genbank also indicate that mRNAs encoding only the HAD domain may also be transcribed in plants. *Physcomitrella patens*, a moss that diverged at the base of the land plant lineage, has a protein containing all three domains, but alternative splicing may produce a protein containing only the HAD domain. Interestingly, two closely related C4 plants, *Zea mays* and *Sorghum bicolor,* lack a protein that contains all three domains. *Zea mays* has a protein with the HAD domain but no predicted proteins with the Trx-like or NHL domains, and in *Sorghum bicolor* a gene has inserted in the middle of the protein disrupting the NHL domain.

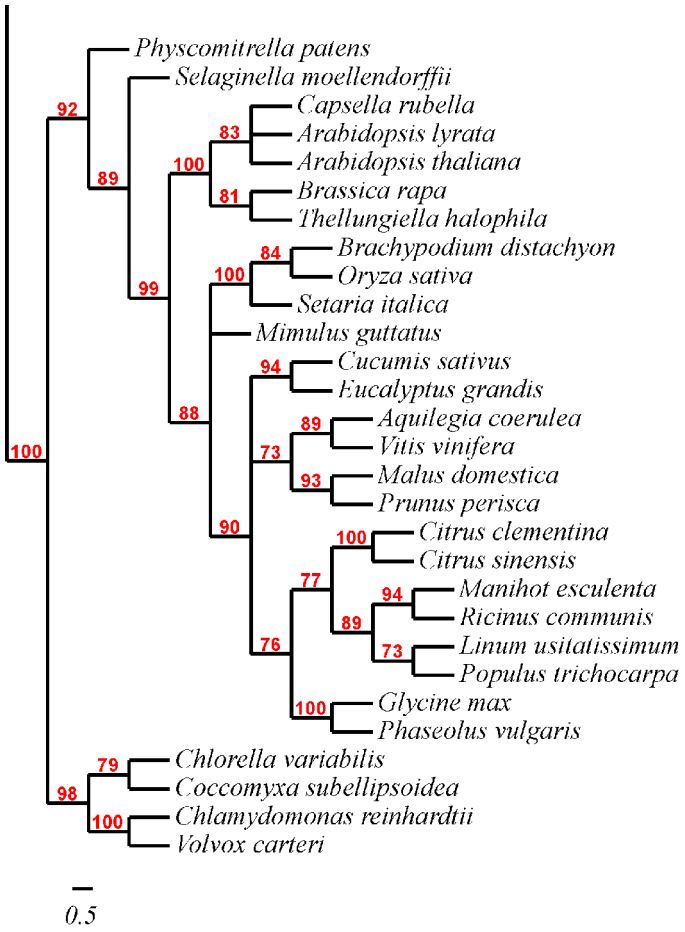

Figure 2.14: Phylogenetic tree of SOQ1 homologs in plants
The tree was generated as described in the methods section. The outgroup used was other eukaryotic proteins containing the Trx-like/NHL domains (not shown).

The TRX-like and NHL domain are found together without the HAD domain in a much broader group of species, including animals and bacteria, but no sequenced fungi. A phylogenetic tree was constructed from BLAST hits (Figure 2.15). The sequence similarity between these orthologs from species separated by large evolutionary distances is remarkable. For example, the Trx-like/NHL portion of the proteins from Arabidopsis and *Homo sapiens* have 45% identity and 65% similarity over 98% of the sequence. None of these proteins from any other species has been characterized previously.

In contrast to the TRX-like and NHL domains, the HAD domain has far less sequence similarity with other HAD proteins beyond the homologs found in land plants.

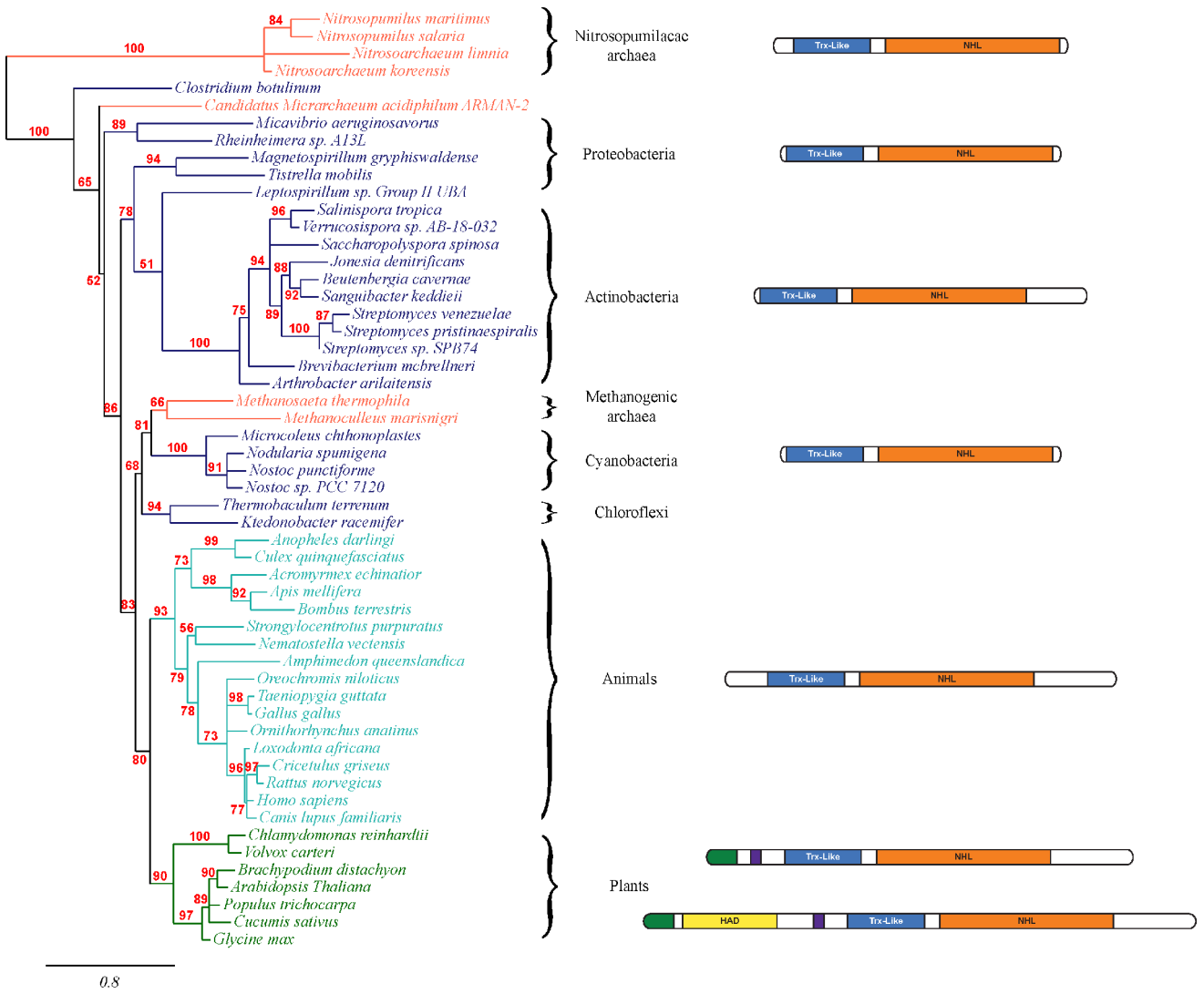

Figure 2.15: Phylogenetic tree of Trx-like and NHL regions of SOQ1 and similar proteins
The phylogenetic tree was made as described in the methods section. The domain architecture for the different groups is shown on the right. Note that the plant, animal and actinobacteria have C-terminal extensions beyond the NHL domain. Each of these contain conserved cysteines.

Domains Required for the NPQ Phenotype

Which domains of SOQ1 are involved in the NPQ phenotype seen in *soq1* plants? One of the point mutations, *soq1-2*, affects a conserved residue of the NHL domain but still expresses the protein (not shown), suggesting that the NHL domain is required for SOQ1 function. To test the involvement of the other domains, *soq1-1* was transformed with a series of point mutant and truncation constructs (Figure 2.16). Transformation of *soq1-1* with a point mutant construct, D80N, which lacks the catalytic aspartate residue of the HAD domain as determined by alignments with other HAD-containing proteins, resulted in successful complementation of the mutant phenotype as assessed by screening of transformants by fluorescence video imaging and PAM fluorescence. To confirm that the HAD domain is not required, *soq1-1* plants were transformed with a construct lacking the entire HAD domain (ΔHAD). The ΔHAD construct successfully complemented the NPQ phenotype. However, a construct lacking both the HAD domain and the putative transmembrane helix (ΔHAD/TM) did not complement *soq1-1*, suggesting that the transmembrane domain is required. Similarly, a requirement for the Trx-like domain was shown by transforming *soq1-1* plants with C431S or C434S point mutants, which lack the first or second catalytic cysteines of the Trx-like domain, respectively. Neither of these point mutant constructs was able to complement *soq1-1*. For the ΔHAD/TM and cysteine mutant constructs, several hundred transformants were obtained and screened, but none of them exhibited complementation of the NPQ phenotype.

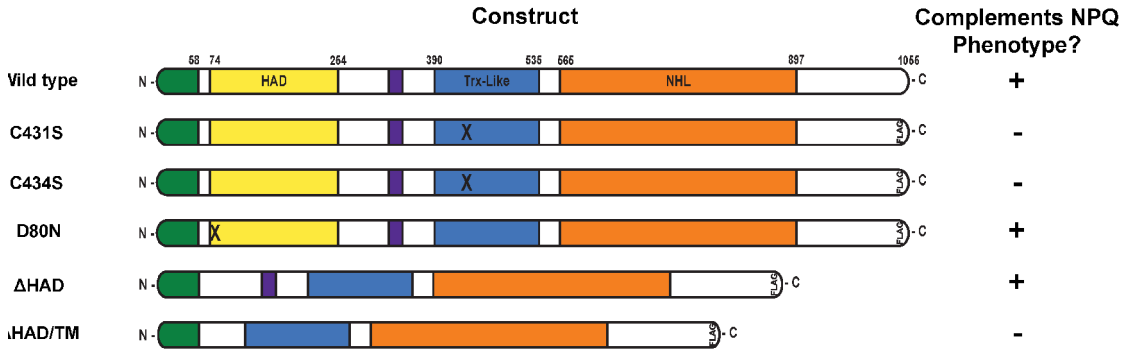

Figure 2.16: Complementation of *soq1-1* with SOQ1 containing various mutations
Diagram of the different truncated and point mutant constructs tested for complementation. Numbers above the wild type protein indicate amino acid positions. Green bar is the chlorplast transit peptide, and purple bar is the putative transmembrane domain.

Localization and Topology of SOQ1

Proteomics results from other labs suggest that the SOQ1 protein may possibly be associated with the thylakoid membrane [69]. The *soq1-1* mutant has significantly more NPQ than the wild type in both isolated chloroplasts and thylakoid membranes when measured using a PAM fluorometer (Figure 2.17A). It should be noted that the total

amount of NPQ as well as the kinetics of induction and relaxation differ significantly between isolated thylakoids/chloroplasts and whole leaves. Immunoblot analysis of these samples shows that SOQ1 was undetectable in the whole leaf extract but clearly present in the thylakoid preparation (Figure 2.17B). The stromal protein rubisco activase was absent from the thylakoid fraction, whereas the PSII subunit D2 was enriched. These results suggest that the SOQ1 protein is located in the thylakoid membrane or lumen.

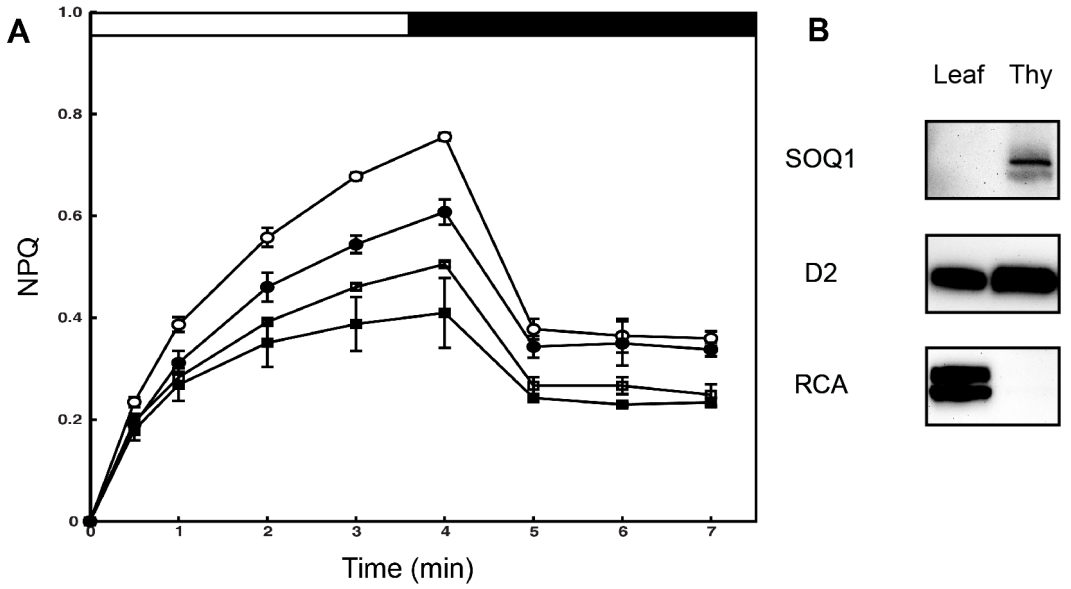

Figure 2.17: NPQ phenotype of isolated *soq1-1* chloroplasts and thylakoids
A) Isolated chloroplasts from wild type (closed squares) and *soq1-1* (closed circles) as well as isolated thylakoids from wild-type (open squares) and *soq1-1* (open circles) were illuminated with actinic light at 500 µmol photons m^{-2} s^{-1} for 4 minutes (white bar) and allowed to relax for 3 minutes (black bar). Data represent means ± SD (n = 3). B) Immunoblot analysis showing enrichment of SOQ1 in the thylakoid preparation. D2 and Rubisco Activase (RCA) were used as thylakoid and stromal controls, respectively.

To determine the specific location and possible transmembrane topology of SOQ1, isolated thylakoids were treated with either trypsin or thermolysin prior to immunoblotting (Figure 2.18). Samples not treated with protease had a SOQ1 band at the expected size of 110 kDa, whereas those treated with protease and detergent were completely digested. Trypsin or thermolysin treatment of unsolubilized thylakoids resulted in the rapid appearance of an approximately 80 kDa band in the SOQ1 blot. The lumenal protein PsbO was protected from digestion except in the presence of detergent, and the stroma-exposed PsaD and FNR proteins were completely cleaved in 20-40 minutes, forming smaller polypeptides thate were protected from further digestion as described previously [26,53].

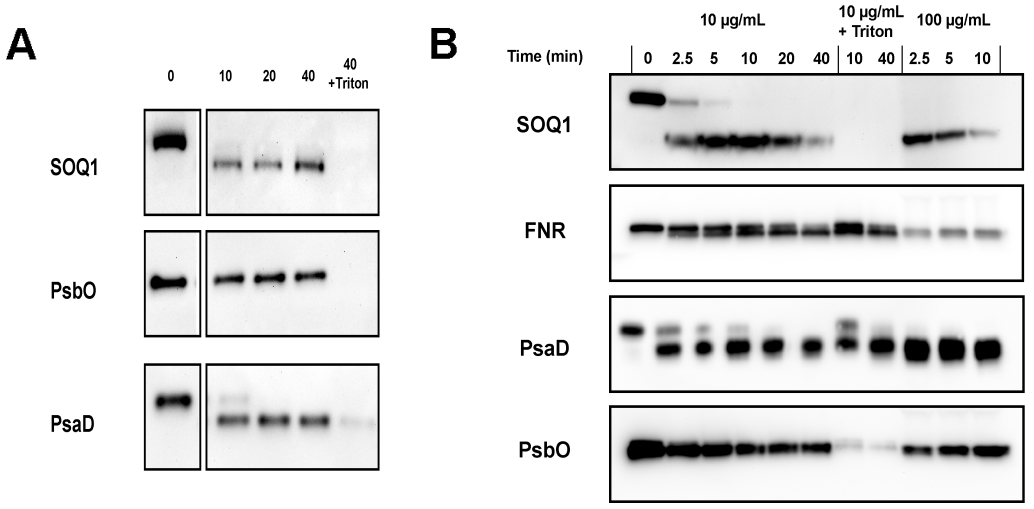

Figure 2.18: Protease protection assay
Isolated thylakoids were treated with A) trypisn or B) thermolysin for the indicated amount of time and proteins were separated by SDS-PAGE. Membranes were also treated with protease in the presence of 1% (v/v) Triton X-100 to solubilze the membrane and to allow access to the lumen. PsbO and PsaD (or FNR) were used as lumenal and stromal controls, respectively.

Discussion

The dominant NPQ mechanism for dealing with rapid fluctuations in light intensity is qE, which has been the focus of much research on photoprotection. Because of the large contribution of the qE component to the total amount of NPQ, screening for *npq* mutants has mainly uncovered those with a defect in qE, and mutants that affect other NPQ components have probably been overlooked. Here, by screening in an *npq4* background that lacks qE, we have found Arabidopsis *soq1* mutants that affect a slowly reversible qI type of NPQ.

The higher NPQ phenotype of the recessive, loss-of-function *soq1* mutations indicates that the wild-type SOQ1 protein is primarily involved in preventing the formation of a slowly relaxing quenching pathway when plants are exposed to high light. Other screens have identified mutants with higher qE resulting from additional cyclic electron flow [48], and recent studies on the *npq4* mutant have shown that qE-like quenching can form in the absence of PsbS after prolonged illumination with moderate light intensities [37] or with the aid of chemicals that increase the pH gradient [36,38]. This led us to ask if the quenching seen in *soq1* is related to qE or other known components of NPQ. The NPQ phenotype in the *soq1* single mutant suggested that the quenching was not the result of a sustained pH gradient after removal of the actinic light, because the qE component was able to completely relax while the additional quenching

remained. Formation of the pH gradient was also unnecessary to produce the quenching in *soq1* as shown by treatment with the uncoupler nigericin (Figure 2.5). The third component known to be required for qE *in vivo*, the xanthophyll cycle, is also not required for the quenching in *soq1* as demonstrated by the inhibition of VDE with DTT (Figure 2.6), by crossing *soq1-1* to the *npq1* and *npq2* mutants (Figure 2.7) and by its pigment profile (Table 2.1). Thus, the independence of *soq1* quenching from any of the three known qE requirements indicates that it is distinct from qE. While much less is known about the qZ type of quenching, these results would also suggest that *soq1* is not involved in that pathway as it also requires zeaxanthin formation.

State transitions balance light absorption between PSI and PSII using the redox state of the PQ pool as an indicator of light quality [52]. When PSII is being preferentially excited, the PQ pool will become reduced, leading to activation of the STN7 kinase. In high light, when both reaction centers are being over excited the PQ pool will also be reduced, however there is believed to be a mechanism that exists to prevent state transitions [32,63]. Because the additional NPQ in *soq1* is high light dependent, we hypothesized that the SOQ1 protein might be responsible for inhibiting STN7 or removing phosphate groups from LHCII in high light. If this were true, then the STN7 protein would be required for the NPQ, and a *soq1 stn7* double mutant would no longer have the NPQ phenotype seen in *soq1*. Figures 2.8 shows that the additional NPQ remained in this double mutant and along with the phosphothreonine immunoblot and 77K measurements, clearly indicates that the quenching is not a result of state transitions or LHCII phosphorylation.

Another possibility is that the quenching seen in *soq1* is the result of an increase in oxidative damage or the inability of the mutant to efficiently repair damaged reaction centers [5,42,49,70], leading to more photoinhibitory qI quenching. If this were the case, one might expect other known repair mutants to have been identified in our screen. Although the screen was not saturating, none of the known repair mutants were identified from the nearly 30,000 M2 plants screened, and all three mutants that were recovered had mutations in the same gene, *SOQ1*. Many repair mutants also display visible growth phenotypes, especially when grown in high light [5,11,65,69], whereas *soq1* grew just as well as wild-type in constant high light or temperature stress. During light curves, the photochemical efficiency as measured by ΦPSII and qP did not deviate from wild-type levels, also suggesting that reaction centers maintained their ability to do charge separation [15]. Finally, sustained quenching of F_o' after light exposure and experiments using the chloroplast protein synthesis inhibitor lincomycin suggest that quenching in the *soq1* mutant is occurring in the antenna and not reaction centers (Figure 2.9) [73].

Having ruled out the other known components of NPQ, we conclude that the quenching in *soq1* is a form of qI that is unrelated to PSII photoinhibition. It has been observed that the amount of qI in plants treated with high light can often not be explained by the amount of damaged PSII [73], suggesting that qI is heterogenous and consists of multiple mechanisms. Photoprotective qI has been observed in many species including overwintering evergreens and shade plants transferred to high light [1]. While this quenching is always correlated with zeaxanthin formation, in some cases it also requires the pH gradient [27,72]. It is interesting to speculate that the quenching seen in *soq1* may be a form of sustained quenching that is activated during prolonged stress by down regulation or inhibition of the SOQ1 protein. High light exposure in these stressed plants

and the slow kinetics of this quenching could be a form of molecular memory preventing damage from subsequent high light exposure. This is similar to the role proposed for zeaxanthin in qE and qZ [14,16] but with a more prolonged effect. This possibility is supported by the fact that the quenching in *soq1* decreases the average lifetime of excited chlorophyll (Figure 2.11). As this quenching in *soq1* does not depend on zeaxanthin formation, it would either be a completely new form of quenching or indicate that the observed relationship between qI and zeaxanthin is a coincidence. Further experiments will be required to test this hypothesis and determine if and under what conditions this quenching occurs in wild-type plants.

The *soq1* mutations mapped to a previously uncharacterized gene encoding a chloroplast-targeted protein. Multiple alleles, including several T-DNA lines, and complementation with untagged and tagged versions of the SOQ1 cDNA confirmed that it was the locus responsible for the phenotype. The SOQ1 protein contains three domains, but only the Trx-like and NHL domains are required for the NPQ phenotype as demonstrated by complementation with a truncated version of the protein lacking the HAD domain. Immunoblot analysis confirmed proteomics data showing that SOQ1 is located in the thylakoid membrane. We have also demonstrated by protease protection assays (Figure 2.18) that SOQ1 likely has a transmembrane spanning helix from amino acids 325-344. The 80 kDa fragment that is protected from proteolysis would correspond to the Trx-like and NHL domains, which would be located in the thylakoid lumen. The stroma-exposed HAD domain is readily digested by either trypsin or thermolysin. While it is possible that the protein is entirely stroma-exposed and simply partially resistant to digestion as is the case with PsaD and FNR, this possibility seems unlikely as the 80 kDa fragment degraded rapidly with the addition of detergent similarly to the the lumenal PsbO protein, whereas the smaller PsaD and FNR fragments remained resistant to proteolysis even in the presence of detergent. There are also 111 trypsin and 316 thermolysin cleavage sites found throughout the protein, and presumably some of these are surface-exposed and readily available to cleavage.

Phylogenetic analysis of SOQ1 supports the hypothesis that the Trx-like/NHL domains have a different origin than the HAD domain and possibly a unique function. Many species outside of the plant kingdom contain a homolog corresponding to the Trx-like/NHL domains of SOQ1. As none of the Trx-like/NHL proteins from animals and bacteria have a HAD domain, it seems possible that a gene fusion occurred early in the evolution of the Viridiplantae, resulting in targeting of the Trx-like/NHL domains to the chloroplast where they have developed a role in photosynthetic regulation and light harvesting. This view is reinforced by the loss of the HAD domain in certain algal clades, the loss of the NHL domain in Maize and Sorghum, and the possibility that proteins with only the HAD domain are made by alternative splicing.

The Trx-like domain of SOQ1 is a member of the unique TlpA-like subgroup within the Trx superfamily. The proteins within this family appear to be distantly related to the DsbD protein from bacteria. DsbD is a transmembrane protein involved in transferring reducing power into the oxidizing periplasmic space [67]. Cysteines within the membrane of DsbD are reduced by cytoplasmic Trx, and then those electrons are transferred to soluble receiver domains of DsbD in the periplasm [64]. From there, the reduction pathway can split into at least three different routes: the cytochrome biogenesis pathway through DsbE/CcmG [23], the protein isomerization pathway through DsbC

[62], or a pathway to reduce sulfenic groups through DsbG [17]. Members of the TlpA family appear to have similar functions, with characterized roles in cytochrome maturation [9,22] and methionine sulfoxide reductase regeneration [75].

The oxidizing environment of the bacterial periplasm is analogous to that of the thylakoid lumen and mitochondrial intermembrane space [31,33]. The structure of the SOQ1 Trx-like domain and the localization of this domain in the thylakoid lumen suggest that it may have a function similar to that of the bacterial proteins in this family. Several proteins have already been identified as playing a role in the cytochrome biogenesis pathway of green algal and plant thylakoids: the CCS pathway that was characterized in *Chlamydomonas reinhardtii* [54,76] and the CCDA/HCF164 pathway characterized in Arabidopsis [44,58]. SOQ1 is not required for cytochrome biogenesis, however, as the *soq1* mutant does not have the drastic growth and high chlorophyll fluorescence phenotypes seen in these other cytochrome assembly mutants. The oxidizing environment of the thylakoid lumen would presumably require a system to maintain the folding of proteins, similar to what is seen in bacteria and with the protein disulfide isomerases of the endoplasmic reticulum [29,74]. A system to reduce oxidized cysteines or methionines may also be necessary in the thylakoid lumen. It is interesting to speculate that SOQ1 may be involved in reducing immunophilins, given their presence in both animals and plants and their role in protein folding [30].

Further characterization of SOQ1 will be required to determine its exact role in photosynthetic regulation. Presumably this form of quenching is undesirable for healthy plants growing in naturally fluctuating light conditions as it is important that any quenching mechanism can be turned off rapidly when the stress is removed. Experiments, currently underway, in which wild-type and *soq1* plants are given high light stress and then transferred to very low light may result in a growth phenotype if this hypothesis is correct. Alternatively, growth under variable light, such as plants would experience in their natural environment, may also help address this question.

References

1. Adams III, W.W., Zarter, C.R., Mueh, K.E., Amiard, V., and Demmig-Adams, B. (2006). Energy Dissipation and Photoinhibition: A Continuum of Photoprotection. Photoprotection, Photoinhibition, Gene Regulation, and Environment. pp. 49–64.
2. Amarnath, K., Zaks, J., Park, S.D., Niyogi, K.K., and Fleming, G.R. (2012). Fluorescence lifetime snapshots reveal two rapidly reversible mechanisms of photoprotection in live cells of Chlamydomonas reinhardtii. Proc. Natl. Acad. Sci. U.S.A. *109*, 8405–8410.
3. Andersson, J., Walters, R.G., Horton, P., and Jansson, S. (2001). Antisense Inhibition of the Photosynthetic Antenna Proteins CP29 and CP26: Implications for the Mechanism of Protective Energy Dissipation. The Plant Cell Online *13*, 1193 –1204.
4. Anisimova, M., and Gascuel, O. (2006). Approximate likelihood-ratio test for branches: A fast, accurate, and powerful alternative. Syst. Biol. *55*, 539–552.

5. Armbruster, U., Zühlke, J., Rengstl, B., Kreller, R., Makarenko, E., Rühle, T., Schünemann, D., Jahns, P., Weisshaar, B., Nickelsen, J., et al. (2010). The Arabidopsis Thylakoid Protein PAM68 Is Required for Efficient D1 Biogenesis and Photosystem II Assembly. The Plant Cell Online *22*, 3439 –3460.
6. Bellafiore, S., Barneche, F., Peltier, G., and Rochaix, J.-D. (2005). State transitions and light adaptation require chloroplast thylakoid protein kinase STN7. Nature *433*, 892–895.
7. Brooks, M.D., and Niyogi, K.K. (2011). Use of a pulse-amplitude modulated chlorophyll fluorometer to study the efficiency of photosynthesis in Arabidopsis plants. Methods Mol. Biol. *775*, 299–310.
8. Burroughs, A.M., Allen, K.N., Dunaway-Mariano, D., and Aravind, L. (2006). Evolutionary genomics of the HAD superfamily: understanding the structural adaptations and catalytic diversity in a superfamily of phosphoesterases and allied enzymes. J. Mol. Biol. *361*, 1003–1034.
9. Capitani, G., Rossmann, R., Sargent, D.F., Grütter, M.G., Richmond, T.J., and Hennecke, H. (2001). Structure of the soluble domain of a membrane-anchored thioredoxin-like protein from Bradyrhizobium japonicum reveals unusual properties. J. Mol. Biol. *311*, 1037–1048.
10. Chen, C.K.-M., Chan, N.-L., and Wang, A.H.-J. (2011). The many blades of the β-propeller proteins: conserved but versatile. Trends Biochem. Sci. *36*, 553–561.
11. Chen, M., Choi, Y., Voytas, D.F., and Rodermel, S. (2000). Mutations in the Arabidopsis VAR2 locus cause leaf variegation due to the loss of a chloroplast FtsH protease. The Plant Journal *22*, 303–313.
12. Chevenet, F., Brun, C., Bañuls, A.-L., Jacq, B., and Christen, R. (2006). TreeDyn: towards dynamic graphics and annotations for analyses of trees. BMC Bioinformatics *7*, 439.
13. Clough, S.J., and Bent, A.F. (1998). Floral dip: a simplified method for Agrobacterium-mediated transformation of Arabidopsis thaliana. Plant J. *16*, 735–743.
14. Dall'Osto, L., Caffarri, S., and Bassi, R. (2005). A Mechanism of Nonphotochemical Energy Dissipation, Independent from PsbS, Revealed by a Conformational Change in the Antenna Protein CP26. The Plant Cell Online *17*, 1217 –1232.
15. Demmig, B., and Björkman, O. (1987). Comparison of the effect of excessive light on chlorophyll fluorescence (77K) and photon yield of O2 evolution in leaves of higher plants. Planta *171*, 171–184.
16. Demmig-Adams, B., and Adams III, W.W. (1996). The role of xanthophyll cycle carotenoids in the protection of photosynthesis. Trends in Plant Science *1*, 21–26.
17. Depuydt, M., Leonard, S.E., Vertommen, D., Denoncin, K., Morsomme, P., Wahni, K., Messens, J., Carroll, K.S., and Collet, J.-F. (2009). A Periplasmic Reducing System Protects Single Cysteine Residues from Oxidation. Science *326*, 1109–1111.

18. Dereeper, A., Audic, S., Claverie, J.-M., and Blanc, G. (2010). BLAST-EXPLORER helps you building datasets for phylogenetic analysis. BMC Evol. Biol. *10*, 8.
19. Dereeper, A., Guignon, V., Blanc, G., Audic, S., Buffet, S., Chevenet, F., Dufayard, J.-F., Guindon, S., Lefort, V., Lescot, M., et al. (2008). Phylogeny.fr: robust phylogenetic analysis for the non-specialist. Nucleic Acids Res. *36*, W465–469.
20. Elrad, D., Niyogi, K.K., and Grossman, A.R. (2002). A Major Light-Harvesting Polypeptide of Photosystem II Functions in Thermal Dissipation. The Plant Cell Online *14*, 1801 –1816.
21. Emanuelsson, O., Nielsen, H., Brunak, S., and von Heijne, G. (2000). Predicting subcellular localization of proteins based on their N-terminal amino acid sequence. J. Mol. Biol. *300*, 1005–1016.
22. Erlendsson, L.S., Acheson, R.M., Hederstedt, L., and Le Brun, N.E. (2003). Bacillus subtilis ResA is a thiol-disulfide oxidoreductase involved in cytochrome c synthesis. J. Biol. Chem. *278*, 17852–17858.
23. Fabianek, R.A., Hennecke, H., and Thöny-Meyer, L. (1998). The Active-Site Cysteines of the Periplasmic Thioredoxin-Like Protein CcmG of Escherichia coli Are Important but Not Essential for Cytochrome c Maturation In Vivo. Journal of Bacteriology *180*, 1947 –1950.
24. Fleischmann, M.M., Ravanel, S., Delosme, R., Olive, J., Zito, F., Wollman, F.-A., and Rochaix, J.-D. (1999). Isolation and Characterization of Photoautotrophic Mutants ofChlamydomonas reinhardtii Deficient in State Transition. Journal of Biological Chemistry *274*, 30987 –30994.
25. Follo, C., and Isidoro, C. (2008). A fast and simple method for simultaneous mixed site-specific mutagenesis of a wide coding sequence. Biotechnol. Appl. Biochem. *49*, 175–183.
26. Gadda, G., Aliverti, A., Ronchi, S., and Zanetti, G. (1990). Structure-function relationship in spinach ferredoxin-NADP+ reductase as studied by limited proteolysis. J. Biol. Chem. *265*, 11955–11959.
27. Gilmore, A.M., and Björkman, O. (1995). Temperature-sensitive coupling and uncoupling of ATPase-mediated, nonradiative energy dissipation: Similarities between chloroplasts and leaves. Planta *197*, 646–654.
28. Guindon, S., and Gascuel, O. (2003). A simple, fast, and accurate algorithm to estimate large phylogenies by maximum likelihood. Syst. Biol. *52*, 696–704.
29. Hatahet, F., and Ruddock, L.W. (2009). Protein disulfide isomerase: a critical evaluation of its function in disulfide bond formation. Antioxid. Redox Signal. *11*, 2807–2850.
30. He, Z., Li, L., and Luan, S. (2004). Immunophilins and Parvulins. Superfamily of Peptidyl Prolyl Isomerases in Arabidopsis. Plant Physiology *134*, 1248 –1267.
31. Herrmann, J.M., Kauff, F., and Neuhaus, H.E. (2009). Thiol oxidation in bacteria, mitochondria and chloroplasts: Common principles but three unrelated machineries? Biochimica Et Biophysica Acta (BBA) - Molecular Cell Research *1793*, 71–77.

32. Hou, C.-X., Pursiheimo, S., Rintamäki, E., and Aro, E.-M. (2002). Environmental and metaboliccontrol of LHCII protein phosphorylation: revealing the mechanismsfor dual regulation of the LHCII kinase. Plant, Cell & Environment *25*, 1515–1525.
33. Hu, J., Dong, L., and Outten, C.E. (2008). The Redox Environment in the Mitochondrial Intermembrane Space Is Maintained Separately from the Cytosol and Matrix. Journal of Biological Chemistry *283*, 29126 –29134.
34. Jander, G., Norris, S.R., Rounsley, S.D., Bush, D.F., Levin, I.M., and Last, R.L. (2002). Arabidopsis Map-Based Cloning in the Post-Genome Era. Plant Physiology *129*, 440 –450.
35. Jenny, A., Mark, W., Robin G., W., Caroline A., H., Alexander V., R., Peter, H., and Stefan, J. (2003). Absence of the Lhcb1 and Lhcb2 proteins of the light-harvesting complex of photosystem II – effects on photosynthesis, grana stacking and fitness. The Plant Journal *35*, 350–361.
36. Johnson, M., Zia, A., and Ruban, A. (2012). Elevated ΔpH restores rapidly reversible photoprotective energy dissipation in *Arabidopsis* chloroplasts deficient in lutein and xanthophyll cycle activity. Planta *235*, 193–204.
37. Johnson, M.P., and Ruban, A.V. (2010). Arabidopsis plants lacking PsbS protein possess photoprotective energy dissipation. The Plant Journal *61*, 283– 289.
38. Johnson, M.P., and Ruban, A.V. (2011). Restoration of Rapidly Reversible Photoprotective Energy Dissipation in the Absence of PsbS Protein by Enhanced ΔpH. Journal of Biological Chemistry *286*, 19973 –19981.
39. Kemena, C., and Notredame, C. (2009). Upcoming challenges for multiple sequence alignment methods in the high-throughput era. Bioinformatics *25*, 2455–2465.
40. Koonin, E.V., and Tatusov, R.L. (1994). Computer analysis of bacterial haloacid dehalogenases defines a large superfamily of hydrolases with diverse specificity. Application of an iterative approach to database search. J. Mol. Biol. *244*, 125–132.
41. Kovács, L., Damkjær, J., Kereïche, S., Ilioaia, C., Ruban, A.V., Boekema, E.J., Jansson, S., and Horton, P. (2006). Lack of the Light-Harvesting Complex CP24 Affects the Structure and Function of the Grana Membranes of Higher Plant Chloroplasts. The Plant Cell Online *18*, 3106 –3120.
42. Krilov, L.R., Rubin, L.G., Frogel, M., Gloster, E., Ni, K., Kaplan, M., and Lipson, S.M. (1990). Disseminated adenovirus infection with hepatic necrosis in patients with human immunodeficiency virus infection and other immunodeficiency states. Rev. Infect. Dis. *12*, 303–307.
43. Kyle, D.J., Staehelin, L.A., and Arntzen, C.J. (1983). Lateral mobility of the light-harvesting complex in chloroplast membranes controls excitation energy distribution in higher plants. Archives of Biochemistry and Biophysics *222*, 527–541.
44. Lennartz, K., Plücken, H., Seidler, A., Westhoff, P., Bechtold, N., and Meierhoff, K. (2001). HCF164 Encodes a Thioredoxin-Like Protein Involved in the Biogenesis of the Cytochrome b6f Complex in Arabidopsis. The Plant Cell Online *13*, 2539 –2551.

45. Li, X.-P., Bjorkman, O., Shih, C., Grossman, A.R., Rosenquist, M., Jansson, S., and Niyogi, K.K. (2000). A pigment-binding protein essential for regulation of photosynthetic light harvesting. Nature *403*, 391–395.
46. Li, X.-P., Phippard, A., Pasari, J., and Niyogi, K.K. (2002). Structure–function analysis of photosystem II subunit S (PsbS) *in vivo*. Functional Plant Biol. *29*, 1131–1139.
47. Li, Z., Ahn, T.K., Avenson, T.J., Ballottari, M., Cruz, J.A., Kramer, D.M., Bassi, R., Fleming, G.R., Keasling, J.D., and Niyogi, K.K. (2009). Lutein Accumulation in the Absence of Zeaxanthin Restores Nonphotochemical Quenching in the Arabidopsis thaliana npq1 Mutant. The Plant Cell Online *21*, 1798 –1812.
48. Livingston, A.K., Cruz, J.A., Kohzuma, K., Dhingra, A., and Kramer, D.M. (2010). An Arabidopsis Mutant with High Cyclic Electron Flow around Photosystem I (hcef) Involving the NADPH Dehydrogenase Complex. The Plant Cell Online *22*, 221 –233.
49. Lu, Y. (2011). The occurrence of a thylakoid-localized small zinc finger protein in land plants. Plant Signal Behav *6*, 1881–1885.
50. Messens, J., and Collet, J.-F. (2006). Pathways of disulfide bond formation in Escherichia coli. Int. J. Biochem. Cell Biol. *38*, 1050–1062.
51. Michelmore, R.W., Paran, I., and Kesseli, R.V. (1991). Identification of markers linked to disease-resistance genes by bulked segregant analysis: a rapid method to detect markers in specific genomic regions by using segregating populations. Proc. Natl. Acad. Sci. U.S.A. *88*, 9828–9832.
52. Minagawa, J. (2011). State transitions—The molecular remodeling of photosynthetic supercomplexes that controls energy flow in the chloroplast. Biochimica Et Biophysica Acta (BBA) - Bioenergetics *1807*, 897–905.
53. Minai, L., Cohen, Y., Chitnis, P.R., and Nechushtai, R. (1996). The precursor of PsaD assembles into the photosystem I complex in two steps. Proceedings of the National Academy of Sciences *93*, 6338 –6342.
54. Nakamoto, S.S., Hamel, P., and Merchant, S. (2000). Assembly of chloroplast cytochromes b and c. Biochimie *82*, 603–614.
55. Neff, M.M., Neff, J.D., Chory, J., and Pepper, A.E. (1998). dCAPS, a simple technique for the genetic analysis of single nucleotide polymorphisms: experimental applications in Arabidopsis thaliana genetics. Plant J. *14*, 387–392.
56. Niyogi, K.K., Bjorkman, O., and Grossman, A.R. (1997). Chlamydomonas Xanthophyll Cycle Mutants Identified by Video Imaging of Chlorophyll Fluorescence Quenching. The Plant Cell Online *9*, 1369 –1380.
57. Niyogi, K.K., Grossman, A.R., and Björkman, O. (1998). Arabidopsis Mutants Define a Central Role for the Xanthophyll Cycle in the Regulation of Photosynthetic Energy Conversion. The Plant Cell Online *10*, 1121 –1134.
58. Page, M.L.D., Hamel, P.P., Gabilly, S.T., Zegzouti, H., Perea, J.V., Alonso, J.M., Ecker, J.R., Theg, S.M., Christensen, S.K., and Merchant, S. (2004). A homolog of prokaryotic thiol disulfide transporter CcdA is required for the assembly of the cytochrome b6f complex in Arabidopsis chloroplasts. J. Biol. Chem. *279*, 32474–32482.

59. Peers, G., Truong, T.B., Ostendorf, E., Busch, A., Elrad, D., Grossman, A.R., Hippler, M., and Niyogi, K.K. (2009). An ancient light-harvesting protein is critical for the regulation of algal photosynthesis. Nature *462*, 518–521.
60. Porra, R.J. (2002). The chequered history of the development and use of simultaneous equations for the accurate determination of chlorophylls a and b. Photosyn. Res. *73*, 149–156.
61. Pribil, M., Pesaresi, P., Hertle, A., Barbato, R., and Leister, D. (2010). Role of Plastid Protein Phosphatase TAP38 in LHCII Dephosphorylation and Thylakoid Electron Flow. PLoS Biol *8*, e1000288.
62. Rietsch, A., Belin, D., Martin, N., and Beckwith, J. (1996). An *in vivo* pathway for disulfide bond isomerization in Escherichia coli. Proceedings of the National Academy of Sciences *93*, 13048 –13053.
63. Rintamäki, E., Martinsuo, P., Pursiheimo, S., and Aro, E.-M. (2000). Cooperative regulation of light-harvesting complex II phosphorylation via the plastoquinol and ferredoxin-thioredoxin system in chloroplasts. Proceedings of the National Academy of Sciences *97*, 11644 –11649.
64. Rozhkova, A., Stirnimann, C.U., Frei, P., Grauschopf, U., Brunisholz, R., Grütter, M.G., Capitani, G., and Glockshuber, R. (2004). Structural basis and kinetics of inter- and intramolecular disulfide exchange in the redox catalyst DsbD. EMBO J. *23*, 1709–1719.
65. Sakamoto, W., Tamura, T., Hanba-Tomita, Y., Sodmergen, and Murata, M. (2002). The VAR1 locus of Arabidopsis encodes a chloroplastic FtsH and is responsible for leaf variegation in the mutant alleles. Genes to Cells *7*, 769–780.
66. Shapiguzov, A., Ingelsson, B., Samol, I., Andres, C., Kessler, F., Rochaix, J.-D., Vener, A.V., and Goldschmidt-Clermont, M. (2010). The PPH1 phosphatase is specifically involved in LHCII dephosphorylation and state transitions in Arabidopsis. Proceedings of the National Academy of Sciences *107*, 4782 – 4787.
67. Stewart, E.J., Katzen, F., and Beckwith, J. (1999). Six conserved cysteines of the membrane protein DsbD are required for the transfer of electrons from the cytoplasm to the periplasm of Escherichia coli. EMBO J. *18*, 5963–5971.
68. Sun, Q., Zybailov, B., Majeran, W., Friso, G., Olinares, P.D.B., and van Wijk, K.J. (2009). PPDB, the Plant Proteomics Database at Cornell. Nucleic Acids Research *37*, D969 –D974.
69. Sun, X., Fu, T., Chen, N., Guo, J., Ma, J., Zou, M., Lu, C., and Zhang, L. (2010). The Stromal Chloroplast Deg7 Protease Participates in the Repair of Photosystem II after Photoinhibition in Arabidopsis. Plant Physiology *152*, 1263 –1273.
70. Takahashi, S., Bauwe, H., and Badger, M. (2007). Impairment of the photorespiratory pathway accelerates photoinhibition of photosystem II by suppression of repair but not acceleration of damage processes in Arabidopsis. Plant Physiol. *144*, 487–494.
71. Di Tommaso, P., Moretti, S., Xenarios, I., Orobitg, M., Montanyola, A., Chang, J.-M., Taly, J.-F., and Notredame, C. (2011). T-Coffee: a web server for the

multiple sequence alignment of protein and RNA sequences using structural information and homology extension. Nucleic Acids Res. *39*, W13–17.
72. Verhoeven, A.S., Adams, W.W., and Demmig-Adams, B. (1998). Two forms of sustained xanthophyll cycle-dependent energy dissipation in overwintering Euonymus kiautschovicus. Plant, Cell & Environment *21*, 893–903.
73. Walters, R.G., and Horton, P. (1993). Theoretical assessment of alternative mechanisms for non-photochemical quenching of PS II fluorescence in barley leaves. Photosynthesis Research *36*, 119–139.
74. Wilkinson, B., and Gilbert, H.F. (2004). Protein disulfide isomerase. Biochimica Et Biophysica Acta (BBA) - Proteins & Proteomics *1699*, 35–44.
75. Wu, J., Neiers, F., Boschi-Muller, S., and Branlant, G. (2005). The N-terminal domain of PILB from Neisseria meningitidis is a disulfide reductase that can recycle methionine sulfoxide reductases. J. Biol. Chem. *280*, 12344–12350.
76. Xie, Z., and Merchant, S. (1998). A novel pathway for cytochromes c biogenesis in chloroplasts. Biochimica Et Biophysica Acta (BBA) - Bioenergetics *1365*, 309–318.

Chapter 3

SOQ1 Interacts with Thylakoid Proteins and Affects the Organization of Supercomplexes

Summary

Plants must balance light-harvesting and the protection of the photosynthetic apparatus by quenching excess light and preventing the formation of reactive oxygen species. The SOQ1 protein is a novel thylakoid membrane component that is essential to prevent the formation of a quenching site and maintain photosynthetic efficiency after exposure to high light. This function requires thioredoxin-like (Trx-like) and beta propeller (NHL) domains located in the thylakoid lumen. It was found that SOQ1 binds to thylakoid complexes, likely in substochiometric amounts. While there was little if any difference in the amount of abundant thylakoid proteins, two-dimensional separation of proteins by pKa and molecular weight as well as labeling of reduced thiols using monobromobimane revealed differences between wild-type and mutant plants in high light. To investigate how SOQ1 prevents quenching, identification of interaction partners and targets was attempted by several biochemical methods including single cysteine mutant trap experiments and yeast two-hybrid screening. These results indicate that SOQ1 might have some overlapping functions with the Trx-like thylakoid protein HCF164. Finally, the structure of whole chloroplasts/thylakoids and the organization of photosytem II within grana of the *soq1* mutant were analyzed using electron microscopy and atomic force microscopy, respectively. While chloroplast structure remains similar to wild-type, the organization of photosystem II was unique in *soq1*. The possible significance of these results is discussed in the context of explaining the NPQ phenotype of *soq1* and planning future experiments to further our understanding of this type of quenching.

Preface

Alexander Hertle, Bibiana Onoa, Xin Hou, Patricia Grob and Gigi Kemalyan contributed to the work in this chapter. Alexander Hertle aided with experiments and performed biochemical characterization of SOQ1 including 2-D gels and mBBr experiments. Bibiana Onoa performed the AFM imaging and Patricia Grob and Gigi Kemalyan did the electron microscopy. Xin Hou screened the lumenal yeast two-hybrid library.

Introduction

Plants are able to transfer absorbed light energy to the reaction center and perform charge separation with near 100% quantum efficiency. This requires a very precise

arrangement of pigment molecules within the protein complexes of the thylakoid membrane. At higher light intensities, the amount of light absorbed exceeds that which can be used, and excess absorbed light energy can be dissipated as heat through various nonphotochemical quenching (NPQ) mechanisms. In order to optimize photosynthetic growth, it is important that these quenching mechanisms can be switched on and off in a controlled manner depending on light conditions. The isolation and initial characterization of a novel mutant, *soq1*, that affects NPQ was presented in Chapter 2. We proposed that in wild-type plants the SOQ1 protein plays a role in preventing the formation of a quenching site that is undesirable due to its slow relaxation kinetics. In this chapter we will address how the absence of SOQ1 causes the NPQ phenotype by comparing the changes that occur in wild-type and *soq1* mutant plants upon exposure to high light by biochemical and high-resolution imaging techniques.

The predicted structure of the Trx-like domain in SOQ1 suggested that the protein may function in the transfer of reducing power across the thylakoid membrane and into the lumen. This hypothesis is based on the sequence and secondary structure that indicates SOQ1 is part of the TlpA-DipZ family of thioredoxin-like proteins. This family is a subset of the thioredoxin superfamily and has structural similarity to the soluble C-terminal of DsbD/DipZ [6]. In order to maintain protein folding and to attach cofactors in the oxidizing periplasm, the integral membrane protein DsbD transfers reducing equivalents to other Trx-like intermediates in the periplasm and eventually reduces target proteins [20]. Proteins in the TlpA-DipZ family have been shown to have similar functions in reducing target proteins to facilitate cytochrome biogenesis [6,10] or methionine sulfoxide reductase activity [Wu].

In higher plant thylakoids, reducing power can be transferred to the oxidizing lumen by the CCDA/HCF164 pathway [21]. This system is analogous to the bacterial DsbD pathway with CCDA corresponding to the transmembrane portion of DsbD and HCF164 to DsbE/CcmG [12]. Both CCDA and HCF164 have been shown to be thylakoid membrane proteins and to be involved in cytochrome b_6f biogenesis [18,22]. Despite the oxidizing environment, no protein in the thylakoid lumen has been identified with a role similar to that of DsbG [7] or methionine sulfoxide reductase [4] in reducing oxidized amino acids, or that of DsbC in maintaining protein folding [24]. Given the the location and sequence of SOQ1, we predict that it is involved in maintaining the folding of thylakoid lumen proteins through reduction of disulfide bridges or individual oxidized amino acid residues. The quenching phenotype in *soq1* plants suggests that a target of this activity, either directly or indirectly, is a component of the PSII antenna

The mechanisms of NPQ are also known to be closely correlated with changes in the stacking properties of thylakoid membranes and organization of complexes within the grana. State transitions are known to involve stacking and unstacking of the thylakoid membrane as it switches between state 1 and state 2 [8]. Recent work on qE has indicated that reorganization of PSII and LHCII in the thylakoid membrane may act as the switch between light harvesting and quenching of absorbed energy [15]. Photoinhibition is also thought to involve expansion of the thylakoid lumen and structural changes to the membrane in order facilitate diffusion of damaged PSII to the stroma lamellae where they are reassembled [16]. Could the quenching in *soq1* be the result of aberrant organization of thylakoids or the supercomplexes within the grana? If so, it will also need to be determined if SOQ1 has a role in maintaining organization or if the

change is simply the consequence of the SOQ1 protein being absent.

In this chapter, these questions are addressed by comparing dark- and high-light-treated *soq1* mutant plants to wild type. This was done using several several biochemical techniques to analyze the protein and supercomplex content from isolated thylakoids as well as using high-resolution imaging techniques to look at chloroplast and thylakoid structures. Finally, interactions between SOQ1 and possible targets are explored by a variety of methods.

Methods

Mono-Cysteine Trap Experiment - His-tagged C434S SOQ1 protein was purified as described in Chapter 2 in the presence of DTT to keep it in the reduced state. *soq1-1* plants were treated with high light for 30 minutes, and then chloroplasts were isolated as described in Chapter 2. Chloroplasts were solublized with either 1% (v/v) Triton X-100, or 0.5% (w/v) n-dodecyl-alpha-D-maltoside (alpha-DM) for 30 minutes at 4ºC. Unsolubilized material was pelleted by centrifugation at 20,000 g for 15 minutes, and 1 mg of purified SOQ1 protein was added to the supernatant and allowed to mix at 4ºC for 2-3 hours. The sample was then applied to a nickel column and washed extensively with resuspension buffer containing 40 mM imidazole and 0.2% alpha-DM. Elutions were done with resuspension buffer containing 500 mM imidazole and 0.2% alpha-DM.

For transient expression, C-terminal FLAG-tagged C431S and C434S SOQ1 constructs were made in pEarleygate100 [9]. Constructs were transformed into Agrobacterium, and cells were resuspended in freshly prepared induction medium (10 mM $MgCl_2$, 10 mM MES pH 5.6, 150 mM acetosyringone) and incubated for 2-3 hours. The OD_{600} of the solution was then adjusted to 0.5, and *Nicotiana benthamiana* leaves from 4-6 week-old plants were infiltrated with a 1 mL syringe. Plants were placed under continuous light for 72 hours. Infiltrated leaves were exposed to high light for 20 minutes, and chloroplasts were isolated and solubilized as described above. The FLAG-Immunoprecipitation Kit (Sigma, USA) was used following the manufacturer's instructions with the addition of 0.5% (w/v) alpha-DM and Halt Protease Inhibitor Cocktail (Thermo Fisher Scientific Inc., USA). Protein was eluted with 40 µL 3xFLAG peptide in wash buffer. 2-D gels were run by adding 4x LDS buffer to half the sample and running it under non-reducing conditions for the first dimension on a NuPAGE 3-8% Tris-Acetate Gel (Invitrogen, USA). Lanes were cut from the gel and soaked in a solution containing 100 mM DTT before running the second dimension on a 10% Tris-glycine SDS gel.

Blue Native PAGE, Isoelectric Focusing and mBBr - Wild-type and *soq1-1* mutant plants were treated with high light (2,000 µmol photons m^{-2} sec^{-1}) for 90 minutes. Leaves were homogenized in thylakoid isolation buffer (100 mM Tricine/NaOH pH 7.8, 400 mM sorbitol, 10 mM NaF, 10 mM PMSF) at 4°C. Chloroplasts and thylakoids were obtained by centrifugation at 1,400 g for 5 min at 4°C. The chloroplasts and thylakoids were resuspended in resuspension buffer (100 mM HEPES, pH 7.6, 5 mM EDTA) for 30 min. The suspension was centrifuged with 10,000 g for 5 min at room temperature. The pellet was resuspended in 25 mM Bis/Tris pH 7.0, 20% glycerol.

For mBBr labeling, thylakoids (50 μg of chlorophyll) in resuspension buffer (100 mM HEPES, pH 7.6, 5 mM EDTA) were supplemented with 20 mM mBBr and incubated for 30 minutes at room temperature. Excess mBBr was removed by protein precipitation using 4 volumes of 20% TCA (dissolved in acetone) at -20°C for at least 1 hour. Proteins were centrifuged at 12,000 g for 3 minutes. and the precipitate was resuspended in IEF sample buffer (9 M urea, 2 M thiourea, 4% CHAPS, 2.5 mM EGTA, 2.5 mM EDTA and $1/100^{th}$ volume of Biolyte™). After incubation for 1 hour at room temperature, samples were centrifuged at 16,000 g for 1 minute, and the supernatant was applied to an IEF strip, pH gradient 3-10 (Biorad, USA). Following 16 hours of rehydration at room temperature, proteins were focused using a Protean IEF Cell (Biorad, USA). IEF strips were equilibrated in 2x Laemmli buffer containing 100 mM DTT for 30 minutes at room temperature and acetylated for 30 minutes at room temperature in 2x Laemmli buffer containing 200 mM iodacetamide. IEF Strips were applied on top of a 4% stacking gel of a 15% SDS-PAGE gel, and proteins were separated in the second dimension by SDS-PAGE. Following run with 15 mA constant current gels were incubated in 5% acetic acid for at least 16 hours at room temperature. mBBr-labeled proteins were visualized by using UV light of 265 nm.

For Blue Native (BN) gels, thylakoid solubilization was performed as described [25]. Solubilized thylakoids corresponding to 30 μg of chlorophyll were loaded per well and separated on 3-12% native gels (Invitrogen, USA) with 30 V at 4 °C. Lanes were cut and frozen at -20 °C until used. For 2D-BN/SDS-PAGE, BN-PAGE lanes were solubilized in 2x Laemmli buffer containing 100 mM DTT for 45 min. Lanes were applied on top of a 4% stacking gel and separated on 15% SDS-PAGE gels at 15 mA constant current. Following separation, gels were either stained with Coomassie or transferred to nitrocellulose membranes for immunodetection.

Atomic Force Microscopy - BBY particles [2] were prepared from 7-10 week-old plants as described [5] with some modifications. Buffers were made fresh and along with all equipment used were cooled to 4°C before the experiments. All steps were carried out on ice and in the dark. Leaves were cut from plants, and approximately 3-5 g of leaf material per 100 mL B1 (20 mM tricine-KOH pH 7.8, 400 mM NaCl, 2 mM $MgCl_2$, 0.2 mM benzmidine, 1 mM aminocaproic acid) was homogenized in a commercial blender by 8-10 half second pulses. This was filtered through a 41 μm nylon membrane using a light hand-generated vacuum. The solution was then centrifuged for 10 minutes at 4,000 g at 4°C. Supernatant was resuspended in B2 (20 mM Tricine-KOH pH 7.8, 150 mM NaCl, 5 mM $MgCl_2$, 0.2 mM benzamidine, 1 mM aminocaproic acid) and centrifuged for 10 minutes at 6,000 g at 4°C. The supernatant was then resuspended in a small volume of buffer B3 (20 mM HEPES pH 7.5, 15 mM NaCl, 5 mM $MgCl_2$), and the chlorophyll concentration was adjusted to 2.5 mg/mL. To this solution 3/16 volumes of solubilization buffer (7.6% (w/v) alpha-DM, 15 mM NaCl, 5 mM $MgCl_2$) was added and the sample was incubated with gentle rocking for 20 minutes at 4°C in the dark. Insoluble material was then pelleted by centrifuging at 3,500 g for 5 minutes. The supernatant was then centrifuged for 30 minutes at 40,000 g. The pellet was washed once with buffer B3 to remove excess detergent, and the previous spin was repeated. The final pellet was resuspended in a small amount of buffer B4 (20 mM HEPES pH 7.5, 400 mM sorbitol, 15 mM NaCl and 5 mM $MgCl_2$. Sample was frozen immediately in liquid N_2 as 5-10 μL

aliquots.

Grana aliquots were diluted 1:15 in deposition buffer (10 mM Tris-HCl pH 7.5, 150 mM KCl and 25 mM $MgCl_2$) on freshly cleaved ultra-clean grade V mica (Ted Pella Inc., USA) and incubated at room temperature for 1-3 hours. The mica discs were then rinsed with purified 18.2 MΩ deionized water ten times and dried using a gentle N_2 gas flow, perpendicular to the mica surface. AFM measurements were performed with a Multimode AFM Nanoscope V (Bruker Corporation, USA) equipped with a vertical engagement E-scanner (15-µm x 15-µm x 2.5-µm vertical range). The samples were imaged in tapping mode; the probes were excited on resonance with free amplitudes of 2-15 nm and phases of 20-30 degrees. The image amplitude (set point A_s) and free amplitude (A_0) ratio (A_s/A_0) was kept at ~0.8. Images were acquired using silicon cantilevers (Nanosensors), with a high-resonance frequency in the range of 280-350 kHz and a spring constant of 46 N/m. Images (512 x 512 pixels) were captured in the trace direction the scan angle was maintained at 0 degrees. All samples were measured at room temperature in air, at a relative humidity of 30%.

Electron Microscopy - Wild type (Col-0) and the *soq1-1* mutant plants grown on agar plates for 4 weeks were exposed to high light for 30 minutes or dark-acclimated. Isolated chloroplasts and whole leaf samples were high-pressure frozen with a Leica EM PACT2 prior to chemical fixation and resin embedding. Isolated chloroplasts in a re-suspension buffer containing 10% BSA as a cryo-protectant were pipetted into 1.5 mm x 0.1 mm Leica membrane carriers and high-pressure frozen. Samples from whole leaves were removed with a 1.2 mm Harris uni-core punch, immediately coated with a cryo-protectant paste made of dried yeast and 10% methanol, placed into 1.5 mm x 0.2 mm Leica membrane carriers and high-pressure frozen. The frozen samples were transferred to cryo vials containing a liquid N_2-frozen fixative cocktail consisting of 1.0% osmium tetroxide and 0.1% uranyl acetate in 100% acetone, and quick-freeze substituted for 90 minutes [19]. After coming to room temperature, the samples were rinsed in 100% acetone, then microwave infiltrated with Eponate 12 resin, embedded in molds and polymerized at 60˚C for 48 hours. The resin blocks were thin sectioned at 60 nm with a Leica UC7 ultramicrotome, and sections were collected on 3 mm Formvar and carbon coated copper grids. Grids were poststained with 2% uranyl acetate and 0.1% Reynold's lead citrate. Images were acquired with an FEI Tecnai 12 TEM with an accelerating voltage of 120 kV at 18500x magnification.

Yeast Two-Hybrid Analysis - Each construct was built by cDNA fragments amplified by PCR and cloned into the pGBT9.BS and pGAD.GH vectors. The lithium acetate method was used to introduce BD and AD plasmids into yeast strain AH109 [13]. Transformants were selected in SC-Leucine-Tryptophan media and transferred on the interaction selection media (SC-Adenine-Histidine-Leucine-Tryptophan) to score growth as an indicator of protein-protein interaction. For serial dilution assay, exponentially grown yeast cells were harvested and adjusted to OD_{600} = 0.5 with sterilized double-distilled water and diluted 1/10, 1/100 and 1/1000. Yeast cells, 2 µL, were spotted onto SC-Leucine-Tryptophan media and SC-Adenine-Histidine-Leucine-Tryptophan media.

Results

SOQ1 Co-migrates With Thylakoid Complexes

Previous work showed that SOQ1 is a thylakoid membrane protein with domains in the stroma and lumen. To determine if SOQ1 associates with any photosynthetic complexes, we performed blue native PAGE (BN-PAGE) on solubilized thylakoid membranes from high light treated wild-type and *soq1* plants. Complexes were labeled by comparison to previously published BN-PAGE on thylakoid membranes [14]. No obvious differences were observed in the amount or presence of any specific complex when comparing wild-type and mutant gels (Figure 3.1). The lanes were then run in a second dimension with SDS-PAGE and blotted for SOQ1 protein. In wild-type thylakoids, SOQ1 clearly co-migrated with photosynthetic complexes and not as a monomer which would be smaller than the approximately 140 kDa LHCII trimer. The protein signal for SOQ1 formed a streak covering a range of sizes from LHCII trimers to PSII supercomplexes. In addition, there was a strong signal from the wild-type sample that corresponds to what would be very large molecular weight complexes. The sample from the *soq1* mutant unexpectedly had a signal at approximately the expected size for SOQ1, however the shape of the spot suggests that it is non-specific background.

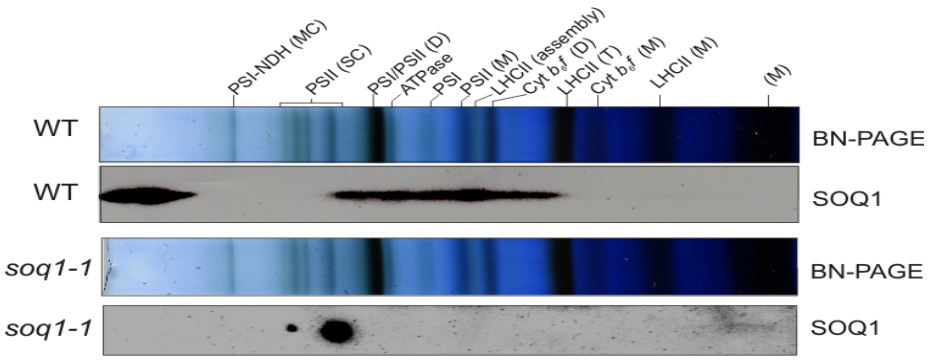

Figure 3.1: Separation of thylakoid complexes by BN-PAGE
Thylakoids were isolated from wild-type (WT) and *soq1-1* plants treated with high light (2,000 µmol photons m^2 s^{-1}) for 90 minutes, and complexes were separated by BN-PAGE as described in the methods. The protein complexes were labeled based on Järvi *et al.* [14]. Lanes from the BN-gels were run in a second dimension by SDS-PAGE and probed for SOQ1.

Absence of SOQ1 Does Not Alter the Composition of Complexes

The phenotype of the *soq1* mutant and the results of the BN-PAGE shown above do not suggest that the mutant is severely impaired in any particular photosynthetic complex, but more subtle differences in the amount or composition of a complex may be different. In order to investigate this possibility, BN-gels from high-light-treated plants

were run in a second dimension using SDS-PAGE and proteins were stained with coomassie (Figure 3.2). The gels showed that most of the complexes from the BN-gel contain all of the expected proteins with similar intensities.

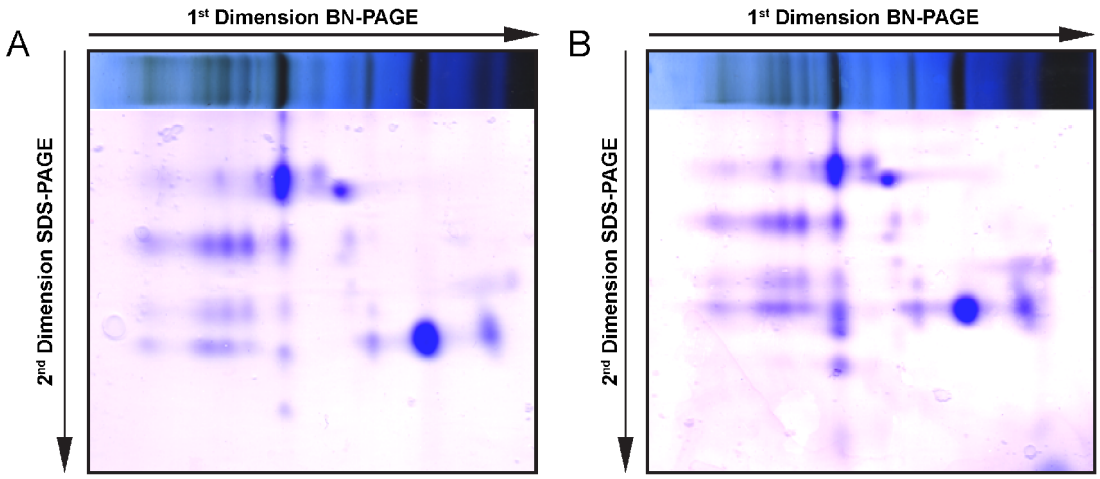

Figure 3.2: 2-D gels of thylakoid protein complexes
Solubilized thylakoids from A) wild-type and B) *soq1-1* leaves treated with high light (2,000 µmol photons m^2 s^{-1}) for 90 minutes. Complexes were first separated by BN-PAGE and then by SDS-PAGE and stained with coomassie.

Isoelectric Focusing/SDS-PAGE Separation of Proteins

Thylakoid proteins from wild type and *soq1* were also separated by their pKa using isoelectric focusing. This method allows the separation of proteins of the same size but with different charge, as well as modified proteins with a different charge (e.g. phosphorylation) from the unmodified protein. Isoelectric focusing was followed by SDS-PAGE in order to further separate proteins based on molecular weight. 2-D gels were made in this way from wild-type (Figure 3.3A) and *soq1* (Figure 3.3B) plants exposed to high light and then stained with coomassie. In order to make differences between the gels more apparent, they were false-colored so that wild-type is red and *soq1* is green and then overlaid (Figure 3.3C). Spots that were unique to one gel or the other were marked with a white square. All but one of these differences are proteins that are found in wild type but not in *soq1*. The identity of these proteins remains to be determined. This can be done by probing for potential interactors identified by other methods (see below) or by excising gel pieces and doing mass spectrometry.

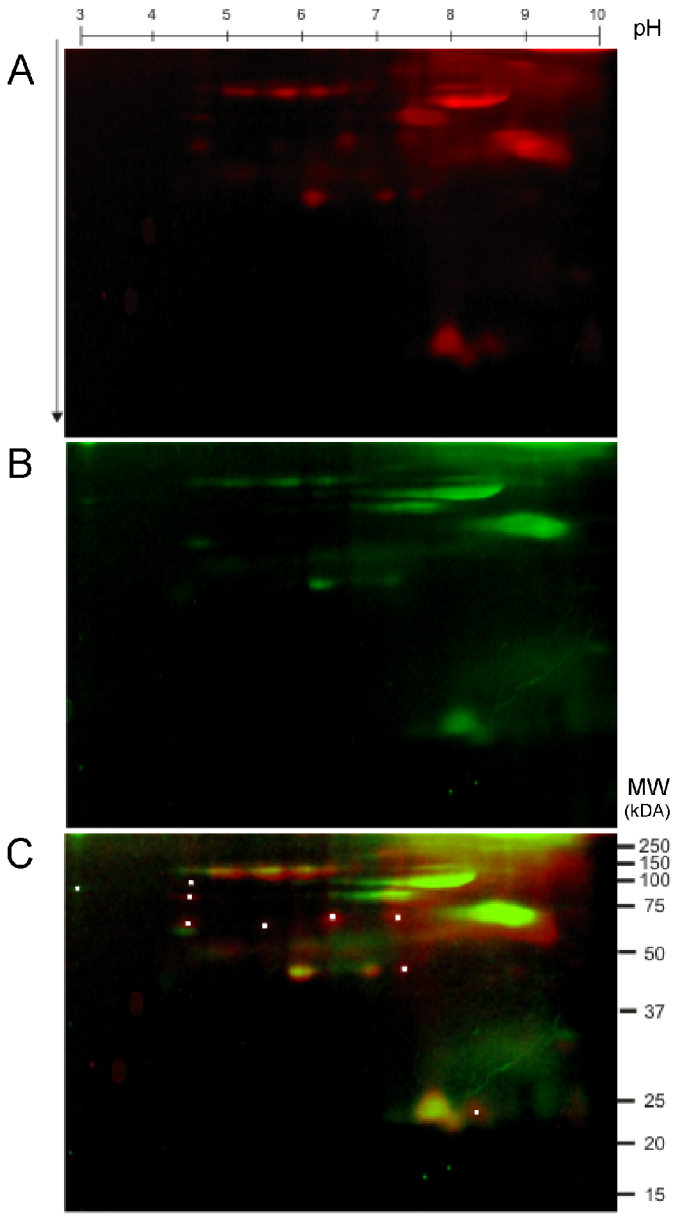

Figure 3.3: 2-D gels separating proteins by pKa and molecular weight
A) Wild-type and B) *soq1* thylakoid proteins isolated from leaves exposed to 2,000 µmol photons m^2 s^{-1} for 90 minutes were separated by isoelectric focusing followed by SDS-PAGE. After staining with coomassie and scanning the gels, images were false-colored and C) overlain in order emphasize differences. White dots indicate spots that only appeared or were shifted in one sample or the other.

Mono-Cysteine Trap Experiments

We undertook several approaches to identify potential targets of the Trx-like domain of SOQ1. Mono-cysteine trap experiments, in which the second cysteine of the Trx-domain is mutated and the target protein cannot be released after formation of the

mixed-disulfide intermediate, has become a common way to identify targets of Trx and Trx-like proteins. Trap experiments were first attempted using recombinant His-tagged C434S SOQ1 from *E. coli* and mixing the purified protein with solubilized thylakoid membranes. Recombinant SOQ1 along with any proteins trapped by a disulfide bond were then purified on a nickel column and separated by SDS-PAGE. Addition of DTT to the sample should reduce the mixed-disulfide and release the target protein (Figure 3.4)

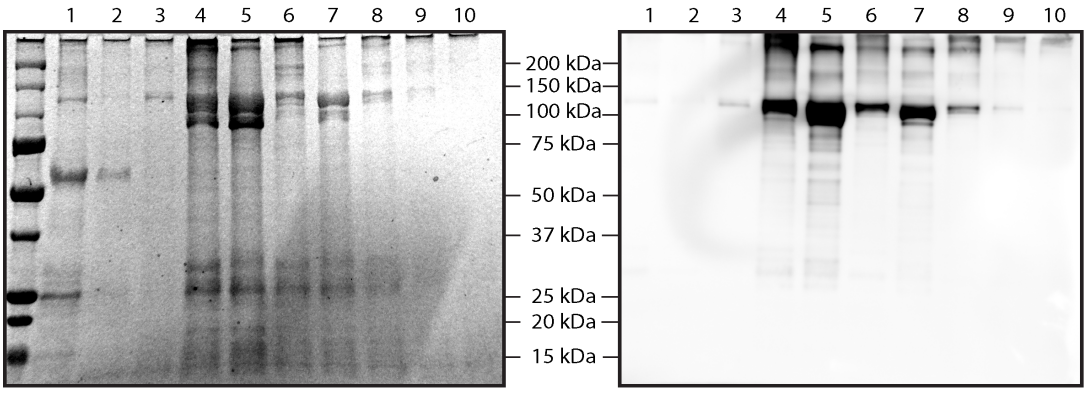

Figure 3.4: Mono-cysteine trap experiment using His-tagged C434S SOQ1
Commassie stained gel (left) and immunoblot using SOQ1 antibody (right) of samples from a mono-cysteine trap experiment using His-tagged C434S SOQ1. Lanes: 1 – flowthrough, 2 – wash, 3 – elution 1, 4 – elution 2, 5 – elution 2 + DTT, 6 – elution 3, 7 – elution 3 + DTT, 8 – elution 4, 9 – elution 5, 10 – elution 6.

Though there are additional bands besides SOQ1 visible in the gel after elution from the column, few of them increase in intensity with the addition of DTT as would be expected for proteins trapped by a mixed disulfide. One band, slightly smaller than SOQ1, does appear to increase in intensity upon DTT treatment and does not appear to be SOQ1 from the Western blot. Mass spectrometry analysis of these bands returned hits for SOQ1, RBCL, RBCS, ATPB and a single hit to a small protein annotated as a rapid alkanization factor-like protein (AT4G11510), which is not predicted to be chloroplast localized.

With the hope of obtaining cleaner samples, pulldowns were also attempted using FLAG-tagged mono-cysteine SOQ1 protein transiently expressed in *Nicotiana benthamiana*. After treatment with high light for 20 minutes, thylakoids from these plants were isolated and solubilized completely with detergent before immunoprecipitation. Eluted samples were run on an SDS-PAGE gel either in the presence of absence of reducing agent (Figure 3.5A). Along with SOQ1 with mutations in the first (lanes 3 and 4) and second (lanes 5 and 6) cysteine of the Trx-like domain, violaxanthin de-epoxidase was also expressed and purified as a lumen-localized control (lanes 1 and 2). The expectation is that mutants in the second cysteine will form mixed disulfides with target proteins but cannot be released unless reduced with DTT. While some bands do appear to be more intense in the DTT treated samples (lanes 2,4,6), none of these bands appears to be specific to the second cysteine mutant. To achieve better separation of proteins, we

performed 2-D gel electrophoresis with both C431S (figure 3.5C) and C434S (Figure 3.5B) purified samples. The first dimension was non-reducing, and mixed disulfides should be maintained, therefore we used a low percentage tris-acetate gel to separate larger proteins. Lanes cut from this gel were reduced to break the mixed disulfides and release interacting proteins, and the second dimension utilized a higher percentage gel to separate smaller proteins. The dashed white arcs on the gels represent the "diagonal" where proteins that run at the same size during both steps will appear. The majority of the SOQ1 protein was found on this arc and is circled in Figure 3.5. Other proteins along this arc and found in both mutants may be interacting proteins that did not form a mixed disulfide with SOQ1 and were released with the addition of sample buffer. Proteins to the left of the arc ran larger in the first dimension than the second and may be targets of the Trx-like domain.

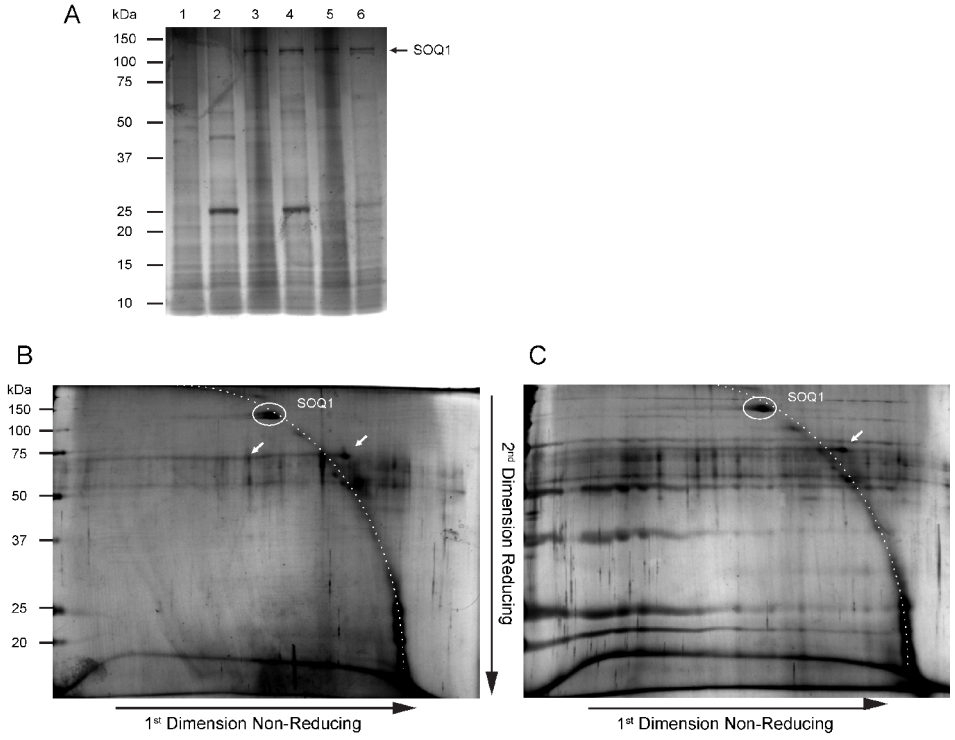

Figure 3.5: Transient mono-cysteine trap in *Nicotiana benthamiana*
Transient expression and FLAG immunoprecipitation was done as described in the methods section. A) SDS-PAGE of VDE (lanes 1 and 2) C431S SOQ1:FLAG (lanes 3 and 4) and C434S SOQ1:FLAG (lanes 5 and 6) either reduced with 100 mM DTT (lanes 2, 4,6) or unreduced (lanes 1,3,5). B) 2-D gel electrophoresis of C434S SOQ1 and C) C431S SOQ1, separated under non-reducing conditions in the first dimension and reducing conditions in the second dimension. The dashed line is the "diagonal," SOQ1 is in the white circle, and arrows indicate potential interacting proteins.

Identification of Potential Targets by mBBr Staining

If SOQ1 plays a role in reducing disulfides or sulfenic groups on proteins, another possible approach to determine targets of SOQ1 is to look for proteins that have a different oxidation state in the mutant compared to wild type when plants are treated with high light. To identify candidate proteins, thylakoid samples were solubilized and separated on 2-D gels using IEF in the first dimension and SDS-PAGE for the second dimension. These gels were then labeled with mBBr, a chemical that will alkylate free thiol groups with a fluorescent tag. When this method was used to compare wild-type (Figure 3.6A) and *soq1* (Figure 3.6B) thylakoid proteins, we observed several spots that were unique to one of the gels or the other. To make differences between the two gels more obvious, the area in the dashed box was colorized red for wild type and green for *soq1,* and then overlaid (Figure 3.6C). Because the gels ran slightly differently, the regions do not overlay perfectly, however there are still some clear features. Black areas indicate proteins that were reduced in both wild-type and *soq1,* red spots represent proteins reduced only in wild type and green regions represent proteins only reduced in *soq1*. Several spots are likely background in the image but these tended to have very intense signal with sharp edges compared to proteins which often had blurred edges. Unique spots to wild type or *soq1* were circled in white. Wild type had two unique spots between 20 and 30 kDa, whereas larger molecular weight proteins appear to be more reduced in *soq1*. The shape of several of the more intense spots is slightly different between the two samples, however the cause of this difference is difficult to determine.

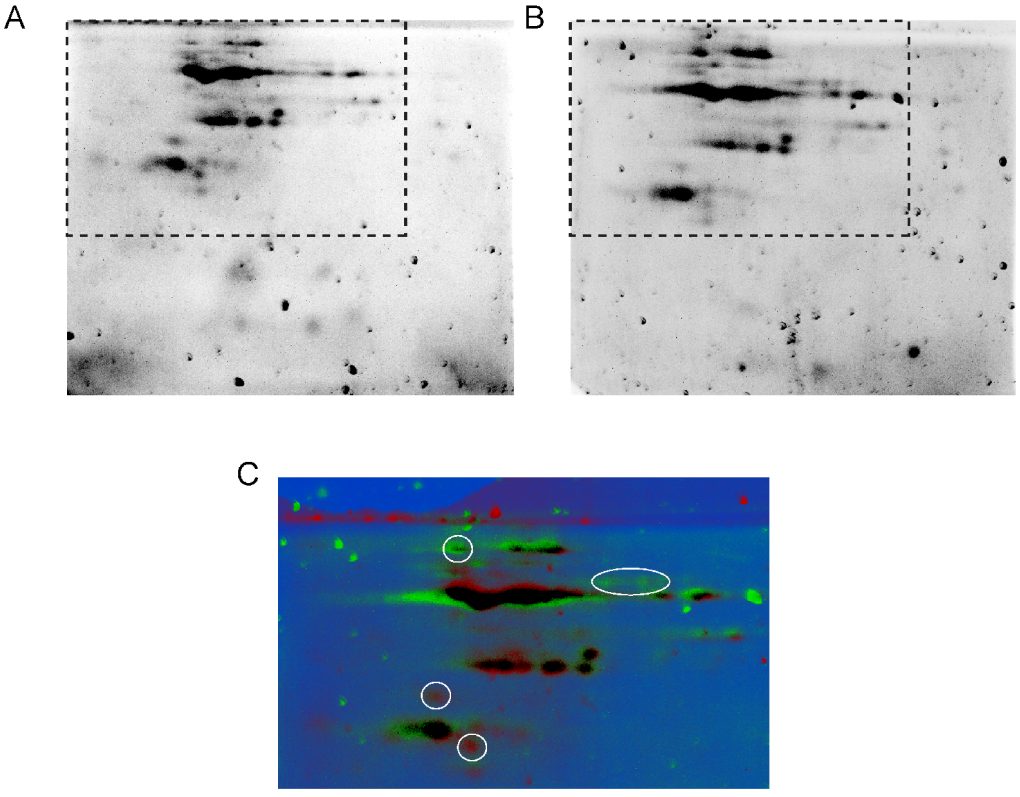

Figure 3.6: Fluorescent staining of free thiols with mBBr
2-D gels were made as described in the methods from thylakoids isolated from A) wild-

type and B) *soq1* plants treated with high light (2,000 µmol photons m^2 s^{-1}) for 90 minutes. The gels were then treated with mBBr to fluorescently tag reduced thiols and imaged by excitation at 488 nm. C) The region in the dashed box was colorized (wild-type turned red and *soq1* colored green) and the images were overlaid. White circles denote spots that are unique to one sample or the other.

Probing Lumen Interactions With Yeast Two-Hybrid

We have also explored possible interactions between the Trx-like/NHL domains of SOQ1 with other lumen localized proteins using Y2H and a library of lumen proteins generated in the laboratory of Prof. Sheng Luan. The portion of SOQ1 beginning after the transmembrane helix and containing the entire Trx-like and NHL domains (amino acids 345-1055) was cloned into the Y2H shuttle vectors pGAD and pGBT9 so that the protein was in-frame with the GAL4 activation and binding domains, respectively. Interaction between SOQ1 and other proteins was then tested with reporter genes for strong and weak interactions. No strong interactions were found, however SOQ1 was found to interact weakly with HCF136 and a bit more strongly with At2g26340 (Figure 3.7).

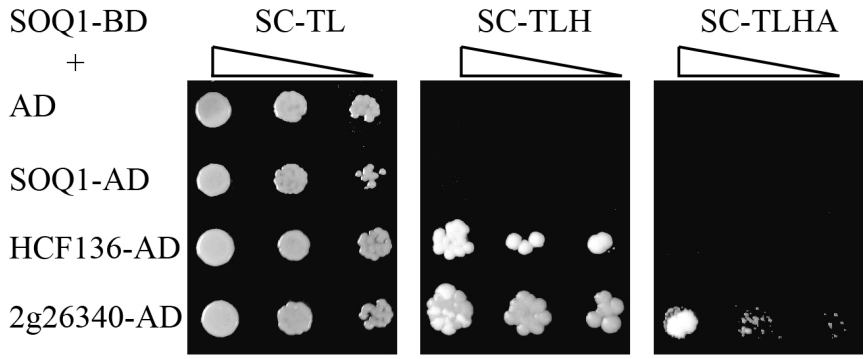

Figure 3.7: Yeast two-hybrid assay for interactions with thylakoid lumen proteins SOQ1 interacts with HCF136 and At2G26340 in yeast two-hybrid assays. Transformants were diluted and plated on synthetic complete medium (SC). Absence of tryptophan (T) and leucine (L) was used to select for transformants. Histidine (H) and adenine (A) were omitted to test reporter genes. SOQ1 did not interact with itself (SOQ1-AD) or the activation domain alone (AD).

PSII Supercomplexes Arrays Assume Different Arrangement in *soq1*

Current models for the activation of quenching mechanisms involve the rearrangement of LHCII antenna and PSII complexes in the grana membrane. Therefore we compared the supercomplex arrangement in wild-type and *soq1-1* by AFM on isolated BBY membranes. Leaves were transferred to ice immediately after light treatment and kept cold for the duration of the isolation in order to maintain the light-adapted conformation of membranes. For both wild-type and *soq1-1,* ordered arrays of particles were more frequently found in grana discs isolated from dark adapted plants. An example of these ordered arrays can be seen in Figure 3.8A and C. The size and frequency in which these arrays are found is higher in *soq1-1* compared to wild-type and can be seen

more clearly at higher resolution as shown in Figure 3.8B and E. In the mutant, the arrays appear to consist of rows of larger particles alternating with rows of smaller particles. In contrast, arrays from wild-type dark-adapted BBYs consist of rows containing particles of a single size. The packing density of particles is also qualitatively lower in wild-type than *soq1*. When BBYs from high-light-treated plants are compared (Figure 3.8C and F), fewer crystalline arrays are found in both wild type and mutant. There still appears to be an increased packing density in the *soq1* mutant compared to wild type. Efforts are currently underway to automate data analysis in order to quantify the differences observed in both the frequency and characteristics of the arrays from various samples.

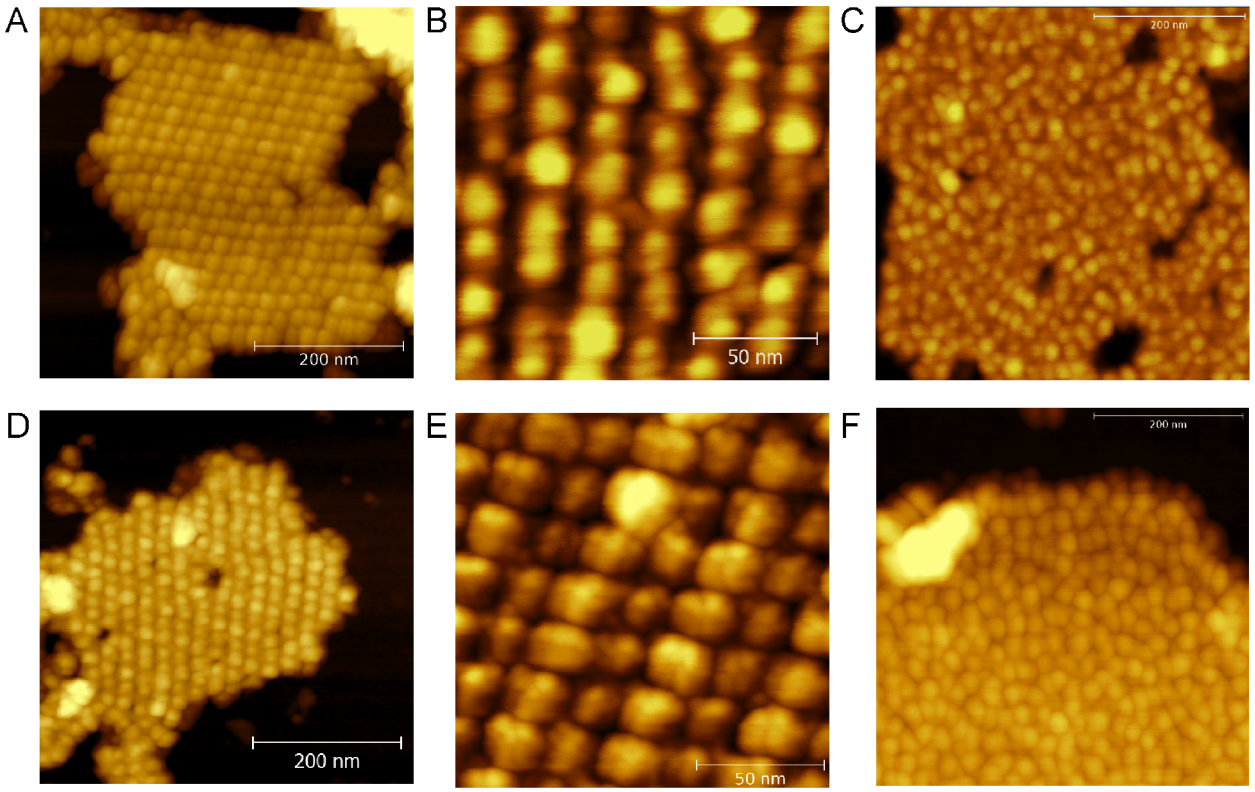

Figure 3.8: Atomic force microscopy of BBY membranes isolated from wild-type and *soq1-1* plants
BBYs were isolated from wild-type (A,B,C) and *soq1-1* (D,E,F) plants as described in the methods section. Plants were either dark-acclimated (A,B,D,E) or treated with high light (1,000 µmol photons m^2 s^{-1}) (C and F) for 30 minutes before isolation of membranes. Images were acquired... B and E are higher resolution images of A and D that highlight the differences in PSII arrays.

Electron Microscopy Reveals Subtle Differences in Chloroplast Structures

The differences in PSII complexes that we observed by AFM led us to ask if there were larger differences in chloroplast structures between wild-type and *soq1-1*. To answer this question, electron microscopy (EM) was performed on leaves from low and high light treated leaves. In contrast to the samples used for AFM, whole leaves from young plants were used, and approximately 15-30 minutes passed between the light treatment and high-pressure freezing of the samples, allowing the more rapid NPQ components to fully relax. Representative images are shown in Figure 3.9. In both low- and high-light-treated leaves, there was no obvious difference between wild-type and mutant in the density of thylakoids within the chloroplast or in the number of stacks or the size of individual grana. Compared to wild type, in both low and high light the *soq1* mutant appears to contain more spherical structures within the chloroplasts that resemble plastoglobules. The lumen distance also appears to be greater in *soq1* compared to wild-type in low- and high-light-treated leaves. Work is currently in progress to quantify these differences and to confirm the results with additional samples.

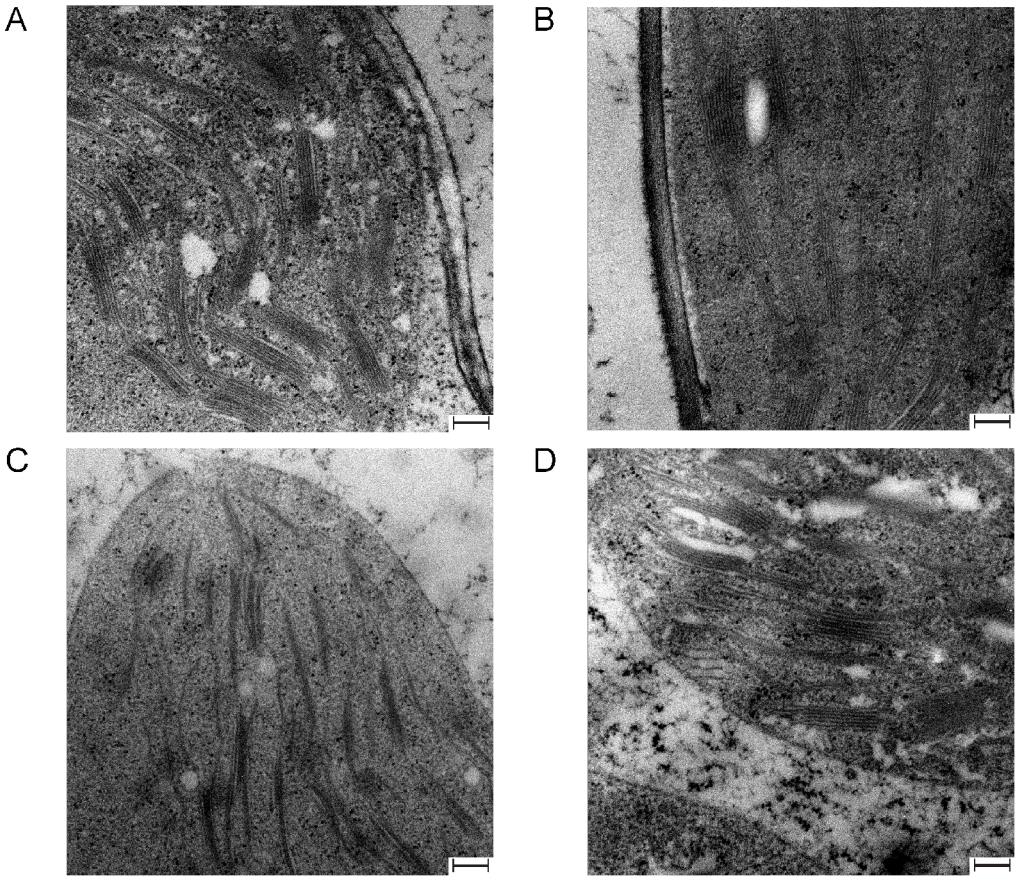

Figure 3.9: Electron micrographs of wild-type and *soq1-1* leaves
Wild-type (A and B) and *soq1-1* (C and D) leaves from 4 week old plants were prepared by high-pressure freezing before (A and C) or after (B and D) exposure to high light (1,000 μmol photons m^2 s^{-1}) for 30 minutes. Scale bar represents 200 nm.

Discussion

Previous work on the localization of SOQ1, its role in NPQ, and its domain structure/evolution led us to hypothesize that the SOQ1 protein may play a role in reducing proteins in oxidizing environments such as the lumen. Furthermore a target of SOQ1 is predicted to be part of the LHCII antenna. This interaction could be a direct reduction of LHCII protein(s) by SOQ1 or through some intermediate protein. The work presented in this chapter addresses these hypotheses.

SOQ1 was previously shown to contain a transmembrane domain and to be associated with thylakoid membranes. We have confirmed this result with BN-PAGE and shown that in wild-type plants the protein is likely associated with photosynthetic complexes (Figure 3.1). No signal was seen at the position expected for SOQ1 monomers, suggesting that the binding affinity of SOQ1 for other proteins is maintained during the mild solublization procedure used in BN-PAGE. Given that *soq1* is 110 kDa, if it were absent from a complex, that band would display a significant decrease in molecular weight. However we observed a banding pattern for the *soq1* mutant that was indistinguishable from wild-type. This was not unexpected though, as we predicted SOQ1 to be present in thylakoids at low amounts based on immunoblot analysis comparing known concentrations of recombinant protein to isolated thylakoids. Unfortunately this makes it difficult to determine the specific complex that SOQ1 is interacting with due to the large size shift, low abundance and the multiple overlapping signals detected in the anti-SOQ1 immunoblot.

Identifying SOQ1 interactions from wild-type plants may prove difficult, because it is membrane protein and present in low amounts. To address these issues we took the approach of immunoprecipitating targets of the Trx-like domain using a mono-cysteine mutant of SOQ1. With this technique we were able to overcome the abundance issue by using recombinant protein or transiently overexpressing SOQ1 in *N. benthamiana* and using epitope tags to do the pull-downs. This method will covalently link the two proteins as a mixed disulfide, giving the added benefit that stringent wash conditions can be used without disrupting the interaction. Results obtained in the initial experiments described above indicate that SOQ1 can be overexpressed transiently in *N. benthamiana* and that it is targeted to the thylakoid. However after doing pull-downs with this tissue, as well as when using recombinant protein, the majority of SOQ1 migrated at its monomeric size, suggesting that very little of the mutant SOQ1 is forming mixed disulfides under the conditions used. This could be due to the low amount of target protein present, possibly because the high light treatment used to oxidize targets was insufficient. Optimization of the light conditions used, either high light for a slightly longer time period or moderate light for a significantly longer period may lead to more protein forming mixed disulfides with SOQ1.

Another approach used to identify proteins that interact with SOQ1 was yeast two-hybrid screening [11]. As we are interested in interactions between the Trx-like/NHL domains and target proteins, we were able to use the lumen library created in the lab of Prof. Sheng Luan. Our screen identified two proteins that interacted with SOQ1. One of the identified proteins was HCF136, a lumen protein thought to be involved in PSII assembly and repair [17,23]. In contrast to *soq1* plants, *hcf136* mutants have a high chlorophyll fluorescence phenotype and cannot grow photoautotrophically due to a deficiency in PSII. This suggests that SOQ1 is not required for PSII assembly or HCF136 function. HCF136 also does not contain any cysteine residues in the mature peptide, indicating that it is unlikely to be a direct target of the Trx-like domain of SOQ1, unless it reduces oxidized methionines. The other protein that SOQ1 interacted with is At2g26340, a small lumen protein of unknown function. At2g26340 is unique to green plants and contains one well conserved cysteine, but because it does not contain any known domains or have a characterized phenotype it is difficult to predict its function and potential relationship to SOQ1.

Through mBBr labeling of free thiols [1], several differences between wild-type and *soq1* were seen in the oxidation of thylakoid proteins. There are at least two spots that were more reduced in wild-type than *soq1* when leaves were treated with high light. At this point we can only speculate about the identity of these proteins, but the possibility that they are minor antenna complexes is intriguing. Both Lhcb4 and Lhcb5 contain only one cysteine residue, and both are conserved in higher plants. In Lhcb4, this residue is located in the first transmembrane helix near the chlorophyll that ligates chlorophyll *a* and when oxidized could affect the environment of this chlorophyll molecule. The cysteine in Lhcb5 is located in the lumenal loop between the first and second transmembrane helices and is near the protonatable glutamate residue shown to bind DCCD [26]. It has also been shown that HCF164 interacts with Lhcb5 through mono-cysteine trap experiments [21], although this interaction was not explored further.

Another possibility is that the NPQ phenotype in *soq1* is due to changes in the supercomplex organization or thylakoid membrane structure. To address this we used high-resolution imaging techniques to compare wild-type and mutant plants from low and high light. EM results revealed that the chloroplasts in the mutant have only very minor differences compared to the wild type in both dark- and light-treated samples. We observed a possible increase in the number of plastoglobules in *soq1* chloroplasts when compared to wild type. If this difference can be confirmed, it is interesting as plastoglobules are thought to form in response to stress conditions [3]. This may indicate that *soq1* plants are more stressed than wild-type or that they perceive stress as the result of a signaling intermediate being affected. We are also in the process of quantifying more subtle differences in the thylakoid (eg. dimensions, number of stacks and lumen spacing) by statistically analyzing the images we have obtained.

To assess the organization of photosystem II within the thylakoid, isolated grana membranes were examined by AFM. The *soq1* mutant appeared to be different from wild-type in the arrangement, packing density and frequency of PSII particles seen in these preparations. It remains to be seen whether these differences are due to the absence of the lumen domains or the stromal portion of SOQ1, as they may have independent functions. This can be tested by imaging grana membranes from mutant plants that have been complemented with SOQ1 protein containing mutations that inactivate specific

domains. Because we know that point mutations in the Trx-like and NHL domains have the same NPQ phenotype as knockouts in SOQ1, looking at grana membranes from these mutants would be an easy way to test whether the changes in organization are the result of a defect in the activity of the protein versus the absence of SOQ1 from the thylakoid membrane. In this way we will be able to isolate the cause of the additional quenching in *soq1* and determine if there is a relationship between structural changes and the redox activity SOQ1 on target protein(s).

The work in this chapter follows up on the initial characterization of SOQ1 and is a further step towards understanding the functional role of the protein and how it is involved in NPQ. We have provided evidence that SOQ1 can interact with proteins in the thylakoid membrane and that its absence affects the organization and density of grana supercomplexes. Interestingly, these changes do not appear to significantly affect the stability of complexes and how well they are solubilized by detergent (Figure 3.1). By using several methods to look for interacting proteins and targets of SOQ1, we have preliminary evidence that it is indeed involved in a pathway to reduce target proteins in the lumen, however these interactions will need to be confirmed and studied further in order to fully understand the role of SOQ1 in the thylakoid membrane.

References

1. Balmer, Y., Vensel, W.H., Hurkman, W.J., and Buchanan, B.B. (2006). Thioredoxin target proteins in chloroplast thylakoid membranes. Antioxid. Redox Signal. *8*, 1829–1834.
2. Berthold, D., Babcock, G., and Yocum, C. (1981). A Highly Resolved, Oxygen Evolving Photosystem II Preparation From Spinach Thylakoid Membranes. FEBS Letters *134*, 231–234.
3. Bréhélin, C., Kessler, F., and van Wijk, K.J. (2007). Plastoglobules: versatile lipoprotein particles in plastids. Trends in Plant Science *12*, 260–266.
4. Cabreiro, F., Picot, C.R., Friguet, B., and Petropoulos, I. (2006). Methionine Sulfoxide Reductases. Annals of the New York Academy of Sciences *1067*, 37–44.
5. Caffarri, S., Kouril, R., Kereiche, S., Boekema, E.J., and Croce, R. (2009). Functional architecture of higher plant photosystem II supercomplexes. EMBO J *28*, 3052–3063.
6. Capitani, G., Rossmann, R., Sargent, D.F., Grütter, M.G., Richmond, T.J., and Hennecke, H. (2001). Structure of the soluble domain of a membrane-anchored thioredoxin-like protein from Bradyrhizobium japonicum reveals unusual properties. Journal of Molecular Biology *311*, 1037–1048.
7. Depuydt, M., Leonard, S.E., Vertommen, D., Denoncin, K., Morsomme, P., Wahni, K., Messens, J., Carroll, K.S., and Collet, J.-F. (2009). A Periplasmic Reducing System Protects Single Cysteine Residues from Oxidation. Science *326*, 1109 –1111.
8. Dietzel, L., Bräutigam, K., Steiner, S., Schüffler, K., Lepetit, B., Grimm, B., Schöttler, M.A., and Pfannschmidt, T. (2011). Photosystem II supercomplex remodeling serves as an entry mechanism for state transitions in Arabidopsis.

Plant Cell *23*, 2964–2977.
9. Earley, K.W., Haag, J.R., Pontes, O., Opper, K., Juehne, T., Song, K., and Pikaard, C.S. (2006). Gateway-compatible vectors for plant functional genomics and proteomics. Plant J. *45*, 616–629.
10. Erlendsson, L.S., Acheson, R.M., Hederstedt, L., and Le Brun, N.E. (2003). Bacillus subtilis ResA Is a Thiol-Disulfide Oxidoreductase involved in Cytochrome c Synthesis. Journal of Biological Chemistry *278*, 17852 –17858.
11. Fields, S., and Song, O. (1989). A novel genetic system to detect protein–protein interactions. Nature *340*, 245–246.
12. Gabilly, S.T., Dreyfuss, B.W., Karamoko, M., Corvest, V., Kropat, J., Page, M.D., Merchant, S.S., and Hamel, P.P. (2010). CCS5, a Thioredoxin-like Protein Involved in the Assembly of Plastid c-Type Cytochromes. Journal of Biological Chemistry *285*, 29738 –29749.
13. Ito, H., Fukuda, Y., Murata, K., and Kimura, A. (1983). Transformation of intact yeast cells treated with alkali cations. Journal of Bacteriology *153*, 163 –168.
14. Järvi, S., Suorsa, M., Paakkarinen, V., and Aro, E. (2011). Optimized native gel systems for separation of thylakoid protein complexes: novel super- and mega-complexes. Biochemical Journal *439*, 207–214.
15. Johnson, M.P., Goral, T.K., Duffy, C.D.P., Brain, A.P.R., Mullineaux, C.W., and Ruban, A.V. (2011). Photoprotective Energy Dissipation Involves the Reorganization of Photosystem II Light-Harvesting Complexes in the Grana Membranes of Spinach Chloroplasts. The Plant Cell Online *23*, 1468 –1479.
16. Kirchhoff, H., Hall, C., Wood, M., Herbstová, M., Tsabari, O., Nevo, R., Charuvi, D., Shimoni, E., and Reich, Z. (2011). Dynamic control of protein diffusion within the granal thylakoid lumen. Proceedings of the National Academy of Sciences *108*, 20248 –20253.
17. Komenda, J., Nickelsen, J., Tichý, M., Prásil, O., Eichacker, L.A., and Nixon, P.J. (2008). The cyanobacterial homologue of HCF136/YCF48 is a component of an early photosystem II assembly complex and is important for both the efficient assembly and repair of photosystem II in Synechocystis sp. PCC 6803. J. Biol. Chem. *283*, 22390–22399.
18. Lennartz, K., Plücken, H., Seidler, A., Westhoff, P., Bechtold, N., and Meierhoff, K. (2001). HCF164 Encodes a Thioredoxin-Like Protein Involved in the Biogenesis of the Cytochrome b6f Complex in Arabidopsis. The Plant Cell Online *13*, 2539 –2551.
19. McDonald, K.L., and Webb, R.I. (2011). Freeze substitution in 3 hours or less. Journal of Microscopy *243*, 227–233.
20. Messens, J., and Collet, J.-F. (2006). Pathways of disulfide bond formation in Escherichia coli. Int. J. Biochem. Cell Biol. *38*, 1050–1062.
21. Motohashi, K., and Hisabori, T. (2006). HCF164 Receives Reducing Equivalents from Stromal Thioredoxin across the Thylakoid Membrane and Mediates Reduction of Target Proteins in the Thylakoid Lumen. Journal of Biological Chemistry *281*, 35039 –35047.
22. Page, M.L.D., Hamel, P.P., Gabilly, S.T., Zegzouti, H., Perea, J.V., Alonso, J.M., Ecker, J.R., Theg, S.M., Christensen, S.K., and Merchant, S. (2004). A homolog of prokaryotic thiol disulfide transporter CcdA is required for the

assembly of the cytochrome b6f complex in Arabidopsis chloroplasts. J. Biol. Chem. *279*, 32474–32482.
23. Plücken, H., Müller, B., Grohmann, D., Westhoff, P., and Eichacker, L.A. (2002). The HCF136 protein is essential for assembly of the photosystem II reaction center in Arabidopsis thaliana. FEBS Lett. *532*, 85–90.
24. Rietsch, A., Belin, D., Martin, N., and Beckwith, J. (1996). An in vivo pathway for disulfide bond isomerization in Escherichia coli. Proceedings of the National Academy of Sciences *93*, 13048 –13053.
25. Shimizu, H., Peng, L., Myouga, F., Motohashi, R., Shinozaki, K., and Shikanai, T. (2008). CRR23/NdhL is a Subunit of the Chloroplast NAD(P)H Dehydrogenase Complex in Arabidopsis. Plant and Cell Physiology *49*, 835 – 842.
26. Walters, R.G., Ruban, A.V., and Horton, P. (1996). Identification of proton-active residues in a higher plant light-harvesting complex. Proceedings of the National Academy of Sciences *93*, 14204 –14209.

Chapter 4

The Haloacid Dehalogenase-Like Hydrolase of SOQ1 is Likely a Pentose Phosphate Phosphatase

Summary

We predicted that the HAD domain of SOQ1 is most likely a phosphatase based on the function of other HAD domain-containing proteins. Recombinant SOQ1 is capable of removing the phosphate group from a general phosphatase substrate. The catalytic nucleophile of the SOQ1 HAD domain, as predicted by alignment to other HAD proteins, is required for this activity. To determine the possible substrate of SOQ1 phosphatase, a variety of small molecule phospho-substrates were screened using the malachite green assay to monitor phosphate release. We show that SOQ1 has a strong preference for sugar phosphates, particularly pentose phosphates, with the highest activity seen for ribose-5-phosphate. This activity was greatest at a neutral pH, consistent with the protein's localization to the stroma. In addition, we have begun using mass spectrometry to characterize possible changes in leaf sugar content resulting from deletion of the SOQ1 protein. This work discusses the possible role of the HAD domain of SOQ1 in chloroplast sugar metabolism.

Preface

I would like to acknowledge the contributions of Alex Schultink, who performed the mass spectrometry work done in this chapter.

Introduction

The identification of a novel thylakoid protein involved in non-photochemical quenching (NPQ) has been presented in previous chapters. This protein contains three structural domains: a haloacid dehalogenase-like hydrolase (HAD) domain, a thioredoxin-like domain and a NHL beta-propeller domain. The focus of this chapter is to determine the enzymatic function and substrate specificity of the HAD domain.

HAD proteins were first characterized by their ability to detoxify chlorinated hydrocarbons through hydrolysis of the carbon-halogen bond, but were subsequently shown to catalyze a wide range of reactions, most commonly the removal of phosphate groups [10]. In fact, it is predicted that HAD domain proteins make up the largest family of small molecule phosphatases, and they are present in all kingdoms of life [11]. The reaction catalyzed by HAD proteins utilizes an invariant aspartate residue in the active site as the nucleophile and requires Mg^{2+} [10]. HAD proteins contain few conserved residues, but are well defined by their unique Rossmannoid α/β fold. The family is divided into three subfamilies based on the presence and position of a capping domain thought to influence substrate binding [6]. SOQ1 belongs to subfamily 1 in which the capping domain is found between the first and second motifs.

To elucidate the function of the HAD domain of SOQ1, we sought to determine the substrate and enzymatic activity of the protein. In *E. coli* it was shown that 21 of 23 soluble HAD proteins had phosphatase activity *in vitro*, and that substrate specificity was variable for

most of these proteins [11]. It was also found that the sequence similarity between HAD-containing proteins often had little bearing on the similarity between substrates. To identify the substrate of SOQ1, we took a similar approach, first testing its phosphatase activity on a general phospho-substrate, followed by narrowing possible *in vivo* substrates using the malachite green assay [13]. Finally, we used mass spectrometry to monitor changes in leaf sugar content that result from deletion of SOQ1 in Arabidopsis.

Methods

Sequence Alignment - The HAD domain of SOQ1 (amino acids 61-271) was aligned to representatives of the HAD superfamily using the web server at UCSF's Structure Function Linkage Database (http://sfld.rbvi.ucsf.edu/django). This alignment was opened in Jalview [18] and annotated with secondary structure features predicted by Phyre2 (http://www.sbg.bio.ic.ac.uk/phyre2) [9].

Phosphatase Assays - Recombinant His-tagged full-length SOQ1 protein and a truncated version consisting of only the HAD-domain (amino acids 58-367) were purified as described in the previous chapter. Protein was tested for general phosphatase activity using the *p*-nitrophenyl phosphate (pNPP) assay. Protein was diluted to between 0.25 and 0.60 mg/mL in 1x colorimetric assay buffer (20 mM Tris-HCl, pH 7.5, 5 mM $MgCl_2$, 0.1 mg/mL bovine serum albumin). Samples containing no enzyme and calf alkaline phosphatase were included as negative and positive controls, respectively. An aliquot of 100 mM pNPP stock solution in 1x colorimetric assay buffer was added to a 96-well plate and diluted with 1x colorimetric assay buffer so that the desired final concentration was reached in a 62.5 µL volume. To begin the reaction, the enzyme mix was added to columns of the plate at regular intervals with a multichannel pipet. The reaction was allowed to proceed for 45 minutes and then quenched with 20 µL of 5 N NaOH added at the same interval. The mixture was incubated at room temperature for 30 seconds and then the absorbance was measured at 405 nm. The molar extinction coefficient for pNPP is 18,000 M^{-1} cm^{-1}. The blank was subtracted from the experimental values to account for any nonenzymatic phosphate release. The K_m and V_{max} were calculated using BioDataFit 1.02 (http://www.changbioscience.com/stat/ec50.html).

The malachite green assay was done to test specific phospho-substrates using the BIOMOL GREEN kit (Enzo Life Sciences International Inc, USA). For the initial screen, substrate stocks were made at 10 mM in 1x colorimetric assay buffer and diluted to a final concentration of 1 mM upon addition to a 96-well plate. To start the reaction, 10 µL of diluted enzyme containing 17 µg of protein was added. The reaction was allowed to proceed for 30 minutes and was terminated by addition of 150 µL of BIOMOL GREEN reagent to each well. The plate was then incubated at room temperature for 20-30 minutes and the A_{620} was measured using a plate reader. Phosphatase activity was determined by comparing the amount of phosphate released in each reaction to phosphate standards. Controls lacking enzyme were included in order to account for substrate interactions with the malachite compound. Concentration of substrate and enzyme were adjusted as necessary for further experiments in order to observe activity or determine kinetics for reactions that were outside the linear range of phosphate release. Dithiothreitol (DTT) and oxidized glutathione (GSSG) were added to the enzyme mix at 15 mM and allowed to equilibrate for 20 minutes before starting the assay where indicated.

Sugar Mass Spectrometry- Sugars and sugar phosphates were extracted from Arabidopsis leaves using a chloroform/methanol method [2]. Depending on the experiment, 10-100 mg of wild-type or *soq1* leaves were frozen in liquid nitrogen and ground to a fine powder. The powder was transferred to a microfuge tube, and 250 µL of ice-cold chloroform/methanol (3:7 v/v) was added per 10-20 mg tissue. The tubes were vortexed and incubated at -20°C for 2 hours. After incubation, 200 µL of ice-cold water was added per 10-20 mg tissue, and warmed to 4°C with repeated shaking. The extract was centrifuged at 18,000 g for 10 minutes at 4°C, and the upper aqueous-methanol phase containing sugars was transferred to a new tube. A second extraction with 200 µL ice-cold water was done, and the extracts were combined. The sugar sample was then evaporated to dryness using a vacuum centrifuge. Separation of sugars by liquid chromatography-mass spectrometry was performed as described [2].

Results

In Vitro Phosphatase Activity of the HAD-Domain From SOQ1

A colorimetric assay using the general phosphatase substrate *p*-nitrophenyl phosphate (pNPP) was used to test whether SOQ1 has phosphatase activity *in vitro*. Both acid and alkaline phosphatases act on pNPP, generating the product *p*-nitrophenol, which can be quantified by its absorbance at 405 nm. When purified recombinant His-tagged SOQ1 was used in this assay, there was a low level of phosphatase activity detected (Figure 4.1). The specific activity was approximately 5 µmoles min^{-1} mg^{-1}. The optimal pH was determined to be approximately 5.5, and the amount of activity was approximately 3-fold higher at this lower pH. Based on the alignment of SOQ1 with other HAD proteins (Figure 4.2), we identified the putative nucleophilic aspartate residue at amino acid position D80. To test this assignment, recombinant D80N SOQ1 was purified and assayed for phosphatase activity using the aforementioned assay. Phosphatase activity observed in the mutant was significantly reduced relative to that of wild-type protein activity. The HAD-domain purified on its own also displayed the same specific activity as the full-length protein (data not shown).

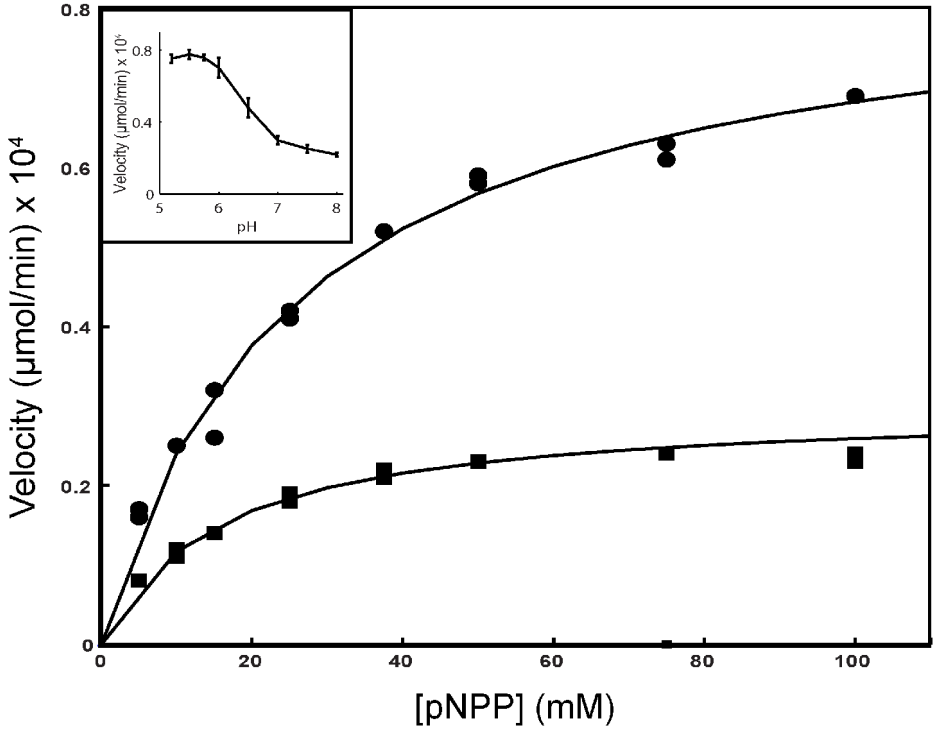

Figure 4.1: Enzyme kinetics of recombinant SOQ1 on pNPP
Plot of reaction rate versus concentration of pNPP for wild type SOQ1 protein (circles) and D80N SOQ1 (squares). Reactions were done with 10 µg of protein at 30ºC and pH 7.0. For wild type and D80N protein, K_m values were calculated as 25.5 and 15.5 mM and the V_{max} was 0.857 and 0.299 µmol/min, respectively. Inset – pH optimum curve for SOQ1 pNPP phosphatase activity. Data represent means $\pm$ SD (n = 4).

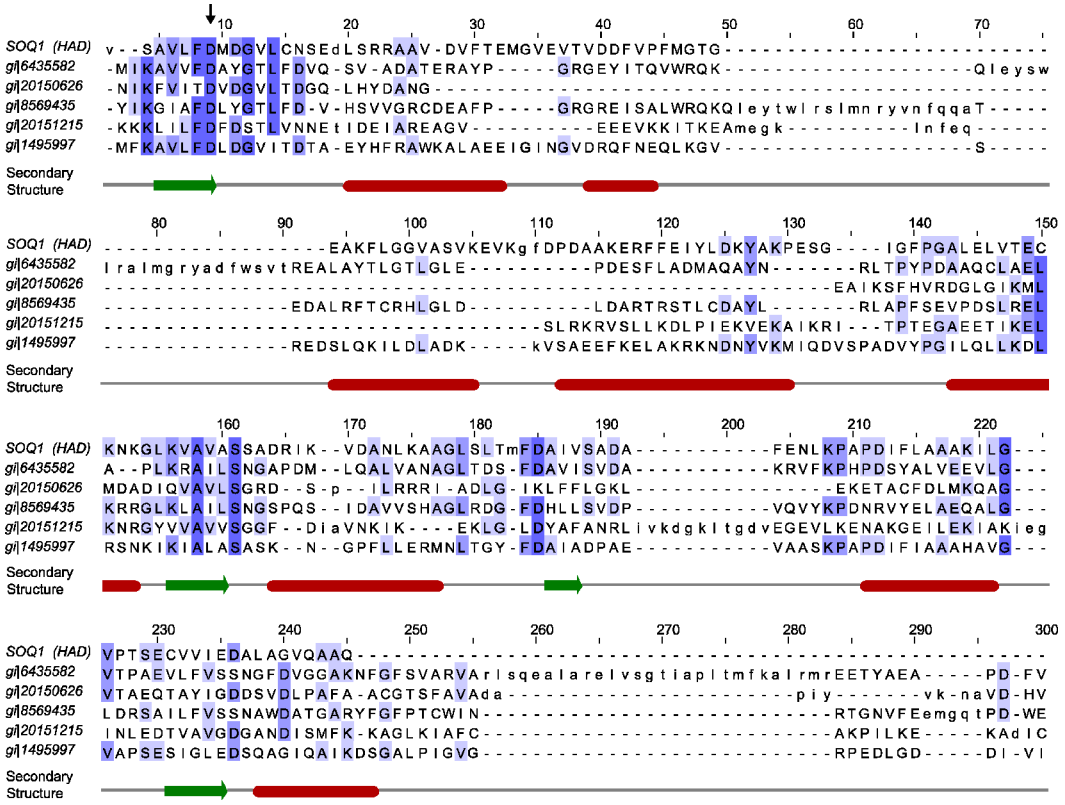

Figure 4.2: Alignment of the SOQ1 HAD domain with representative HAD-domain proteins
The HAD domain of SOQ1 was aligned to representatives of the HAD superfamily with secondary structure as predicted by the Phyre2 web program. Green arrows in the secondary structure represent beta-sheets, red bars are helices. Blue shading corresponds to the conservation of amino acids at that position. Arrow indicates the catalytic aspartate residue.

To determine the potential substrate of the phosphatase, we tested SOQ1 activity on a broad range of phosphorylated substrates including sugars, nucleotides, amino acids and lipids. We used the malachite green assay to measure phosphate released during these reactions and compared these levels to those of known standards. SOQ1 displayed little activity on most of the substrates tested including all of the phosphopeptides, phospholipids and phosphonucleotides (Figure 4.3). In contrast, significantly more activity was seen when phosphorylated sugars were used in this assay. SOQ1 had the highest activity on the five-carbon sugar ribose-5-phosphate (R5P), with the next highest activity observed on phosphorylated fructose sugars.

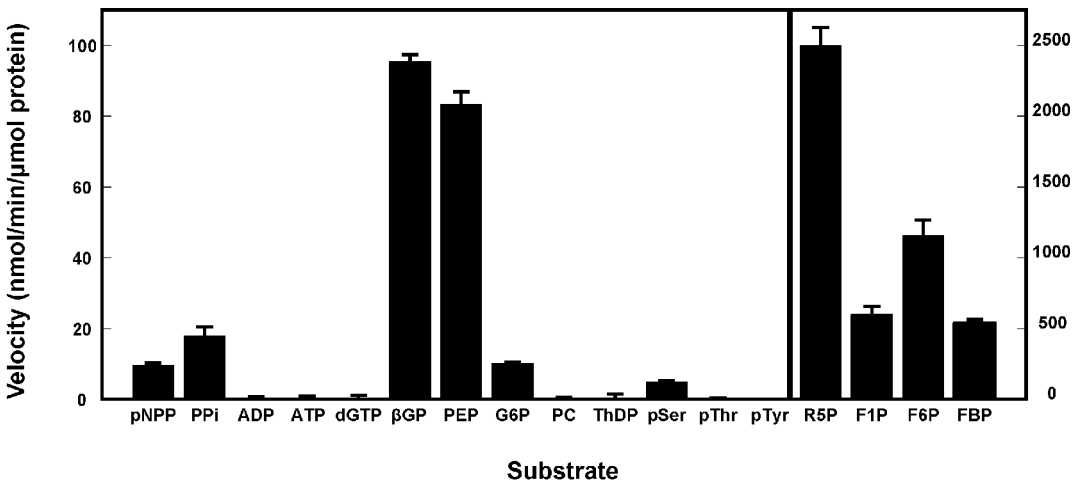

Figure 4.3: SOQ1 phosphatase activity on various phosphorylated substrates
The malachite green assay was used to test SOQ1 phosphatase activity on various substrates at 1 mM concentrations. 10-20 µg of full-length SOQ1 or a truncation consisting of only the HAD domain were used with similar results. Note the different scales for the right and left panels of the figure. Substrates tested were: pNPP – *p*-nitrophenyl phosphate, PPi – pyrophosphate, ADP – adenosine diphosphate, ATP – adenosine triphosphate, dGTP – deoxyguanosine triphosphate, βGP – beta-glycerophosphate, PEP – phosphenolpyruvate, G6P – glucose-6-phosphate, PC – phosphatidylcholine, ThDP – thaimine diphosphate, pSer – phosphoserine, pThr – phosphothreonine, pTyr – phosphotyrosine, R5P – ribose-5-phosphate, F1P – fructose-1-phosphate, FBP – fructose-1,6-bisphosphate. Data represent means ± SD (n = 3).

Attempts to determine kinetic properties for SOQ1 phosphatase activity on R5P were unsuccessful due to interference of higher sugar concentrations with the assay, however the K_m was likely in the range of 3-7 mM. Similar difficulties with substrate interference also prevented the measurement of SOQ1 activity on other sugars such as ribulose-1,5-bisphosphate. In contrast to what we observed when SOQ1 acted on the pNPP substrate, the optimal pH of SOQ1 activity on R5P was determined to be closer to pH 7.0 (Figure 4.4). The D80N mutant of SOQ1 had only 3% of the activity on R5P when compared to the wild-type protein at the same pH and substrate concentration. To test if the SOQ1 protein was redox regulated, we measured its activity in the presence of either the reducing agent DTT or oxidized glutathione (GSSG). The phosphatase activity was nearly abolished when the protein was oxidized with GSSG. Interestingly, the activity was also slightly lower in the presence of DTT than without any reducing agent.

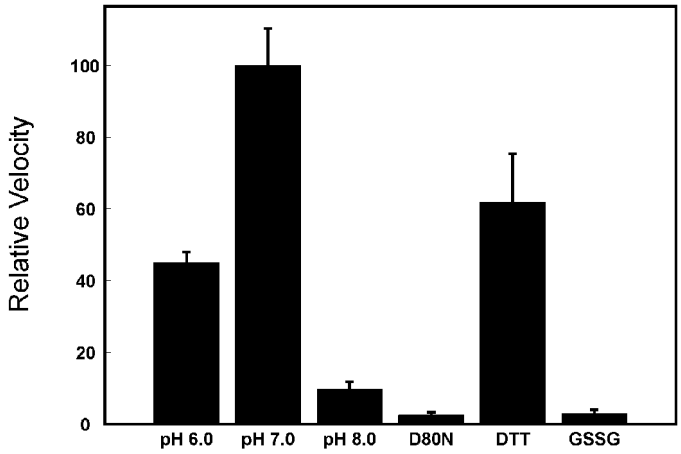

Figure 4.4: Effect of pH, active site mutation and redox conditions on phosphatase activity Full-length SOQ1 activity on R5P was assayed at different pH. Activity in the presence of the reductant DTT or the oxidant GSSG, as well as with the D80N point mutation, were tested at pH 7.0. All reactions were done with R5P at 1 mM using 1 μg of purified protein per reaction. The reaction velocity of the wild-type protein at pH 7.0 was set to 100% activity. Data represent means ± SD (n = 3).

Sugar Phosphate Content of Wild-type and *soq1* Plants

Based on the *in vitro* phosphatase assays above, we hypothesized that the absence of the SOQ1 HAD-domain might have an effect on the sugar content of leaf cells. To test this, we extracted sugars from wild-type and *soq1* plants and analyzed the samples by LC-MS [2]. We first attempted to extract sugars from isolated chloroplasts equivalent to 10 mg of leaf tissue based on chlorophyll concentration. The LC-MS signal for sugar phosphates from these samples was low, possibly due to the long preparation time. Instead of these over-processed samples, we used whole leaves for the subsequent experiments. Sugar phosphate standards included were ribose-5-phosphate, fructose-1-phosphate and glucose-1-phosphate. In addition, glucose, trehalose, and sucrose were used as neutral sugar standards. Figure 4.5 shows a typical LC-MS analysis of leaf tissue from wild type and *soq1-1* plants. Additional channels besides those for which we had standards were included to determine if SOQ1 had activity on, or affected the accumulation of, other sugars or sugar phosphates.

We were able to see clear signals in several channels, including all those for which we had a standard. Some peaks were specific to either wild type or *soq1,* for example in Figure 4.5 the peak at 9.89 minutes in the *m/z* 273 channel is possibly a sugar acid that accumulates in *soq1-1* but not in wild type. Differences in the disaccharides (data not shown) were also seen. Further experiments and optimization of the procedure will be necessary to show the reproducibility of these differences.

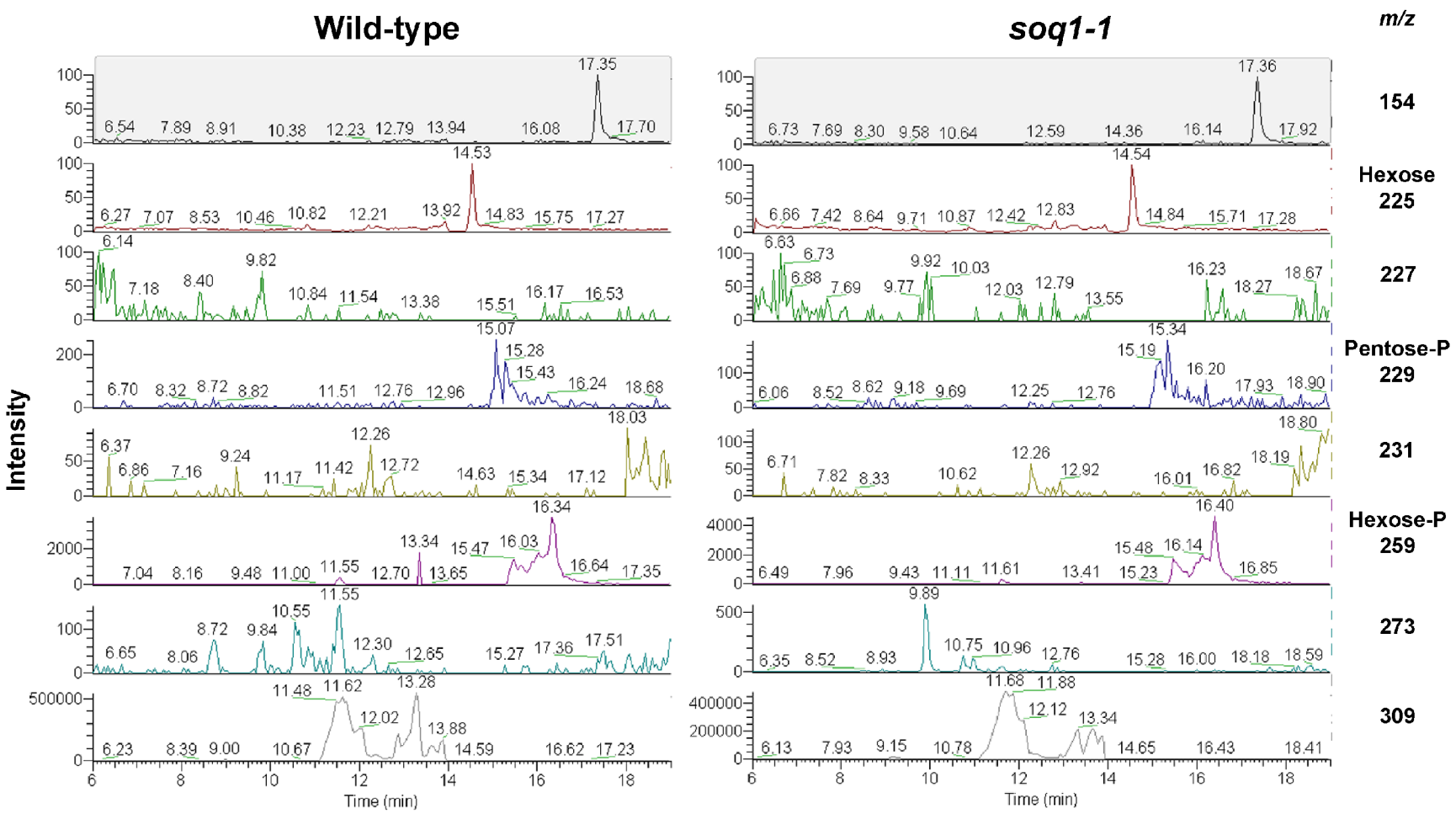

Figure 4.5: Chromatograms of sugar and sugar phosphates from wild-type and *soq1-1* leaves
Sugars were extracted from whole leaves as described in the methods section and separated by LC-MS. Samples were detected as deprotonated negatively charged ions for phosphorylated sugars or as formylated molecules for neutral sugars. The mass-to-charge ratio (*m/z*) was used to distinguish between different groups of sugar isomers (i.e., hexose phosphates versus pentose phosphates).

Discussion

This work demonstrates that the SOQ1 protein has phosphatase activity *in vitro,* as predicted based on the presence of the HAD domain. It was first shown that SOQ1 was able to remove phosphate groups from the general phosphatase substrate pNPP (Figure 4.1). Because the specific activity and turnover rate for this reaction were low, we tested whether the phosphatase activity was attributable to SOQ1, or rather to the presence of a contaminating protein that was not removed during the purification. Mutation of the catalytic aspartate in the active site of the HAD domain resulted in a significant decrease in phosphatase activity. The pH optimum for SOQ1 phosphatase activity on pNPP was found to be around 5.5. This value was surprisingly low for a phosphatase predicted to be localized in the stroma (see Chapter 2).

Various HAD-containing proteins have been shown to have phosphatase activity on diverse substrates including inorganic pyrophosphate [8], nucleotides [3], sugars [12], and proteins [17]. Other HAD proteins have been shown to display a remarkable promiscuity with regards to substrate specificity [11]. Using sequence similarity to determine substrate specificity of HAD proteins has proven difficult [11,15]. To narrow the list of possible substrates of SOQ1, we used the malachite green assay to monitor phosphate release when the protein was incubated with a broad range of phospho-substrates. SOQ1 was shown to have little or no activity on inorganic phosphate or phosphorylated nucleotides, lipids and amino acids (Figure 4.3). Highest activity was seen with sugar phosphates, prompting us to test additional sugar substrates. We found that the highest SOQ1 phosphatase activity was observed for pentose phosphates, specifically R5P. The specificity of SOQ1 for pentose phosphates was relatively high, having 20-fold more activity on these substrates than on triose phosphates and 100-fold more activity compared to pyrophosphate.

Consistent with localization to the stroma, the phosphatase activity of SOQ1 on R5P was found to be more active at a neutral pH (Figure 4.4). The D80N mutation had only 3% of the activity of the wild-type protein, indicating that this activity was indeed due to the HAD domain of SOQ1. Given the presence of the Trx-like domain on the full-length protein, we also tested whether SOQ1 phosphatase activity was redox regulated. Under oxidizing conditions, the activity of SOQ1 was reduced to less than 5% of the activity seen in the absence of GSSG. Oddly, the addition of DTT also reduced activity by nearly half. To determine if these effects are attributable to the Trx-like domain or possibly due to redox-active cysteines within the HAD domain, a truncation lacking the C-terminus of the protein will need to be tested under different redox conditions.

We have also begun to look at the sugar phosphate content in wild type and *soq1* plants by MS. Using whole leaf tissue, we have observed sugar and sugar phosphates. Unfortunately, in many cases instead of a clear single peak, we have observed multiple peaks, possibly indicating a mixture of closely related sugars in the sample. While there were some differences between wild-type and *soq1-1* sugar composition, most of these differences were in peaks with low intensities below the noise threshold, making it difficult to reproduce these differences between leaf samples. Variation between leaf samples from the same plant and between plants must also be considered when analyzing these results.

Ultimately, we plan to look for differences in the sugar content of chloroplasts from wild type and *soq1* plants under different conditions. Currently, the relatively low abundance of sugar extracted from these samples has stymied our efforts. One possibility is that sugar phosphates are

rapidly metabolized during the lengthy chloroplast isolation procedure and using a more crude extract that can be frozen immediately may be required. It is also possible that the native amount of SOQ1 protein present may be too low to result in accumulation of differences between *soq1* mutant and wild-type plants, especially if the *in vivo* substrate is an abundant sugar such as R5P. To address this concern, we are over-expressing truncated forms of SOQ1 containing only the soluble HAD domain in the chloroplast. Hopefully this approach will allow accumulation of the phosphatase above levels seen in wild-type plants and amplify any changes in sugar concentration. Alternatively, adding purified protein to sugars extracted from plants and then performing MS could help identify a substrate that we did not test *in vitro*.

A potential problem with this MS approach is that the sugar that SOQ1 acts on *in vivo* might be present only at very low levels. Several phospho-sugar inhibitors of Rubisco such as 2-carboxy-D-arabinitol-1-phosphate [7], D-glycero-2,3-pentodiulose-1,5-bisphosphate [1] and xylulose-1,5-bisphosphate [19] are known to bind tightly to the active site and prevent catalysis even at very low concentrations. Plants prevent this inhibition through removal of the sugars from the active site by Rubisco activase [14] and dephosphorylation into forms that no longer bind tightly [Andralojc]. To determine if any of these photosynthetic inhibitors are the substrate, Dr. Martin Parry's laboratory is testing SOQ1 phosphatase activity on a range of Rubisco inhibitors.

This work could also lead to a clearer understanding of the relationship between the stromal and lumenal domains of SOQ1. While the stroma-exposed HAD domain is not required to complement the NPQ phenotype, it has been suggested that it could function as an inhibitory domain, regulating the lumenal domains. This inhibitory mechanism could be similar to those of the signal receiver domains of two-component regulatory proteins in which a long-lived phospho-aspartyl intermediate is formed [4,16]. The fact that the mechanism employed by HAD phosphatases also involves formation of a phosphor-aspartyl intermediate [6] and that both domains contain a similar Rossman fold [11] supports this possibility. Neofunctionalization of the HAD domain after fusion with the Trx-like and NHL domains would be similar to the proposed evolution of P-type ATPases where the HAD domain is thought to have fused with a transmembrane protein to form an active transport pump [3]. If this hypothesis is correct, then the accumulation of a sugar phosphate intermediate during periods of stress could result in the inactivation of the Trx-like/NHL domains via the stromal HAD domain and activation of the quenching characterized in Chapter 2 to protect against excess light.

References

1. Andralojc, P.J., Madgwick, P.J., Tao, Y., Keys, A., Ward, J.L., Beale, M.H., Loveland, J.E., Jackson, P.J., Willis, A.C., Gutteridge, S., et al. (2012). 2-Carboxy-D-arabinitol 1-phosphate (CA1P) phosphatase: evidence for a wider role in plant Rubisco regulation. Biochemical Journal *442*, 733–742.
2. Antonio, C., Larson, T., Gilday, A., Graham, I., Bergström, E., and Thomas-Oates, J. (2007). Quantification of sugars and sugar phosphates in Arabidopsis thaliana tissues using porous graphitic carbon liquid chromatography-electrospray ionization mass spectrometry. J Chromatogr A *1172*, 170–178.
3. Aravind, L., Galperin, M.Y., and Koonin, E.V. (1998). The catalytic domain of the P-type ATPase has the haloacid dehalogenase fold. Trends Biochem. Sci. *23*, 127–129.
4. Baikalov, I., Schröder, I., Kaczor-Grzeskowiak, M., Grzeskowiak, K., Gunsalus, R.P., and

Dickerson, R.E. (1996). Structure of the Escherichia coli Response Regulator NarL. Biochemistry *35*, 11053–11061.
5. Burroughs, A.M., Allen, K.N., Dunaway-Mariano, D., and Aravind, L. (2006). Evolutionary genomics of the HAD superfamily: understanding the structural adaptations and catalytic diversity in a superfamily of phosphoesterases and allied enzymes. J. Mol. Biol. *361*, 1003–1034.
6. Calderone, V., Forleo, C., Benvenuti, M., Thaller, M.C., Rossolini, G.M., and Mangani, S. (2006). A Structure-based Proposal for the Catalytic Mechanism of the Bacterial Acid Phosphatase AphA belonging to the DDDD Superfamily of Phosphohydrolases. Journal of Molecular Biology *355*, 708–721.
7. Gutteridge, S., Parry, M.A.J., Burton, S., Keys, A.J., Mudd, A., Feeney, J., Servaites, J.C., and Pierce, J. (1986). A nocturnal inhibitor of carboxylation in leaves. Nature *324*, 274–276.
8. Huang, H., Patskovsky, Y., Toro, R., Farelli, J.D., Pandya, C., Almo, S.C., Allen, K.N., and Dunaway-Mariano, D. (2011). Divergence of structure and function in the haloacid dehalogenase enzyme superfamily: Bacteroides thetaiotaomicron BT2127 is an inorganic pyrophosphatase. Biochemistry *50*, 8937–8949.
9. Kelley, L.A., and Sternberg, M.J.E. (2009). Protein structure prediction on the Web: a case study using the Phyre server. Nat Protoc *4*, 363–371.
10. Koonin, E.V., and Tatusov, R.L. (1994). Computer Analysis of Bacterial Haloacid Dehalogenases Defines a Large Superfamily of Hydrolases with Diverse Specificity: Application of an Iterative Approach to Database Search. Journal of Molecular Biology *244*, 125–132.
11. Kuznetsova, E., Proudfoot, M., Gonzalez, C.F., Brown, G., Omelchenko, M.V., Borozan, I., Carmel, L., Wolf, Y.I., Mori, H., Savchenko, A.V., et al. (2006). Genome-wide Analysis of Substrate Specificities of the Escherichia coli Haloacid Dehalogenase-like Phosphatase Family. Journal of Biological Chemistry *281*, 36149 –36161.
12. Lu, Z., Dunaway-Mariano, D., and Allen, K.N. (2005). HAD Superfamily Phosphotransferase Substrate Diversification: Structure and Function Analysis of HAD Subclass IIB Sugar Phosphatase BT4131. Biochemistry *44*, 8684–8696.
13. McAvoy, T., and Nairn, A. (2010). Serine/threonine protein phosphatase assays. Curr Protoc Mol Biol *Chapter 18*, Unit18.18.
14. Portis, A.R., Jr (2003). Rubisco activase - Rubisco's catalytic chaperone. Photosyn. Res. *75*, 11–27.
15. Rawat, R., Sandoval, F.J., Wei, Z., Winkler, R., and Roje, S. (2011). An FMN Hydrolase of the Haloacid Dehalogenase Superfamily Is Active in Plant Chloroplasts. Journal of Biological Chemistry *286*, 42091 –42098.
16. Schnell, R., Agren, D., and Schneider, G. (2008). 1.9 A structure of the signal receiver domain of the putative response regulator NarL from Mycobacterium tuberculosis. Acta Crystallogr Sect F Struct Biol Cryst Commun *64*, 1096–1100.
17. Selengut, J.D. (2001). MDP-1 Is a New and Distinct Member of the Haloacid Dehalogenase Family of Aspartate-Dependent Phosphohydrolases. Biochemistry *40*, 12704–12711.
18. Waterhouse, A.M., Procter, J.B., Martin, D.M.A., Clamp, M., and Barton, G.J. (2009). Jalview Version 2—a multiple sequence alignment editor and analysis workbench. Bioinformatics *25*, 1189 –1191.

19. Zhu, G., and Jensen, R.G. (1991). Xylulose 1,5-Bisphosphate Synthesized by Ribulose 1,5-Bisphosphate Carboxylase/Oxygenase during Catalysis Binds to Decarbamylated Enzyme. Plant Physiology *97*, 1348 –1353.

Chapter 5

Dynamic Mechanical Responses of Thylakoid Membranes During Illumination

Summary

Remodelling of thylakoid membranes in response to illumination is involved in regulation of photosynthesis. Here, we investigate the mechanical responses of the thylakoid network from single isolated chloroplasts. An atomic force microscopy cantilever was used to dynamically probe the mechanics (height, elasticity, and viscosity) of thylakoid membranes from *Arabidopsis thaliana* thylakoid membranes during illumination, and electron microscopy was used to verify proposed changes in ultrastructure. To explore the cause(s) of the observed changes, samples were treated with the uncoupler gramicidin D, or the *stn7* mutant, which is deficient in light-harvesting antenna phosphorylation, was used. The results show that the stiffness of the thylakoid membranes increased immediately upon illumination followed by a delayed height change. The stiffness change primarily depended on the transmembrane pH gradient, whereas the height change required both the pH gradient and STN7-dependent phosphorylation. We propose that the driving force behind the stiffness change is pH-dependent lumen expansion. The height change is also driven by lumen expansion, however it requires disruption of stromal interactions between membranes by phosphorylation. Our results indicate that lumen expansion is not simply a result of the influx of water, and we discuss possible protein interactions within the lumen that could drive these changes.

Preface

This work was a collaboration primarily with Casper Clausen in the lab of Prof. Dan Fletcher. My part of this work consisted of preparing samples, preforming fluorescence measurements, doing Western blots, interpretating results and writing later drafts of the manuscript. Casper performed all of the AFM measurements and wrote the first draft of the manuscript. Tai-De Li was also involved in the AFM measurements. Patricia Grob and Gigi Kemalyan performed the EM imaging in the lab of Prof. Eva Nogales.

Introduction

The mechanisms controlling how a plant acclimates to light and maintains photosynthetic efficiency are of great interest for understanding optimizing photosynthesis. The photosynthetic machinery used to convert light to chemical energy is located in the chloroplast, with the light reactions being carried out by pigment-protein complexes in the thylakoid membrane network. Imbalances between the amount of light absorbed and what can be utilized can result in the production of damaging reactive oxygen species. In order to protect themselves, plants contain multiple mechanisms that balance light absorption and dissipate excess energy [24].

Photosynthetic organisms respond to changes in light intensity and quality by several processes such as energy-dependent quenching [13,24] and phosphorylation of the light-harvesting complex of photosystem II (LHCII) [23]. While these processes have been extensively studied, there are still many aspects that are not yet fully understood [Allen]. A particular area of recent interest is how LHCII and the thylakoid membrane are reorganized in response to light [8,11,14]. These reorganizations are thought to protect the plant from damage, optimize electron transport and facilitate repair [6]. The main mechanism driving mechanical changes of the thylakoid membrane in response to differential excitation of the two photosystems is state transitions, which are thought to balance light harvesting of Photosystem I (PSI) and Photosystem II (PSII) by both molecular and superstructural reorganization [1,8,11].

The effects on thylakoid membrane remodeling as a result of illumination with PSI- and PSII-specific light have been intensely investigated. Most of research has utilized techniques such as electron microscopy (EM) or atomic force microscopy (AFM) in order to describe structural changes to the thylakoid membranes before and after illumination [8,11,17]. In contrast to EM, which involves elaborate sample preparation, AFM has the advantage that it can be performed under conditions that mimic the cellular environment and is a useful tool for investigations of live samples [12]. Several attempts have been made with AFM to image the composition of the thylakoid membrane [16,28] or the thylakoid superstructure [8,15,30]. So far there have been no reports that have used AFM to observe the dynamic changes that occur in response to light as they happen.

This study focuses on characterizing changes in the mechanical properties of thylakoid membranes that occur in the first minutes after illumination with light that specifically excites PSII. The height and rheology changes were investigated using a modified AFM consisting of a Bioscope Catalyst system, where the cantilever was controlled to deploy a fixed average force (height measurement), while a small sinusoidal movement of the cantilever was used to obtain the visco-elastic properties of the thylakoid membrane. An optical microscope was used both as an illumination source and for imaging the thylakoid membrane.

Material and Methods

Plant Material - Wild-type (Col-0) and *stn7* plants [5] were grown in 7.5-cm soil pots in a chamber with a 10-hour day, 14-hour night cycle at 21.5°C and a light intensity of approximately 150 µmol photon m^{-2} s^{-1}. Plants were used for experiments before bolting at an age of 7-10 weeks.

Thylakoid Isolation - De-enveloped chloroplasts were isolated according to Casazza *et al.* [7]. The whole preparation was carried out at 4°C and in the dark. Leaves from Arabidopsis plants as well as all the equipment used were cooled to 4°C one hour prior to the isolation process. The leaves were shredded in a blender by eight 0.5-second pulses in 100 ml buffer, containing 0.4 M sorbitol, 5 mM EGTA, 5 mM EDTA, 5 mM $MgCl_2$, 10 mM $NaHCO_3$, and 20 mM Tricine at pH 8.4. The mixture was filtered through six layers of cheesecloth, and at the end the cloth was gently squeezed in order to obtain a higher yield. The solution was centrifuged for 3 min at 2600 g. The supernatant was discarded, and the pellet was re-suspended in 10 mL of resuspension buffer containing 0.3 M sorbitol, 2.5 mM EDTA, 5 mM $MgCl_2$, 10 mM $NaHCO_3$, 20 mM HEPES at pH 7.6. This step was repeated three times. After the last centrifugation, the supernatant was discarded, and the pellet was resuspended for 5 min in 10 mL of hypotonic

buffer containing 2.5 mM EDTA, 5 mM $MgCl_2$, 10 mM $NaHCO_3$, 20 mM HEPES at pH 7.6. The solution was then centrifuged for 3 min at 200 *g*, and the supernatant was collected and centrifuged for 3 min at 2,600 g. Finally the supernatant was discarded, and the pellet was resuspended in measuring buffer containing 0.3 M sorbitol, 5 mM $MgCl_2$, 10 mM $NaHCO_3$, 20 mM HEPES at pH 7.6. In order to keep the thylakoid membranes active, the experiments were carried out within 2 hours of isolation.

Rheology experiments - Glass coverslips were coated prior to the experiments with poly-L-lysine by adding 0.1% (w/v) poly-L-lysine solution on the coverslips for 30 min and then washing with measuring buffer four times. The solution containing the de-enveloped chloroplast was added and left to settle for 10 min follow by four washing steps with measuring buffer. An incubation period of 10 min was used for the supplementation of electron acceptors (10 μM ferredoxin and 0.6 mM $NADP^+$) and uncouplers (gramicidin D) to the measuring buffer. Cantilevers were prepared by gluing (Norland 61) polystyrene beads (diameter 5 μm) to the tip of the cantilever (Veeco, MLCT-OW, triangular shape, nominal spring constant of 0.01 N/m with no reflective coating and no tip), and their spring constants were determined by the thermal vibration method [27]. The experiments were carried out at room temperature and in the dark. Samples were mounted on a Zeiss Observer 1, and illumination was provided by a Shutter Lambda LS (xenon arc-lamp 300 W bulb) equipped with an ET640/30x filter for red light, a HQ740/40x filter for far red light, and a S484/15x filter for blue light (Chroma Technology). The imaged light was passed through a HQ665LP filter (Chroma Technology). The intensity of the illumination, which was 150 μmol photons m^{-2} s^{-1} for the 640 nm light and 100 μmol photons m^{-2} s^{-1} for the 740 nm light, was measured with a Melles Griot 13PEM001. Optical images were acquired with an Andor Ixon+. Rheology measurements were obtained with a modified Bruker Bioscope Catalyst system (with a Nanoscope V controller). A National Instrument DAQ PCI-6229 card generated the applied signal, and the readout signal was filtered (Krohn-hite 3364) and split between the DAQ card (for sampling of the height data) and a Signal Recovery (model 7270) lock-in amplifier (to acquire amplitude and phase of the signal). For the analysis of the storage and loss modulus, calculations were based on the common Hertz model extended by Tu and Chen models [20].

All AFM data were obtained with an applied force of an average of 0.2 nN and a sinusoid signal with an amplitude of 20 nm and a frequency of 2 Hz. The time constant of the lock-in amplifier was 1 second with the sensitivity at 500 mV. The membrane was illuminated for 7 min with a wavelength of 640 nm. Tests were made after illumination of the membrane and after it was allowed to "relax" in the dark for up to 20 min. During the relaxation period, no changes were observed with the conditions described here.

77 K Fluorescence Measurements - Resuspended chloroplasts in measuring buffer containing 10 μM ferredoxin and 0.6 mM $NADP^+$ were added to a glass cuvette. Glass cuvettes were illuminated for 10 min with the microscope light source by placing the glass cuvette on a cover slip above the microscope objective or by a lamp containing the appropriate filter. After and rapid freezing in liquid nitrogen, an emission spectrum was obtained with a fluorometer (Fluoromax-4, Horiba equipped with the dewar setup for low temperature measurements). The excitation light was 480 nm with a bandpass of 5 nm and emission was detected between 650 and 800 nm at 1 nm increments with a bandpass of 5 nm.

Electron Microscopy - Isolated chloroplasts were high-pressure frozen with a Leica EM PACT2 prior to chemical fixation and resin embedding. Isolated chloroplasts in a re-suspension buffer containing 10% BSA as a cryo-protectant were pipetted into 1.5mm x 0.1mm Leica membrane carriers and high-pressure frozen. The frozen samples were transferred to cryo vials containing a liquid N_2-frozen fixative cocktail consisting of 1.0% osmium tetroxide and 0.1% uranyl acetate in 100% acetone, and quick-freeze substituted for 90 minutes [21]. After coming to room temperature, the samples were rinsed in 100% acetone, then microwave infiltrated with Eponate 12 resin, embedded in molds and polymerized at 60˚C for 48 hours. The resin blocks were thin sectioned at 60 nm with a Leica UC7 ultramicrotome, and sections were collected on 3 mm Formvar and carbon coated copper grids. Grids were poststained with 2% uranyl acetate and 0.1% Reynold's lead citrate. Images were acquired with an FEI Tecnai 12 TEM with an accelerating voltage of 120 kV at 18500x magnification.

Results

Height Increase of Thylakoids in Response to PSII-Specific Light

Figure 5.1A illustrates the modified AFM setup in which the microscope is capable of imaging and illuminating isolated thylakoid membranes simultaneously. The cantilever has a 5 μm bead attached to it in order to contact a broad area of the membrane network (several grana stacks). The AFM system is operated in a feedback loop with a constant applied force in order to measure the changes in height of the membrane. Figure 5.1B shows a typical height response of a thylakoid membrane sample that was illuminated with PSII light (λ = 640 nm). The height of the sample increased by approximately 20% (Figure 5.1C), and a time delay (t_d) was consistently observed between the time when the light was turned on and the time of the height response. Furthermore, this delay was dependent on the light intensity, as shown in Figure 5.1D.

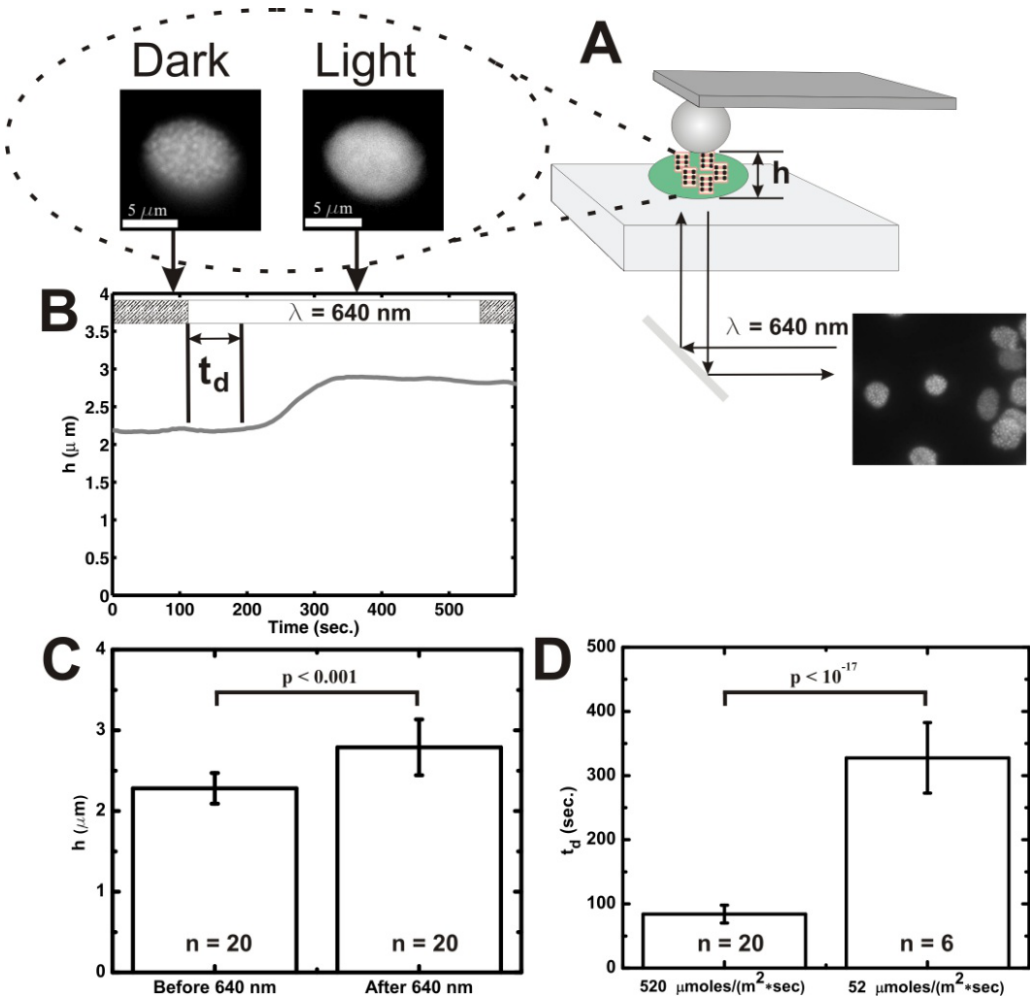

Figure 5.1: Height response of thylakoid membranes when exposed to PSII light
A) Schematic drawing of the AFM setup measuring height (h) and optical changes of thylakoid membranes. B) A typical height response from a thylakoid membrane sample exposed to 640 nm light. There was a time delay (t_d) between when the light was turned on and when changes in the height of the thylakoid membrane occurred. C) Average of start height and end height of 20 thylakoid membranes. D) Average of the time delay at different light intensities.

The Stiffness of Thylakoids Increases Upon Exposure to Light

Figure 5.2 shows the elasticity response of the thylakoid membrane. Figure 5.2A is a schematic representation of the setup with the graph plotting the applied and measured signal of a dark-acclimated membrane sample. A typical response from a thylakoid membrane is shown in Figure 5.2B, with an increase in stiffness occurring upon illumination without the delay seen for the height change. Figure 5.2C plots the average elasticity of thylakoid membranes before and after illumination. There was a very large change in stiffness upon illumination, with light-adapted thylakoids being approximately 10 fold more stiff compared to the dark-acclimated membranes. Thylakoid stacking is known to depend on ions, and specifically depletion of Mg^{2+} is known to cause unstacking. Figure 5.2D shows that when thylakoids were unstacked by Mg^{2+}

depletion, there was a 2-fold decrease in stiffness instead of the increase observed during illumination with 640 nm light.

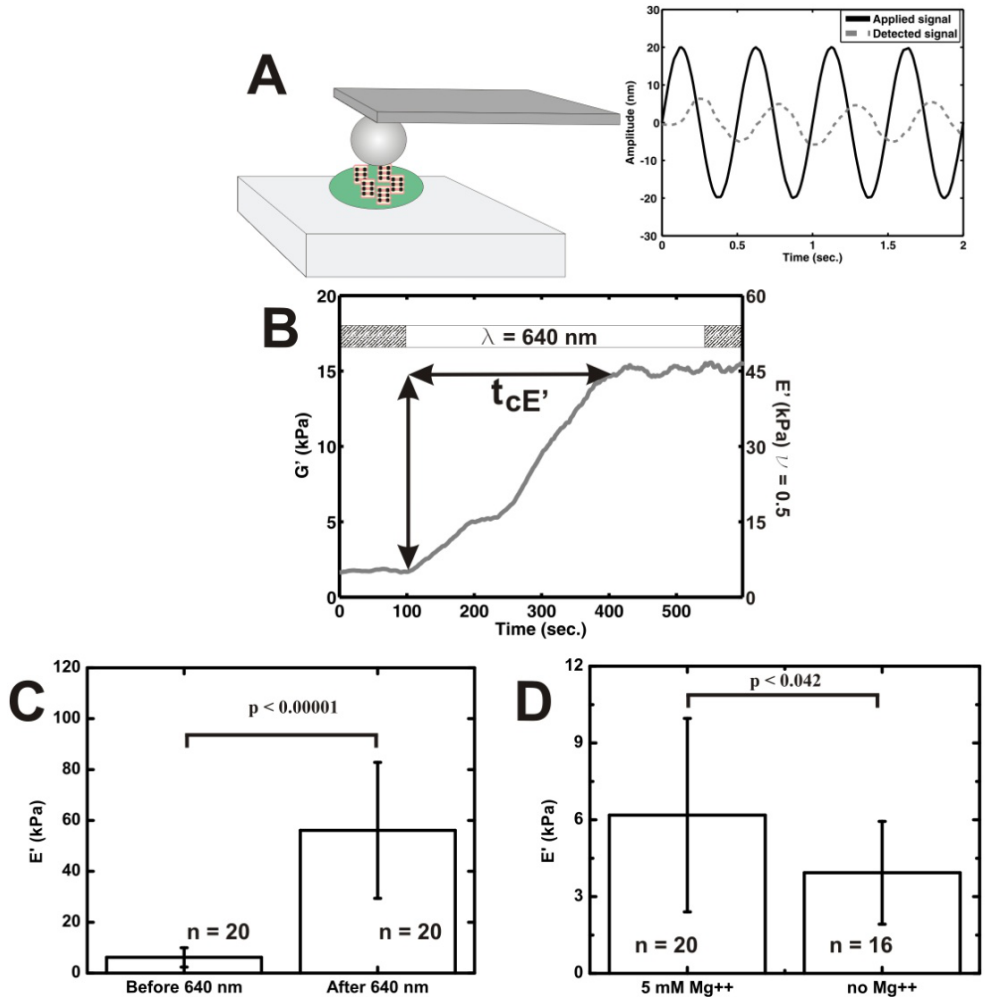

Figure 5.2: Rheology response of thylakoid membrane when exposed to light
A) Schematic representation of the measuring principle. The graph shows the applied signal (black) as well as the measured signal (gray dashed line) of a dark-acclimated thylakoid membrane sample. The time constant of the elasticity change ($t_{cE'}$) was around 5 min. B) Typical mechanical response from a thylakoid membrane exposed to light. C) Average elasticity of 20 thylakoid membranes before and after exposure to light. D) Average elasticity of thylakoid membranes in the presence or absence of Mg^{2+}.

Height and Stiffness Changes are Modulated by the pH Gradient and STN7-Dependent Phosphorylation

To investigate the mechanisms that are responsible for the height and stiffness changes, experiments were carried out on thylakoids isolated from the *stn7* mutant [5]. Transmission EM images obtained from dark-acclimated and illuminated thylakoid membranes from both wild-

type and the *stn7* mutant and the proposed structural changes are illustrated in Figure 5.3A. In addition, thylakoids from wild-type plants were treated with gramicidin D to allow ions to flow across the membrane and prevent the formation of the pH gradient. Figure 5.3B shows the percentage change in elasticity of wild type, *stn7*, and wild type treated with gramicidin D. The *stn7* mutant showed a higher stiffness change compared to the wild-type, whereas treatment with gramicidin D prevented this stiffness change. Furthermore, the relative changes in height of wild type, *stn7*, and wild type treated with gramicidin D are shown in Figure 5.3C. Only the wild-type sample exhibited a significant height change. Figure 5.3D is a plot of the time constant for wild type, *stn7*, and wild type treated with gramicidin D and shows that no statistically significant change was observable in the amount of time it took for the stiffness to reach the maximum level.

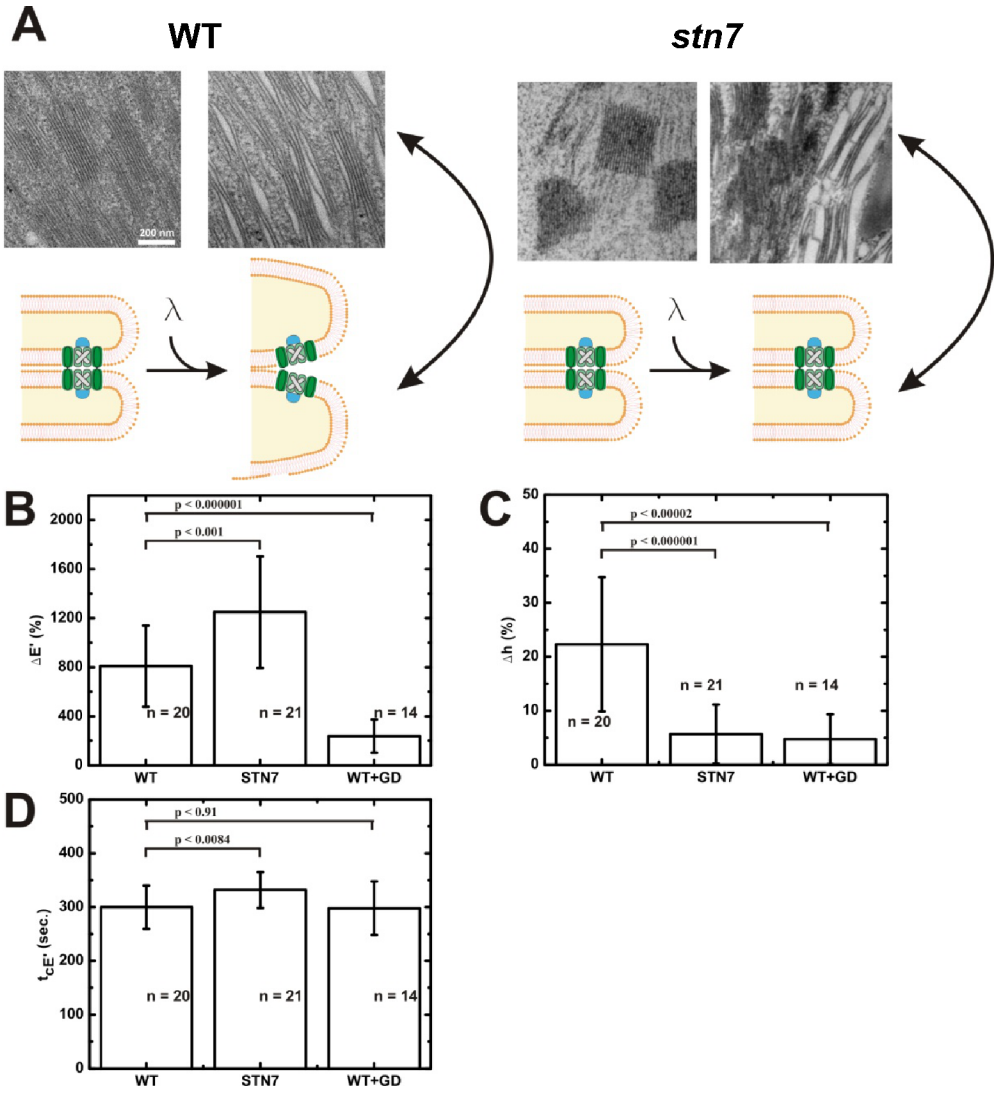

Figure 5.3: Structural comparison between the wild type and *stn7* mutant.
A) Transmission EM images of changes in the thylakoid ultrastructure and the proposed effect of state transition in the wild type (WT) and *stn7* mutant. B) Percentage changes in

elasticity of WT, *stn7*, and WT treated with gramicidin D (GD). C) Percentage changes in height of WT, *stn7*, and WT treated with gramicidin D. D) Time constant for WT, *stn7*, and WT treated with gramicidin D.

Relationship between Height Change and 77 K Fluorescence

The migration of phosphorylated LHCII to PSI during state transitions in plants is thought to occur in order to balance the absorption of the two photosystems. We wanted to determine the timescale of this change as measured by 77 K fluorescence and compare it to the kinetics of the changes in membrane height that we observed. Figure 5.4A shows that the fluorescence changes occurred after an even larger delay compared to the height changes and are likely not even completed by the end of the AFM measurements.

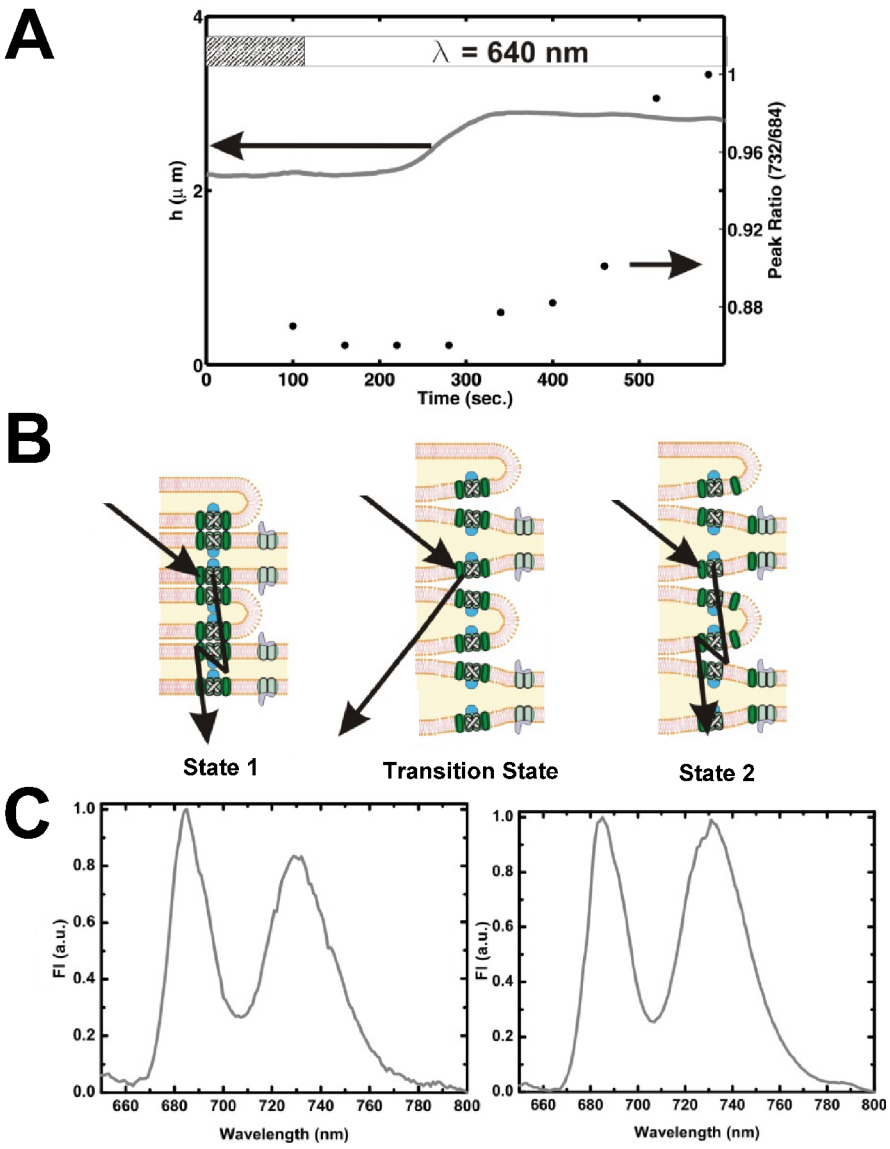

Figure 5.4: Comparison of the kinetics of changes in height and 77 K fluorescence
A) Comparison of the height change (grey line) and fluorescence peak ratio at 77 K (black squares). B) Proposed model of the changes underlying the swelling and stiffening of the thylakoid membrane. Before illumination thylakoids are in state 1, the transition state forms as LHCII becomes phosphorylated and membrane stacking occurs but LHCII remains associated with PSII (~200-350 sec). Prolonged illumination causes LHCII to migrate to PSI and into state 2. C) 77 K fluorescence measurements. Arrows in B point to the 77 K observed during those states

Viscosity and Elasticity of Thylakoid Membranes

The visco-elastic properties of the thylakoid membranes calculated according to Mahaffey *et al.* (17) are shown in Figure 5.5. While the phase (φ) for all the measurements obtained always decreased, there was no consistency for the calculated viscosity (G'). The formula for G" is *am*/(*ap*-*am*)*sin(φ), where *am* is the measured amplitude and *ap* is the applied amplitude. With this model there are limits of *am* = *ap* and φ = 0, where viscosity goes to infinity or zero. The issue here is that both of these conditions are happening, which results in variation of the viscosity response when compared to the elasticity (Figure 5.5 and Figure 5.2B).

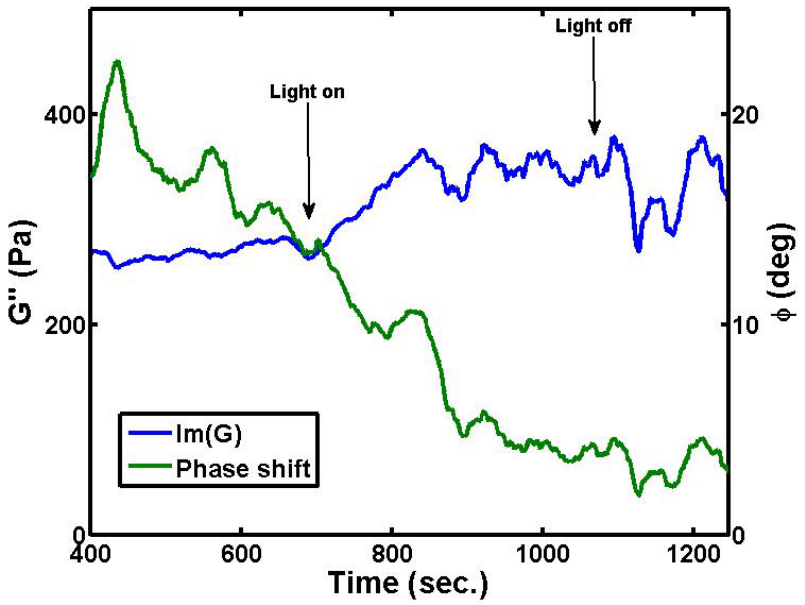

Figure 5.5: Example of changes in visco-elastic properties of the thylakoid membrane
Plot of the calculated viscosity (G", blue curve) and the phase shift (ϕ, green curve). The graph shows that upon illumination the phase lag is shifted around 15 degree for this measurement and was similar for other measurements. No consistency was found in the change in viscosity between samples.

Discussion

This investigation demonstrated that the mechanical properties of dark-acclimated isolated thylakoids are altered by light with a wavelength of 640 nm or less. Longer wavelengths have little effect. The AFM data show that after illumination with PSII-specific light, there was a rapid increase in thylakoid membrane stiffness followed by a height increase after an intensity-dependent time delay (see Figure 5.1B and Figure 5.2B). The height increase was suppressed in the *stn7* mutant and in membranes unable to form a pH gradient (Figure 5.3C). These results indicate that at least two mechanisms control the height change. Previously it has been reported that upon illumination of Arabidopsis leaves with white light, there is a 17% increase in the stacking repeat distance of thylakoids due to lumen expansion and that uncoupling the pH gradient suppresses this effect [17]. This value (17%) is comparable to the height increase found in this investigation using isolated thylakoids (20%; Figure 5.1C), and we partially attribute the height change to lumen expansion. Because there is a significant delay in the height change, the pH gradient, which forms within seconds of illumination [25,26], cannot be sufficient for this effect. Our observation that the height change was abolished in the *stn7* mutant (Figure 5.3C) indicates that STN7-dependent phosphorylation also contributes to this phenomenon when samples are illuminated with PSII-specific light. This is possibly caused by the unstacking of thylakoid membranes [11] that is thought to occur due to disruption of stroma-face interactions between LHCII trimers [4,22]. We propose that lumen expansion or swelling of the thylakoid membrane is the driving force behind the height increase, but only when the molecular interactions holding the grana stacks together are removed as a result of STN7 phosphorylation (Figure 5.3A) can this effect manifest as a height change.

In contrast to the changes in height, Figure 5.3B shows that the increase in stiffness does not require STN7-dependent phosphorylation or unstacking. In fact, we observed that the increase appeared to be greater in the *stn7* mutant compared to the wild type. Formation of the pH gradient was responsible for a large fraction of the stiffness change, as demonstrated by the addition of gramicidin D (Figure 5.3B). The stiffening also differed from the height change in that it did not have a time delay but rather occurred immediately upon illumination (Figure 5.2A). The immediate response in stiffness is in line with it being driven by the formation of the pH gradient, and we attribute most of this effect to lumen expansion. We argue that the unstacking seen in wild-type, which allows the height change, also attenuates the stiffening effect by releasing constraint on the membrane and can explain the increased stiffness seen in *stn7*. Because a 2-3 fold increase in stiffness remained even in the presence of gramicidin D, it is possible that other light-dependent changes contribute to this effect, and the origin of the additional stiffening remains to be determined.

State transitions have been proposed to balance excitation between the two photosystems by decreasing the cross section of PSII and increasing the cross section of PSI [23]. This effect can be monitored by changes in the relative low temperature fluorescence of the two photosystems and involves the migration of LHCII from PSII to PSI. Phosphorylation of LHCII is thought to cause this rearrangement by promoting the unstacking of the grana membranes, which facilitates the movement of complexes. Recently it has been shown that STN7 is important in balancing excitation under fluctuating light, and this function does not involve changes in the 77 K emission spectra [29]. Our results suggest that the height change follows

phosphorylation of LHCII, whereas changes in the 77 K fluorescence only occur once the height change and phosphorylation are nearly complete (Figure 5.4). Lumen expansion has been proposed to facilitate plastocyanin diffusion between the cytochrome *b6/f* complex and PSI, which could improve electron transport [16,17]. Our observation that the lumen expansion is larger in wild-type than in *stn7* thylakoids when illuminated with PSII-specific light (Figure 5.3A) suggests that under these conditions unstacking of the membrane may facilitate not only LHCII migration but also further enhance plastocyanin diffusion and help balance pressure on the two photosystems.

This work also addresses the question of what causes lumen expansion upon exposure to light. If the cause was simply swelling by water influx, one would expect that the elasticity would decrease and the viscosity would increase, however we did not observed this trend during our experiments (Figure 5.5). Therefore we argue that the lumen expansion that causes the stiffening of the thylakoid membrane is most likely to be caused by some form of inter-membrane interaction within the lumen. Whether this is an attractive force between membranes that is disrupted in the light or a repulsive force that is shielded in the dark remains to be determined. Both the attractive and repulsive forces between grana membranes have been explored previously and protein components were implicated in these interactions [2]. The oxygen-evolving complex (OEC) within the lumen is an intriguing candidate for facilitating this interaction. The OEC is the largest lumenal protrusion and is thought to be the main determinant of lumenal spacing [18]. It has been proposed that the PsbQ protein of the OEC is involved in facilitating protein-protein interactions between OECs on opposing membranes [19]. However, the positioning of OECs on opposing lumenal surfaces with respect to each other is an open question due largely to the varying estimates of lumen spacing [10]. Some reports have indicated that the lumen spacing presents no spatial hindrance to OECs being directly opposite one another [18], while others have suggested that this arrangement would not be possible in the dark and that they are more likely to be in an offset arrangement [16,17]. We are currently in the process of obtaining EM images and measuring the lumen spacing in order to determine whether our experiments with PSII-specific light can support either of these scenarios.

We have demonstrated that the mechanical properties of isolated thylakoid membranes can be monitored using a modified AFM. It was found that upon illumination of wild-type thylakoids the stiffness of the membrane increased immediately, followed by a height increase with a light intensity-dependent delay. The height as well as the stiffness increase could be reduced by the addition of the uncoupler gramicidin D. These results indicate that a major molecular mechanism controlling the stiffness and height change of thylakoids is the pH gradient across the membrane, which drives lumen expansion by altering the grana membrane interactions. Using the *stn7* mutant we further showed that in the absence of grana unstacking the height increase is suppressed but the stiffness increase was larger. These results indicate that STN7-dependent phosphorylation releases constraints on the membrane and allows the lumen to expand further. We have also provided evidence that these changes occur more quickly than the migration and docking of LHCII to PSI and support the role of state transitions in rapid acclimation to light changes.

References

1. Albertsson, P. (2001). A quantitative model of the domain structure of the photosynthetic membrane. Trends Plant Sci. *6*, 349–358.
2. Albertsson, P.-Å. (1982). Interaction between the lumenal sides of the thylakoid membrane. FEBS Letters *149*, 186–190.
3. Allen, J.F., and Forsberg, J. (2001). Molecular recognition in thylakoid structure and function. Trends in Plant Science *6*, 317–326.
4. Barber, J. (1982). Influence of Surface Charges on Thylakoid Structure and Function. Annu. Rev. Plant. Physiol. *33*, 261–295.
5. Bellafiore, S., Barneche, F., Peltier, G., and Rochaix, J.-D. (2005). State transitions and light adaptation require chloroplast thylakoid protein kinase STN7. Nature *433*, 892–895.
6. Blankenship, Robert (2002). Molecular Mechanisms of Photosynthesis. Oxford/Malden: Blackwell Science.
7. Casazza, A.P., Tarantino, D., and Soave, C. (2001). Preparation and functional characterization of thylakoids from Arabidopsis thaliana. Photosyn. Res. *68*, 175–180.
8. Chuartzman, S.G., Nevo, R., Shimoni, E., Charuvi, D., Kiss, V., Ohad, I., Brumfeld, V., and Reich, Z. (2008). Thylakoid Membrane Remodeling during State Transitions in Arabidopsis. The Plant Cell Online *20*, 1029 –1039.
9. De Las Rivas, J., Heredia, P., and Roman, A. (2007). Oxygen-evolving extrinsic proteins (PsbO,P,Q,R): Bioinformatic and functional analysis. Biochimica Et Biophysica Acta (BBA) - Bioenergetics *1767*, 575–582.
10. Dekker, J.P., and Boekema, E.J. (2005). Supramolecular organization of thylakoid membrane proteins in green plants. Biochimica Et Biophysica Acta (BBA) - Bioenergetics *1706*, 12–39.
11. Dietzel, L., Bräutigam, K., Steiner, S., Schüffler, K., Lepetit, B., Grimm, B., Schöttler, M.A., and Pfannschmidt, T. (2011). Photosystem II supercomplex remodeling serves as an entry mechanism for state transitions in Arabidopsis. Plant Cell *23*, 2964–2977.
12. Goldsbury, C.S., Scheuring, S., and Kreplak, L. (2009). Introduction to atomic force microscopy (AFM) in biology. Curr Protoc Protein Sci *Chapter 17*, Unit 17.7.1–19.
13. Horton, P., and Ruban, A. (2005). Molecular design of the photosystem II light-harvesting antenna: photosynthesis and photoprotection. Journal of Experimental Botany *56*, 365 –373.
14. Johnson, M.P., Goral, T.K., Duffy, C.D.P., Brain, A.P.R., Mullineaux, C.W., and Ruban, A.V. (2011). Photoprotective Energy Dissipation Involves the Reorganization of Photosystem II Light-Harvesting Complexes in the Grana Membranes of Spinach Chloroplasts. The Plant Cell Online *23*, 1468 –1479.
15. Kaftan, D., Brumfeld, V., Nevo, R., Scherz, A., and Reich, Z. (2002). From chloroplasts to photosystems: in situ scanning force microscopy on intact thylakoid membranes. EMBO J. *21*, 6146–6153.
16. Kirchhoff, H., Hall, C., Wood, M., Herbstová, M., Tsabari, O., Nevo, R., Charuvi, D., Shimoni, E., and Reich, Z. (2011). Dynamic control of protein diffusion within the granal thylakoid lumen. Proceedings of the National Academy of Sciences *108*, 20248 –20253.

17. Kirchhoff, H., Lenhert, S., Buchel, C., Chi, L., and Nield, J. (2007). Probing the Organization of Photosystem II in Photosynthetic Membranes by Atomic Force Microscopy. Biochemistry *47*, 431–440.
18. Kouřil, R., Oostergetel, G.T., and Boekema, E.J. (2011). Fine structure of granal thylakoid membrane organization using cryo electron tomography. Biochimica Et Biophysica Acta (BBA) - Bioenergetics *1807*, 368–374.
19. De Las Rivas, J., Heredia, P., and Roman, A. (2007). Oxygen-evolving extrinsic proteins (PsbO,P,Q,R): Bioinformatic and functional analysis. Biochimica Et Biophysica Acta (BBA) - Bioenergetics *1767*, 575–582.
20. Mahaffy, R.E., Park, S., Gerde, E., Käs, J., and Shih, C.K. (2004). Quantitative Analysis of the Viscoelastic Properties of Thin Regions of Fibroblasts Using Atomic Force Microscopy. Biophys J *86*, 1777–1793.
21. McDonald, K.L., and Webb, R.I. (2011). Freeze substitution in 3 hours or less. Journal of Microscopy *243*, 227–233.
22. McDonnel, A., and Staehelin, L.A. (1980). Adhesion between liposomes mediated by the chlorophyll a/b light-harvesting complex isolated from chloroplast membranes. The Journal of Cell Biology *84*, 40 –56.
23. Minagawa, J. (2011). State transitions—The molecular remodeling of photosynthetic supercomplexes that controls energy flow in the chloroplast. Biochimica Et Biophysica Acta (BBA) - Bioenergetics *1807*, 897–905.
24. Niyogi, K.K. (1999). PHOTOPROTECTION REVISITED: Genetic and Molecular Approaches. Annu. Rev. Plant. Physiol. Plant. Mol. Biol. *50*, 333–359.
25. Po, E.S.-M., and Ho, J.W. (1997). Paraquat Affects Light-Induced Proton Transport Through Chloroplast Membranes in Spinach. Comparative Biochemistry and Physiology Part C: Pharmacology, Toxicology and Endocrinology *118*, 65–69.
26. Rumberg, B., and Muhle, H. (1976). Investigation of the Kinetics of Proton Translocation across the thylakoid membrane. Bioelectrochemistry and Bioenergetics *3*, 393–403.
27. Stark, R.W., Drobek, T., and Heckl, W.M. (2001). Thermomechanical noise of a free v-shaped cantilever for atomic-force microscopy. Ultramicroscopy *86*, 207–215.
28. Sznee, K., Dekker, J.P., Dame, R.T., van Roon, H., Wuite, G.J.L., and Frese, R.N. (2011). Jumping mode atomic force microscopy on grana membranes from spinach. J. Biol. Chem. *286*, 39164–39171.
29. Tikkanen, M., Grieco, M., Kangasjärvi, S., and Aro, E.-M. (2010). Thylakoid Protein Phosphorylation in Higher Plant Chloroplasts Optimizes Electron Transfer under Fluctuating Light. Plant Physiology *152*, 723 –735.
30. Yamada, T., Arakawa, H., Okajima, T., Shimada, T., and Ikai, A. (2002). Use of AFM for imaging and measurement of the mechanical properties of light-convertible organelles in plants. Ultramicroscopy *91*, 261–268.

Chapter 6

Conclusions

Photosynthesis sustains nearly all life on earth and has also been tapped as a fuel source for human-kind. Evolutionary pressures have driven plants to form large light-harvesting antennae that collect as much sunlight as possible. As a consequence, the amount of absorbed light can often exceed that which can be used for photochemical reactions and, left unchecked, could result in the formation of damaging reactive oxygen species [21]. Therefore plants have also evolved several mechanisms that they use to dissipate excess excitation energy [19]. A key feature of these quenching processes is that they can be integrated into the photosynthetic machinery in a manner that allows precise control of the switch between light harvesting and quenching in response to environmental conditions. A complete understanding of this regulatory system will require knowledge of: the proteins and pigments in the system, the structural arrangement of these molecules, the dynamic changes that occur in response to light and the biophysical mechanisms that are involved.

The SOQ1 protein identified in this work is a previously uncharacterized chloroplast protein involved in preventing the formation of a slowly reversible form of quenching. The non-photochemical quenching (NPQ) in *soq1* mutants was shown to be unrelated to the characterized NPQ components and opens a new area of research for understanding how plants maintain photosynthetic efficiency. Under most conditions this quenching is likely to be undesirable as it would compete with photochemistry when light levels are reduced, though it is plausible that it would be beneficial to plants under persistent stress conditions. Indeed, sustained photoprotective quenching has been previously observed in shade plants transferred to full sun and overwintering evergreens [1,2,20]. This type of quenching could possibly occur through the same mechanism as the additional NPQ seen in *soq1* plants. The consistent correlation between sustained quenching and zeaxanthin formation [7,26] may not support this view, but given the versatility of zeaxanthin in photoprotection [10,19] it is conceivable that its accumulation is unrelated to the quenching mechanism. Speeding up the relaxation kinetics of NPQ has been proposed as one way to increase crop yields [18,28], and consideration of *soq1*-type of quenching could be important in these efforts.

A key mechanistic question that remains is how SOQ1 is preventing quenching. Complementation with point mutants and truncated proteins indicated that while the stroma-exposed haloacid dehalogenase-like hydrolase (HAD) domain is not required to prevent quenching, the thioredoxin (Trx)-like and beta-propeller (NHL) domains are essential. The best clue to the function of SOQ1 may lie in the similarity between the Trx-like domain of SOQ1 and the TlpA family of proteins. The TlpA family contains proteins involved in transferring reducing power across the cytoplasmic membrane of bacteria into the periplasmic space [4]. The known pathways present in plant thylakoids that transfer reducing equivalents into the oxidizing lumen utilize proteins that are related to those of the bacterial system [15]. Most of these proteins, such as the thylakoid localized CCDA [22] and HCF164 [17], have been identified through their involvement in cytochrome biogenesis pathways. While the phenotype of *soq1* plants indicates that it is not involved in cytochrome biogenesis, the same pathways in bacteria have been shown to be used for disulfide bond isomerization [23] and reduction of oxidized amino acids [8,27]. Given the oxidizing conditions of the lumen, similar pathways could be involved in maintaining the photosynthetic apparatus.

Establishing how the absence of SOQ1 protein leads to an NPQ phenotype will also be

critical in understanding this type of quenching. Experiments in Chapter 3 begin to address this question by looking for interactions between SOQ1 and other thylakoid proteins and characterizing the changes that occur in *soq1* mutants. One possibility is that an antenna protein is a target of SOQ1, either directly or through another protein. Cysteine and methionine residues on the light-harvesting proteins are intriguing candidates for sites of oxidation. In particular LHCB5 contains a conserved cysteine residue in the first lumenal loop that is conspicuously absent in the prasinophytes, which also lack a SOQ1 homolog. If oxidation of this or any other residue can alter the conformation of an antenna protein, it may alter the pigment interactions and lead to the formation of a quenching site [12,24]. Alternatively, changes in the organization of supercomplexes that we have observed using atomic force microscopy may also explain the NPQ phenotype seen in *soq1* plants. Increased packing density of protein has been proposed to decrease efficiency in isolated grana membranes through quenching of excitation [9]. While a higher packing density of PSII complexes is seen in *soq1* plants compared to wild type, this difference is apparent in both high and low light, making it difficult to explain the high light-dependent phenotype in the mutant.

The HAD domain of SOQ1 also presents an interesting avenue of research. The experiments in Chapter 4 indicate that this domain is likely a phosphatase, specific for a five-carbon sugar. Testing various substrates in vitro has shown that SOQ1 is most active on ribose-5-phosphate, however it remains to be seen if this is also the case in vivo. While the HAD domain could have a function completely independent from that of the Trx-like and NHL domains, it is also possible that it regulates the activity of the lumenal domains of SOQ1. Given that the HAD domain is not required to complement the NPQ phenotype this would have to be an inhibitory effect. A conformational change that occurs due to the formation of the phospho-aspartyl intermediate [16] could affect the other domains, similar to the mechanism employed by two-component systems [25]. In this way, during periods of stress when carbon fixation is limited, the accumulation of stromal photosynthetic intermediates such as ribose-5-phosphate could be a signal to downregulate light harvesting.

A comprehensive model of the switch from light harvesting to NPQ (and back) will also require understanding the structural changes that occur during the switch between these states. While much research has focused on the changes that must occur within proteins in order to activate NPQ [6,24,Ruban], changes in the density and arrangement of supercomplexes within the grana [3,9,12,13] and of the structure of the thylakoid membrane as a whole [5,14], have also been implicated. To further characterize the changes that occur on the level of whole thylakoids, the mechanical properties of isolated thylakoid membranes were monitored as they acclimated to light using a modified AFM instrument. With this technique we were able to observe an increase in the stiffness and height of thylakoids as they responded to PSII-specific light. To our knowledge this is the first time that these measurements have been used to monitor dynamic changes in plants, and it opens the door for future studies on other regulatory processes that control photosynthesis.

Some of the most important challenges facing civilization today, and in the years to come, include food and energy security, climate change, and decreasing bio-diversity. Given the central role photosynthesis plays in the biosphere and the potential it holds for engineering a sustainable fuel source, research in this area will be critical to addressing those and other issues. An understanding of the whole system and the dynamic changes that occur, from the excitation of an electron to the movement of leaves, will be necessary if we wish to manipulate plants to suit our needs.

References

1. Adams III, W.W., Demmig-Adams, B. (2004) Chlorophyll fluorescence as a tool to monitor plant response to the environment, in Chlorophyll a Fluorescence: A Signature of Photosynthesis. pp. 583–604.
2. Adams III, W.W., Zarter, C.R., Mueh, K.E., Amiard, V., and Demmig-Adams, B. (2006). Energy Dissipation and Photoinhibition: A Continuum of Photoprotection. In Photoprotection, Photoinhibition, Gene Regulation, and Environment, (Springer Netherlands), pp. 49–64.
3. Betterle, N., Ballottari, M., Zorzan, S., de Bianchi, S., Cazzaniga, S., Dall'osto, L., Morosinotto, T., and Bassi, R. (2009). Light-induced dissociation of an antenna hetero-oligomer is needed for non-photochemical quenching induction. J. Biol. Chem. *284*, 15255–15266.
4. Capitani, G., Rossmann, R., Sargent, D.F., Grütter, M.G., Richmond, T.J., and Hennecke, H. (2001). Structure of the soluble domain of a membrane-anchored thioredoxin-like protein from Bradyrhizobium japonicum reveals unusual properties. J. Mol. Biol. *311*, 1037–1048.
5. Chuartzman, S.G., Nevo, R., Shimoni, E., Charuvi, D., Kiss, V., Ohad, I., Brumfeld, V., and Reich, Z. (2008). Thylakoid Membrane Remodeling during State Transitions in Arabidopsis. The Plant Cell Online *20*, 1029 –1039.
6. Dall'Osto, L., Caffarri, S., and Bassi, R. (2005). A Mechanism of Nonphotochemical Energy Dissipation, Independent from PsbS, Revealed by a Conformational Change in the Antenna Protein CP26. The Plant Cell Online *17*, 1217 –1232.
7. Demmig-Adams, B., Moeller, D.L., Logan, B.A., and Adams III, W.W. (1998). Positive correlation between levels of retained zeaxanthin + antheraxanthin and degree of photoinhibition in shade leaves of *Schefflera arboricola* (Hayata) Merrill. Planta *205*, 367–374.
8. Depuydt, M., Leonard, S.E., Vertommen, D., Denoncin, K., Morsomme, P., Wahni, K., Messens, J., Carroll, K.S., and Collet, J.-F. (2009). A Periplasmic Reducing System Protects Single Cysteine Residues from Oxidation. Science *326*, 1109–1111.
9. Haferkamp, S., Haase, W., Pascal, A.A., van Amerongen, H., and Kirchhoff, H. (2010). Efficient Light Harvesting by Photosystem II Requires an Optimized Protein Packing Density in Grana Thylakoids. Journal of Biological Chemistry *285*, 17020 –17028.
10. Havaux, M., and Niyogi, K.K. (1999). The violaxanthin cycle protects plants from photooxidative damage by more than one mechanism. Proceedings of the National Academy of Sciences *96*, 8762 –8767.
11. Ilioaia, C., Johnson, M.P., Horton, P., and Ruban, A.V. (2008). Induction of Efficient Energy Dissipation in the Isolated Light-harvesting Complex of Photosystem II in the Absence of Protein Aggregation. Journal of Biological Chemistry *283*, 29505 –29512.
12. Johnson, M.P., Goral, T.K., Duffy, C.D.P., Brain, A.P.R., Mullineaux, C.W., and Ruban, A.V. (2011). Photoprotective Energy Dissipation Involves the Reorganization of Photosystem II Light-Harvesting Complexes in the Grana Membranes of Spinach Chloroplasts. The Plant Cell Online *23*, 1468 –1479.
13. Kereïche, S., Kiss, A.Z., Kouřil, R., Boekema, E.J., and Horton, P. (2010). The PsbS

protein controls the macro-organisation of photosystem II complexes in the grana membranes of higher plant chloroplasts. FEBS Letters *584*, 759–764.
14. Kirchhoff, H., Lenhert, S., Buchel, C., Chi, L., and Nield, J. (2007). Probing the Organization of Photosystem II in Photosynthetic Membranes by Atomic Force Microscopy. Biochemistry *47*, 431–440.
15. Kranz, R., Lill, R., Goldman, B., Bonnard, G., and Merchant, S. (1998). Mmicular mechanisms of cytochrome c biogenesis: three distinct systems. Molecular Microbiology *29*, 383–396.
16. Lahiri, S.D., Zhang, G., Dunaway-Mariano, D., and Allen, K.N. (2003). The Pentacovalent Phosphorus Intermediate of a Phosphoryl Transfer Reaction. Science *299*, 2067 –2071.
17. Lennartz, K., Plücken, H., Seidler, A., Westhoff, P., Bechtold, N., and Meierhoff, K. (2001). HCF164 Encodes a Thioredoxin-Like Protein Involved in the Biogenesis of the Cytochrome b6f Complex in Arabidopsis. The Plant Cell Online *13*, 2539 –2551.
18. Murchie, E.H., and Niyogi, K.K. (2011). Manipulation of Photoprotection to Improve Plant Photosynthesis. Plant Physiology *155*, 86 –92.
19. Niyogi, K.K. (1999). Photoprotection Revisited: Genetic and Molecular Approaches. Annu. Rev. Plant. Physiol. Plant. Mol. Biol. *50*, 333–359.
20. Öquist, G., and Huner, N.P.A. (2003). Photosynthesis of Overwintering Evergreen Plants. Annu. Rev. Plant Biol. *54*, 329–355.
21. Owens, T.G. (2004). Processing of Excitation Energy by Antenna Pigments. In Photosynthesis and the Environment, (Springer Netherlands), pp. 1–23.
22. Page, M.L.D., Hamel, P.P., Gabilly, S.T., Zegzouti, H., Perea, J.V., Alonso, J.M., Ecker, J.R., Theg, S.M., Christensen, S.K., and Merchant, S. (2004). A homolog of prokaryotic thiol disulfide transporter CcdA is required for the assembly of the cytochrome b6f complex in Arabidopsis chloroplasts. J. Biol. Chem. *279*, 32474–32482.
23. Rietsch, A., Belin, D., Martin, N., and Beckwith, J. (1996). An in vivo pathway for disulfide bond isomerization in Escherichia coli. Proceedings of the National Academy of Sciences *93*, 13048 –13053.
24. Standfuss, J., Terwisscha van Scheltinga, A.C., Lamborghini, M., and Kuhlbrandt, W. (2005). Mechanisms of photoprotection and nonphotochemical quenching in pea light-harvesting complex at 2.5 [angst] resolution. EMBO J *24*, 919–928.
25. Stock, J., and Da Re, S. (2000). Signal transduction: Response regulators on and off. Current Biology *10*, R420–R424.
26. Verhoeven, A.S., Adams, W.W., and Demmig-Adams, B. (1998). Two forms of sustained xanthophyll cycle-dependent energy dissipation in overwintering Euonymus kiautschovicus. Plant, Cell & Environment *21*, 893–903.
27. Wu, J., Neiers, F., Boschi-Muller, S., and Branlant, G. (2005). The N-terminal domain of PILB from Neisseria meningitidis is a disulfide reductase that can recycle methionine sulfoxide reductases. J. Biol. Chem. *280*, 12344–12350.
28. Zhu, X., Ort, D.R., Whitmarsh, J., and Long, S.P. (2004). The slow reversibility of photosystem II thermal energy dissipation on transfer from high to low light may cause large losses in carbon gain by crop canopies: a theoretical analysis. Journal of Experimental Botany *55*, 1167 –1175.